12-18-2017

Zeolite Facies and Environmental Change in the Plio-Pleistocene Baringo Basin, Kenya Rift

Karim Minkara

ZEOLITE FACIES AND ENVIRONMENTAL CHANGE IN THE PLIO-PLEISTOCENE BARINGO BASIN, KENYA RIFT

by

KARIM MINKARA

Under the Direction of Daniel Deocampo, PhD, PG

ABSTRACT

Sediments exposed in the Tugen Hills in the Central Rift of Kenya include an important hominin-bearing succession of volcaniclastic and fluvio-lacustrine deposits. The Hominin Sites and Paleolakes Drilling Project (HSPDP) retrieved a ~230 m core through a portion of the Chemeron Formation, containing a highly resolved succession of strata spanning events leading to the Plio-Pleistocene boundary (3.4-2.6 Ma). Trends in the character and abundance of zeolites indicate changes in paleoenvironmental conditions with varying stability identified through distinct facies assemblages. These seem to reflect high amplitude changes accompanying peak earth-orbital eccentricity at ~2.7 Ma, and relative stability at low eccentricity at ~2.9-2.7 Ma. This study suggests a decrease in K/Ca and an increase in Na/Ca with major fluctuations. Zeolites act as terrestrial climate proxies in the absence of biogenic material, aside from intervals of diatom-rich strata, and are suggesting episodes of strongest environmental fluctuations ~2.7-2.6 Ma and environmental stability ~2.9-2.7 Ma.

INDEX WORDS: Paleoclimate, Plio-Pliestocene, Zeolite, Equatorial East Africa, Lake Baringo, Tugen Hills

ZEOLITE FACIES AND ENVIRONMENTAL CHANGE IN THE PLIO0PLEISTOCENE BARINGO BASIN, KENYA RIFT

by

KARIM MINKARA

A Thesis Submitted in Partial Fulfillment of the Requirements for the Degree of

Master of Science

in the College of Arts and Sciences

Georgia State University

2017

ZEOLITE FACIES AND ENVIRONMENTAL CHANGE IN THE PLIO-PLEISTOCENE BARINGO BASIN, KENYA RIFT

by

KARIM MINKARA

Committee Chair: Daniel Deocampo

Committee: W. Crawford Elliott

Lawrence Kiage

Electronic Version Approved:

Office of Graduate Studies

College of Arts and Sciences

Georgia State University

December 2017

DEDICATION

This thesis is dedicated to my father, for providing me an incredible example as a scientist and as an intellectual human being for teaching me to never stop learning. His approach at life and knowledge is why I chose the path I am on and to obtain higher education for the betterment of our planet.

ACKNOWLEDGEMENTS

I would like to acknowledge the immense dedication and collaborative efforts that the HSPDP Tugen Hills team has contributed to the project prior to and after this thesis. Thank you to the drilling and core description team, as well as the LacCore staff for making these analyses possible.

I would not have completed this major accomplishment without the crucial guidance, patience, and understanding of my advisor Dr. Daniel Deocampo, who although might be the busiest man I have ever met, still made the time to point me in the direction of success.

Majority of preliminary XRD data, analysis, and troubleshooting, as well as critical academic and life guidance credited to Nate Rabideaux, who was to me as much of a peer as he was a mentor.

The SEM and EDS analysis would not be possible without Dr. Robert Simmons with the BioImaging Core Facility at Georgia State University.

The assistance with preparation and analysis of the nearly 1,300 core samples are credited to the undergraduate support from Cole Hairston, Morgan Garner, David Davis, Sanam Chaudhary, and Thanh Vo. Thank you all for making the process a little less overwhelming.

I would also like to acknowledge Dr. Brian Meyer, who has played an important role in my academic and professional development for my time as President of the AIPG club as well as being a student in many of his courses.

I would also like to thank my fellow colleagues that I've earned the pleasure of meeting during my time here at GSU as an undergraduate and graduate student. I've grown to enjoy the community that the Department of Geosciences has fostered and will continue to look forward to where all of our careers will take us.

Research for this project is supported by the following grants earned by HSPDP: NSF EAR-1123942, BCS-1241859, EAR-1338553, EAR-1029020, & EAR-1349599.

TABLE OF CONTENTS

LIST OF TABLES

LIST OF FIGURES

LIST OF ABBREVIATIONS

BPRP - Baringo Paleontological Research Project

BTB – Baringo Tugen Hills Barsemoi

EDS – Energy dispersive spectroscopy

HSPDP – Hominin Sites and Paleolakes Drilling Project

Ma – Mega-annum (million years)

SEM – Scanning electron microscope

XRD – X-ray diffraction

1 INTRODUCTION

1.1 The Hominin Sites and Paleolakes Drilling Project

The Hominin Sites and Paleolakes Drilling Project (HSPDP) is an interdisciplinary research effort addressing key questions dealing with the relationship between Earth's climate history and human evolution. Over 2,00 meters of lacustrine sediments forming paleontologically significant sites in Kenya and Ethiopia have been collected to be used in a combined data collection and modeling approach that is aimed to transform the discussion of environmental influence shaping the history of hominin evolution (Cohen et al., 2016). Of particular interest are the timing of early hominin habitats, their climatic conditions, how local and regional scale of climate coupled with tectonic processes to influence the environmental resources and hominin paleoecology, and the evolutionary processes and events observed in hominin lineage (Campisano et al, 2017). Four primary goals of the HSPDP, stated in Campisano et al., 2017 are to: "1) expand paleoenvironmental data collected at key paleoanthropological localities, upon which tests hypotheses about environmental drivers of hominin evolution can be based; 2) enhance the resolution and quality of paleoenvironmental data available to address the role of Earth system dynamics in hominin evolutionary processes; 3) compare overlapping time segments to describe how global climate change is expressed at local levels, and thereby to build a high-resolution regional framework of climate and habitat change during hominin evolution in eastern Africa: and, 4) develop process models of environmental change and ecosystem response during critical intervals of hominin evolution and evaluate these models against our high-resolution core paleorecords."

The Lake Baringo – Tugen Hills basin was selected as a drilling target by the HSPDP community due to 1) its important fossil localities (Table 1), 2) distinctive series of diatomite

units linked to precessional insolation (REFERENCE – Deino et al.?), and 3) its unique record of East African environmental conditions when Northern Hemispheric glaciation first intensified (Campisano et al., 2017).

Table 1 Significant fossil localities of the Tugen Hills (collected from Hill, 2002).

Site Name	Age (Ma)	Archaeological/Paleontological Significance	References
BPRP#2, Chemeron Fm., Tugen Hills	3.3 – 1.6	Earliest known example of the *Homo* genus	Sherwood et al., 1996
Tabarin, Chemeron Fm., Tugen Hills,	4.96 – 4.15	Hominin mandible, possible *Australopithecus afarensis*.	Ward & Hill, 1987
GnJh-42 & GnJh-50, Kapthurin Fm., Tugen Hills	0.55 – 0.51	Earliest blades	Johnson & McBrearty, 2010

The Baringo Basin-Tugen Hills area comprises the most complete late Neogene section known from the African rift, with strata spanning the last 16 Ma (Chapman & Brook, 1978). The Baringo Basin was selected for drilling by the Hominin Sites Paleolakes Drilling Project in order to provide high stratigraphic continuity and resolution for identifying how shifting climate patterns and orbitally-driven cycles influence environmental changes in the Rift Valley (Campisano et al., 2017). In the stratigraphic interval targeted in the Chemeron formation (5.3-1.6 Ma), approximately 100 fossil vertebrate localities including three hominin sites provide opportunities to explore the mechanism of environmental change associated with shifting insolation patterns; more specifically, examining lacustrine response to changing precipitation patterns at precessional timescales to assess terrestrial community responses to pervasive, short-term climatic change during the initiation of Northern Hemispheric glaciation (Kingston et al., 2007; Wilson et al., 2014; Cohen et al., 2016). The diversification of hominin group *Paranthropus* (characterized by robust cranial features and large teeth for strong biting force)

along with genus *Homo,* as well as earliest evidence for stone tool making are also observed in this region (Harmand et al., 2015; Cohen et al., 2016).

Chemeron Formation tuffs stratigraphically bracketing hominin specimen KNM-BC 1, a fossil hominin temporal bone of the genus *Homo,* were dated using single crystal $^{40}Ar/^{39}Ar$ and resulted in the approximate range 2.456-2.393 Ma that is supported by stratigraphically consistent horizons in nearby sections (Deino & Hill, 2002). This succession also contains cyclic diatomite/fluvial cycles that are indicative of periodic freshwater, deep lake development (Deino et al., 2006). These diatomites, termed the Barsemoi diatomites after the nearby Barsemoi River, align with the orbital precessional interval of 23 kyr and are suggested to reflect intervals of orbitally forced wet/dry climatic conditions; insolation models suggest that moisture originating from the northern African monsoon fed the wet times of the record (Deino et al., 2006).The Barsemoi diatomites provide an opportunity to relate short-term climatic changes to hominin habitats and orbitally induced environmental change (Kingston et al., 2007).

1.2 Lake Baringo Basin – Tugen Hills

Modern Lake Baringo is a shallow freshwater lake located in a semi-arid volcanic region on the eastern arm of the central Kenya Rift Valley. The modern lake and the adjoining Loboi Swamp to the south represent the surface of a large (>5km) Pleistocene fault-controlled basin (Renaut, 2000). Lake shape is controlled by the dominant N-S trend of the Tertiary-Holocene rift system and the NW-SE oriented Precambrian metamorphic basement. These lineaments served as major structural controls on Cenozoic extension of the East African Rift along with volcanic damming of a river flowing through the rift valley (Yuretich, 1982; Dunkley et al., 1993; Le Turdu et al., 1995, 1999; Renaut, 2000; Atmaoui & Hollnack, 2003; Ashley et al., 2004).

Volcanism disrupted the drainage patterns of the eastern arm of the central rift, which helped create small, shallow lake basins through new divides (Figure 1). This action diverted water away from the rift and allowed high infiltration so lake development is restricted, explaining why Baringo is such a shallow body of water. Despite the lack of surface outlet in a region of high evaporation, Lake Baringo remains fresh due to subsurface loss of water through the lake floor along with subsequent northward groundwater flows (Yuretich, 1982; Renaut, 2000). Although it is currently a freshwater lake, Lake Baringo has dried up and become moderately saline due to evaporative concentration at time during the past few thousand years (Owen, 1981; Renaut, 2000).

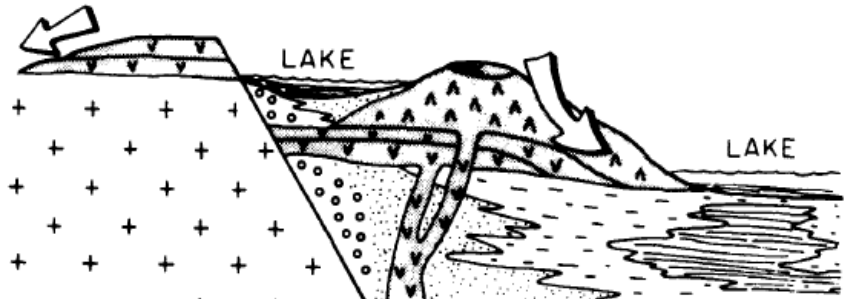

Figure 1 Lake formation through volcanism (Yuretich, 1982)

The Tugen Hills is a structural horst within the Kenya Rift to the west of the modern lake ~1500m above the rift floor consisting of undifferentiated volcanic rocks and clayey soils (Renaut 2000). The Tugen Hills were raised by the Saimo fault block of Neogene lavas, sedimentary rocks, and tuffs which record a gradual eastern migration of the depocenter (Renaut, 2000; Deino et al., 2001; Kingston et al., 2007). Miocene troughs created the rift resulting in a depositional basin housing widespread sedimentary sequences over the past 16 Ma (Chapman & Brook, 1978; King, 1978; Kingston et al., 2007).

The Pliocene and Pleistocene Chemeron Formation is discontinuously exposed in the eastern foothills of the Tugen Hills (Figure 2) and spans ~3.7 million years (5.3 – 1.6 Ma) of strata (Kingston et al., 2007). The Chemeron Formation sediments overlie the Kaparaina Basalts, and are truncated above by an angular disconformity at the base of the overlying Kapthurin Formation (Figure 3). The Kapthurin and Chemeron Rivers that drain from the Tugen Hills eastward to Lake Baringo expose the Chemeron formation. Chemeron sediments are mostly composed of fine-grain terrigenous and lacustrine sediments containing mudstone and siltstone with diatomite, sandstone, and conglomerate intercalations (Deino & Hill, 2002).

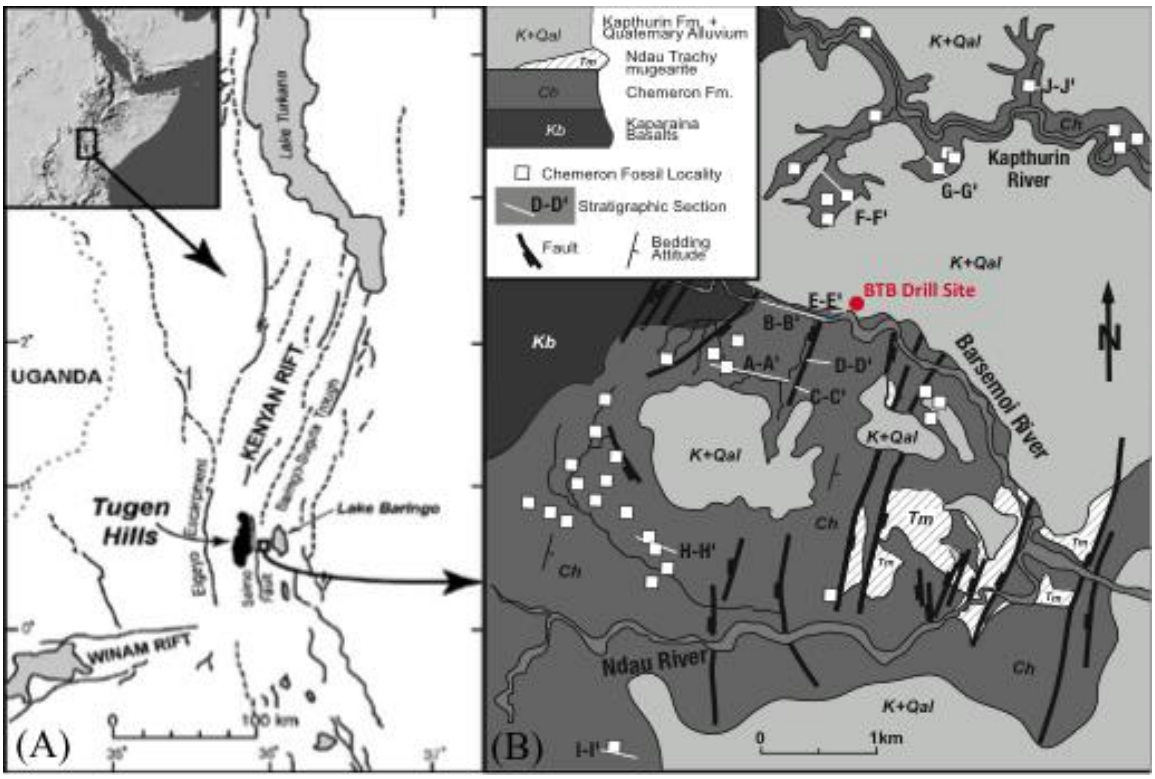

Figure 2 (A) Overview and (B) geologic map of Chemeron Formation, Tugen Hills with BTB drill site labeled (modified from Deino et al., 2006). Cross sections and fossil localities refer to Deino et al., 2006.

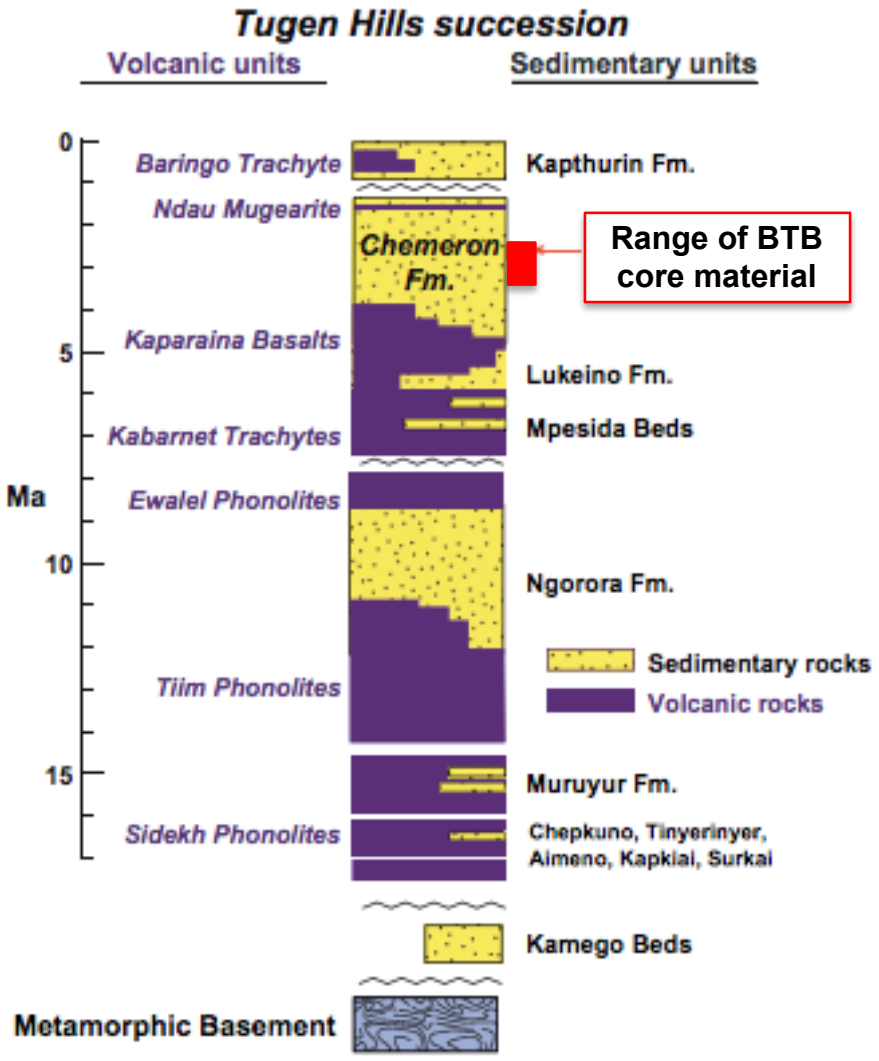

Figure 3 Composite stratigraphy of the Tugen Hills succession (modified from Kingston et al., 2007)

Using the ancient lake classification scheme for tectonic and climate controls from Carroll and Bohacs (1999), core descriptions and mineralogy suggest paleolake Baringo fluctuated between overfilled and balanced-filled lake basin types with lacustrine facies associations changing from fluvial-lacustrine to fluctuating profundal facies associations. Although in a region of high net evaporation and absence of a surface outlet, modern Lake Baringo remains fresh due to subsurface loss of water through the lake floor coupled with

northward flow of groundwater, suggesting that the lake is topographically closed and hydrologically open (Allen & Darling, 1992; Dunkley et al., 1993; Renaut et al., 2000). Fluctuation in size and chemical composition has been explained as responses to short-term seasonal changes to river and stream input (Allen & Darling, 1992), though changes in mineral and lacustrine facies associations can be evidence for long-term changes caused by variations in orbital forcings due to Milankovich cyclicty (Kingston et al., in review).

1.3 Zeolite Diagenesis

The zeolite group of minerals are framework aluminosilicates that are commonly hydrated, and have alkali cation compositions (Klein and Dutrow, 2007). Authigenic zeolite formation is primarily the byproduct of volcanic glass deposited in saline-alkaline waters (Hay, 1970; Hay & Sheppard, 2001). The zeolite crystals typically contain open cavities in the form of channels and cages, usually occupied by H_2O molecules and extra-framework cations that are commonly exchangeable, and large enough to allow the passage of guest species (Lauf, 2014).

Table 2 lists the four major zeolites found throughout the BTB core material (in bold), as well as minor zeolites, with their chemical composition and Dominant Extra Framework Cation (DEC). The most critical requirement for zeolite formation is a high aqueous activity ratio of $(Na^+ + K^+ + Ca^{2+})/H^+$. Because of this, zeolites are formed predominantly in alkaline environments, with the larger concentrations of pure zeolites found primarily in altered vitric tephra deposits of saline-alkaline lakes (pH = 9.5 – 10) (Sheppard & Hay, 2001).

Table 2 Schematic chemical formulae of primary zeolites. DEC = Dominant Extra framework Cation (modified from Passaglia & Shepphard, 2001)

Zeolite	**Formula**	**DEC**
Analcime	$NaAlSi_2O_6$•(H2O)	Na
Wairakite	$CaAl_2Si_4O_{12}$•2(H_2O)	Ca
Natrolite	$Na_2Al_2Si_3O_{10}$•2(H_2O)	Na
Chabazite	$(Ca_{0.5},Na,K)_4[Al_4Si_8O_{24}]$•12($H_2O$)	Ca, Na, K
Clinoptilolite-Heulandite	$(Na,K,Ca_{0.5})_7[Al_7Si_{29}O_{72}]$ •22(H_2O)	Ca, Na, K
Phillipsite	$K_2(Na,Ca_{0.5})_3[Al_5Si_{11}O_{32}]$ •12(H_2O)	K, Na, Ca

Water activity and pore-fluid composition are significant factors in determining zeolite formation. Because the activity of water is reduced at high ionic strength, higher salinity lowers solute temperatures of dehydration and consequently lowers the temperatures at which the less hydrous zeolites are stable (Hay, 1966; Sheppard & Hay, 2001). The proportions of extra-framework cations are also critical in determining which zeolites may form dependent on cation availability. A unique trait defining the zeolite group is the ability to hydrate and dehydrate reversibly during cation exchange between aqueous bodies while resisting major structural changes (Pabalan & Bertetti, 2001). Based on these characteristics, the composition of the dominant extra-framework cations (DECs) of lacustrine zeolites are potentially important indicators for the geochemistry of paleolake waters.

1.4 Plio-Pleistocene East African Paleoclimate

The essential factors that comprise the creation of monsoons, as stated by Webster, 1987, are the following: "(1) the differential seasonal heating of the oceans and continents, (2) moisture processes in the atmosphere, and (3) the earth's rotation". Differences between the East and West African Monsoon systems are affected by the shape of the continent, rainfall variability caused by the rainshadow effect of the Great Rift Valley, large inland lakes that potential modify

monsoon flows, and influences from the Indian monsoon, in addition to the three factors stated above (Davies et al., 1985; Nicholson, 1996; McGregor and Nieuwolt, 1998). Major structural elements of the East African Monsoon system include the ITCZ traveling south of the equator, the Arabian and Mascarene high pressure systems, the East African low level jet stream, West African mid-tropospheric jet stream, the tropical easterly jet stream, and the two subtropical westerly jet streams (McGregor and Nieuwolt, 1998). The rate of moisture transport over East Africa and strength of monsoonal flows are attributed to the two major monsoon wind systems dominating East Africa, which includes the north-easterlies and the south-easterlies, both anticyclones that vary in intensity, location, and orientation (McGregor and Nieuwolt, 1998).

The above describes the modern East African Monsoon system, however Plio-Pleistocene climate variability in this region has been studied through eolian dust from marine sedimentary sequences for the past ~5 Ma (Rea, 1994; deMenocal, 1995). Plio-Pleistocene climate changes in East African must be evaluated in relation to high latitude climate changes, as seen in marine oxygen isotope data recording the onset of high latitude glacial cycles being gradually develop between 3.1-26 Ma (Shackleton et al., 1990; Tiedemann et al., 1994; deMenocal 1995). Previous studies reveal the African climate response to precessional insolation forcing in high and low latitude processes observed during the initial growth and expansion of high latitude ice sheets around 2.8 Ma and 1.0 Ma, respectively; prior to 2.8 Ma the ice sheets were small and relatively constant (Shackleton et al., 1984, 1990; Clemens and Prell, 1991; Jansen and Sjoholm, 1991; deMenocal et al., 1993; Tiedemann et al., 1994; deMenocal, 1995). Because terrestrial paleoclimate data for this time interval have not been recorded as extensively as marine records, the most accurate characterization Plio-Pleistocene African climate can be described as a sequence of alternating wet and dry conditions with significant periods of eolian dust flux

variability occurring around 2.8, 1.7, and 1.0 Ma; these findings are observed as the development of cool, dry conditions after 2.8 Ma followed by the intensification after 1.7 and 1.0 Ma (deMenocal 1995).

1.5 Hypothesis Testing

Past climate reconstruction for this area have been based on outcrops along lake margins or have used marine climate proxies. The lack of abundant biogenic material in the core (other than within diatomite intervals) presents a challenge for paleoclimate reconstruction. Development of these zeolite indicators will contribute a useful set of tools of terrestrial climate proxies for lacustrine systems.

The purpose of this thesis is to test whether major environmental changes in the Baringo–Tugen Hills Basin are represented by trends in the mineralogy of lacustrine sediment. These changes will then be compared to models of orbital variations thought to affect East African paleoclimate in Plio-Pleistocene time, particularly those emphasizing the role of eccentricity in climate control.

Identifying the mineralogy throughout core material collected from the HSPDP Tugen Hills drilling campaign and comparing the trends identified to previous outcrop and marine paleoclimate proxy studies will test this hypothesis.

2 MATERIALS AND METHODS

2.1 Site selection, coring, and initial core descriptions

In order to minimize the likelihood of encountering subsurface faults or associated deformation that might interfere with maximizing stratigraphic resolution, survey data were collected to determine the optimal location for boring prior to drilling (Cohen et al., 2016).

Baringo/Tugen Hills pre-drilling information was based on known outcrop exposures immediately adjacent to the drill site whereas other HSPDP sites used seismic, gravity, and magnetic surveys (Deino et al., 2006; Kingston et al., 2007; Cohen et al., 2016).

HSPDP personnel began drilling June 1, 2013 and successfully recovered a ~227m core. Vertical drilling was possible at the Baringo Basin/Tugen Hills site due to the existing ~20 ° dip of sediments. Geophysical down-hole logging data were collected for natural gamma, magnetic susceptibility (MS), resistivity, borehole temperature, and azimuthal direction (Cohen et al., 2016). MS data were collected from unsplit cores using a multisensory core logger (MSCL, Geotek Ltd.) (Cohen et al., 2016). The core was recovered ~20m from cliff exposures of Chemeron sediments and contains a sedimentary record similar to that known from outcrop studies. The sampling identification system consisted of the project initials (HSPDP), followed by the site name (BTB), then the site hole (1A), core drilled and tool used for drilling (1-81 & Q/Y), section of core (1, 2, 3 or CC) and finally the sediment range in a 2cm interval; example being HSPDP-BTB-1A-32Q-2_33.5-35.5.

The core was subsequently transported to the National Lacustrine Core Facility (LacCore) at the University of Minnesota for scanning, processing, initial core descriptions, and subsampling every 16cm (Cohen et al., 2016). Physical properties of the core were analyzed in detail via MSCL-S for *p* wave locality, gamma density, loop MS, non-contact electrical resistivity, and natural gamma radiation, and MSCL-XYZ for high resolution MS and color reflectance spectrophotometry at 0.5-4cm increments (Cohen et al., 2016). MSCL-CIS digital linescan core imager provided imagery once cores were split in half lengthwise and cleaned (Cohen et al., 2016).

The borehole was located near the cyclic diatomites and mudstone outcrops of the upper Chemeron Formation, which were previously shown to reflect precessional climate variability during the Plio-Pleistocene transition (Deino et al., 2007; Kingston et al., 2007; Cohen et al., 2016). Sediments are dominantly fluviolacustrine and floodplain paleosols in the lower half of the core, with cyclic deep-lake diatomites and subaerially deposited sediments in the upper half, spanning approximately 3.4-2.6 Ma (Kingston et al., 2007; Kingston et al., in review).

2.2 Mineralogy

At Georgia State University, 1078 samples were oven dried at 40°C for 48 hours, then ground to fine powder using ball & pestle impact grinders or by hand using mortar and pestle, depending on hardness of material. The bulk mineralogy of core material was analyzed by powder X-ray diffraction (XRD) using a Panalytical X'pert Pro MPD using CuKα radiation, in the range 5-60°2θ, operating at 45kV and 40mA for a duration of 30 minutes. HighScore+ and Data Viewer software used for mineralogical analysis (Panalytical 2012). 1078 samples were analyzed for mineralogical identification.

Mineralogical identification through XRD consisted of generating mineral ID's from the HighScore+ database and selecting the most applicable match per diffraction peak. These matches were then confirmed through consulting references by hand through d-spacing and 2θ coordinates specific to each mineral (Brindly and Brown, 1980; Moore and Reynolds, 1989).

Mineral occurrence determined from XRD analysis was recorded in a Microsoft Excel spreadsheet listed by relative abundance for the corresponding sample ID (Appendix A). Major zeolite mineral facies were graphed to depth and age using Systat SigmaPlot 13.x software as

XY scatter plots. Age model was created through running stratigraphic heights (mbs) through a Table Interpolation program created by A. Deino at a 97.5% confidence interval.

After mineral identification through XRD, 15 representative samples were selected for scanning electron microscope (SEM) and energy-dispersive spectroscopy (EDS) analysis to provide textural and compositional data for major zeolite facies. Selected samples were carbon coated, and analyzed on a Tescan Vega3 SEM with an EDAX element X-ray detector running Team software, with an accelerating voltage of 10kV with approximately 1nA probe current.

3 RESULTS

3.1 Stratigraphic Variation

The top ~50m of the core contain five diatom-rich intervals (8.73-11.10, 15.10-22.16, 25.22-32.31, 41.52-43.47, and 50.18-52.04 meters below surface) that appear to be the upper Barsemoi Diatomites of Deino et al. (2006). These diatomites have been previously interpreted to record episodic expansions of freshwater lake systems driven by orbital precession (Deino et al., 2006; Kingston et al., 2007). Because biotic proxies are poor outside of these diatom-rich intervals, bulk mineralogical analysis identifies a variety of mineral assemblages from sedimentary sequences nearly exclusive from these diatom-rich zones.

A wide array of alkali and plagioclase feldspars, silica polymorphs, Fe-oxides, Ti-oxides, carbonates, sulfur-bearing minerals, clay minerals, and zeolites are found in abundance throughout the core. Albite, anorthite, and anorthoclase seem to occur sporadically throughout the entire sequence. Silica polymorphs include cristobalite, tridymite, and quartz, as well as opaline silica. Hematite is the most abundant Fe-oxide, although magnetite and magnesioferrite have been identified in lesser amounts. Rutile and anatase are the identified Ti-oxides. Nodular Mg-calcite, dolomite, and calcite are mostly found in areas of paleosol development. Gypsum

and pyrite are seen in individual samples spread across the upper-middle section of the core. Smectite or kaolinite are present in many samples, although detailed clay mineralogical studies on oriented slides have not yet been carried out. Most notably, the distribution of zeolite mineral species forms distinct zones throughout the core. Although zeolites have been noted in the basin before (Renaut et al., 2000; Kerrich, 2002; Ashley et al., 2006) this distinct zonation has not previously been observed in outcrop-based studies.

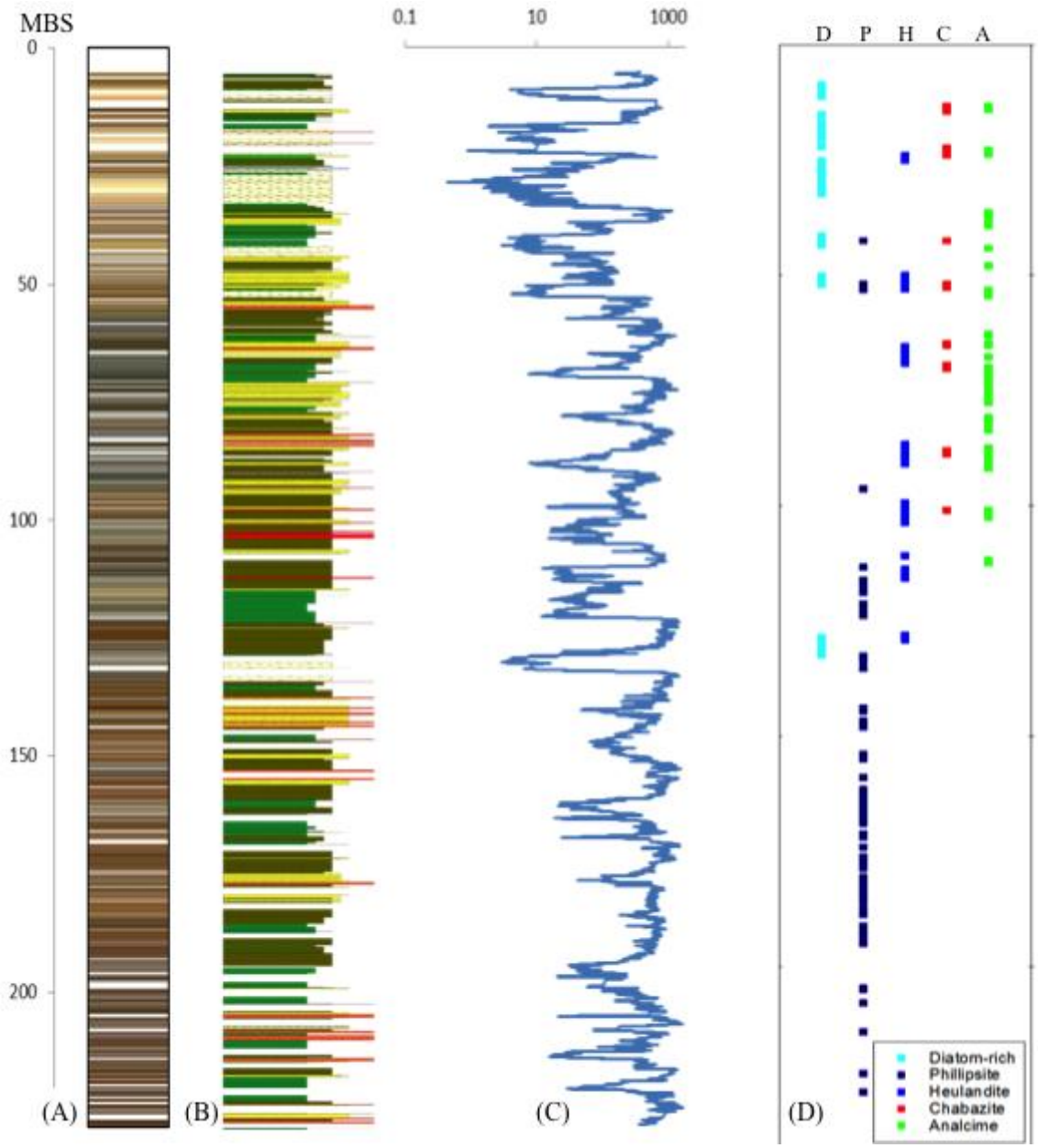

Figure 4 (A) Core color, (B) lithology, and (C) magnetic susceptibility (MS) log data (25-point running mean smooth) from LacCore Geotek XYZ point sensor data (modified from Cohen et al., 2016) compared to (D) major zeolite and diatom-rich facies plotted to depth (mbs)

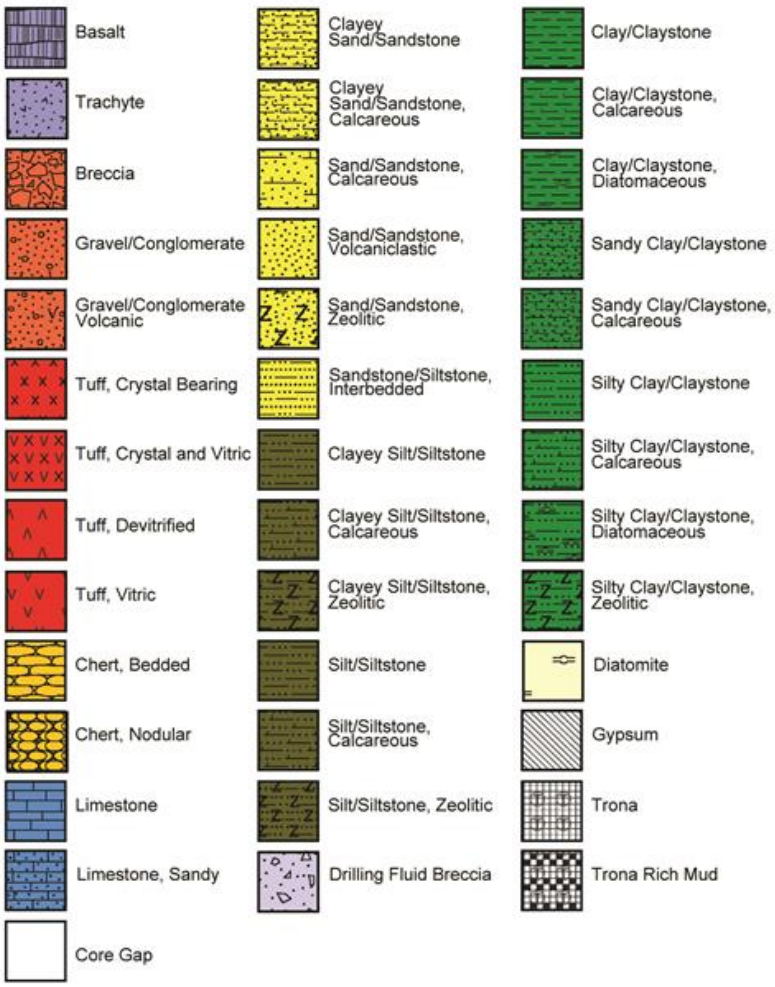

Figure 5 Key to lithological symbols (Cohen et al., 2016)

3.2 Zeolite facies

Although occurrences are variable, facies have been identified for the following zeolite mineral groups up-section, respectively: phillipsite, clinoptilolite-heulandite, chabazite, and analcime. Although other zeolite minerals such as wairakite, natrolite, and mordenite are also found throughout the core, these minerals are subordinate to the other major zeolties, and so are grouped into the facies stated according to their framework type and dominant extra-framework cation (DEC).

3.2.1 Phillipsite facies

Phillipsite is identified in 105 samples and is the most abundant zeolite found in Tugen Hills core material through X-ray diffraction. The phillipsite facies dominates the lower 130m of the core. Phillipsite is also observed in other facies, such as co-occurring with diatomaceous material and other zeolites. A return of the phillipsite facies occurs at the interval 113.35-123.82mbs after clinoptilolite first appears, associated with the deepest observed diatomite (Kingston et al., 2007) and again 67.56-65.50mbs, above which the analcime and chabazite facies dominate (Figure 4). XRD, SEM, and EDS indicate that phillipsite-K is the dominant form of phillipsite in these deposits (Figure 6).

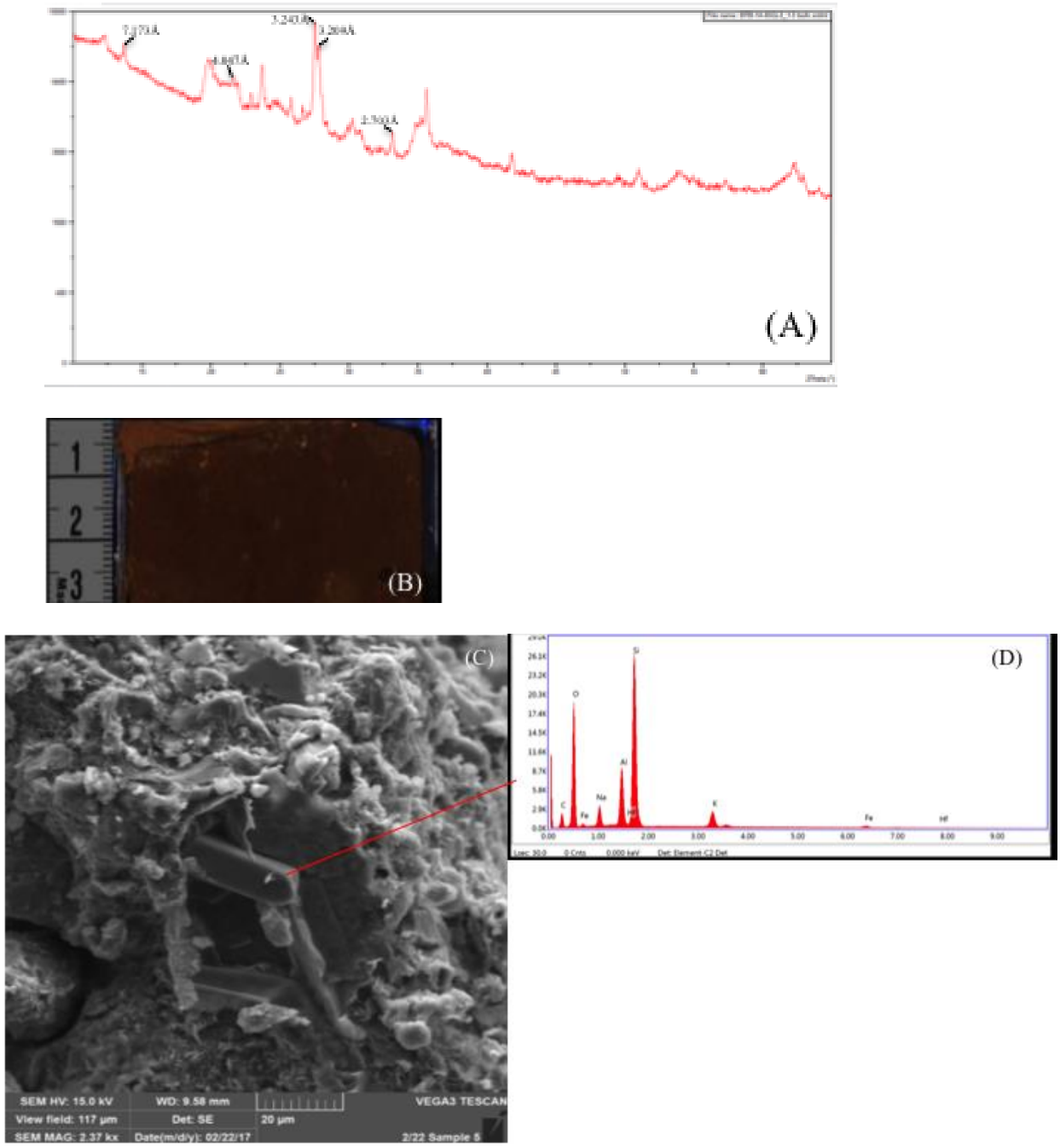

Figure 6 Analysis of philipsite-bearing sample BTB-1A-65Q-2_1-3 (187.73 mbs): (A) diffractogram showing peaks labeled with respective d-spacings, (B) core image described as "orange-brown mottled bioturbated silty clays, some relict bedding, almost completely overprinted pedogenic processes with scattered carbonate nodules, near shore facies

depositional environment" (C) SEM image depicting rectangular phillipsite crystals within a clay matrix, (D) EDS spectrum of phillipsite showing the chemical composition with cations K and Na, major elements of silicate framework Si, O, and Al, trace amounts of Fe, Hf, and C identified in reading attributable to the instrument error and carbon coating process for sample preparation.

3.2.2 Clinoptilolite-heulandite facies

At ~128 mbs, the basal phillipsite facies transitions to the overlying clinoptilolite facies, associated with an interval of the diatomite facies. Although different species of clinoptilolite and heulandite are difficult to distinguish through X-ray diffraction alone, slightly varying diffractogram peaks throughout the core suggest both minerals occur at various depths (Figure 7). Clinoptilolite-heulandite underlies the analcime (110.88-113.8mbs) and chabazite (100.56-101.64mbs) facies as and co-occurs with all major zeolites and diatom-rich intervals.

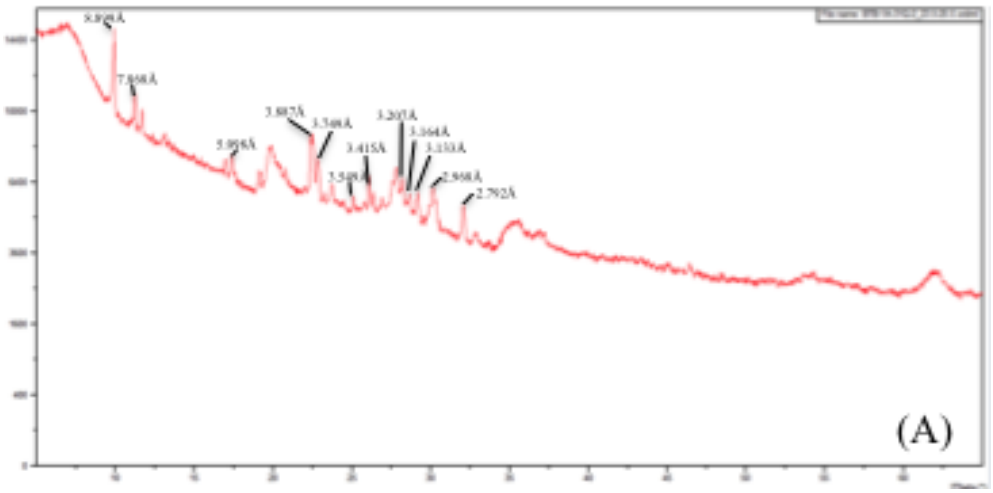

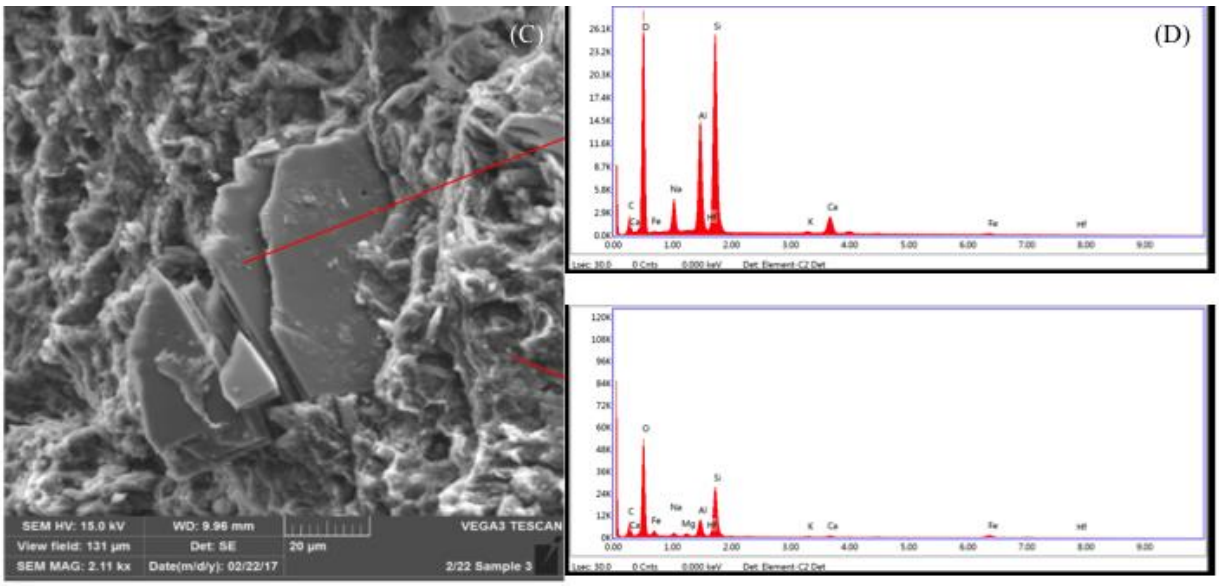

Figure 7 Analysis for heulandite-bearing sample BTB-1A-31Q-2_23.5-25.5 (87.48 mbs): (A) diffractogram showing peaks labeled with respective d-spacings, (B) core image described as "medium brown, medium grain sands, disconformably overlies finegrained lacustrine unit below due to loss of intermediate bedding by channeling and cross cutting represented by this sandy unit, (C) SEM image depicting tabular heulandite crystal fragments in a clay matrix, (D) EDS of heulandite with Ca and Na DEC with trace K and Fe (top) and Al-rich clay with trace Na, Mg, Fe, K, and Ca (bottom).

3.2.3 Chabazite facies

The majority of core material samples containing chabazite also contain other zeolite minerals, most notably, but not exclusively, analcime, clinoptiolite, and phillipsite. The chabazite facies begins at approximately 101mbs and is often interbedded with the analcime facies showing intermittent and simultaneous occurrences of both minerals. The termination of the chabazite facies is interbedded with the analcime facies in the interval between diatomites 4 & 5 in the range 13.33-14.44mbs. The chabazite facies is the least extensive with 23 identified

samples spanning approximately 87m throughout the core. SEM and EDS analyses identify chabazite associated with Al-rich clay (Figure 8).

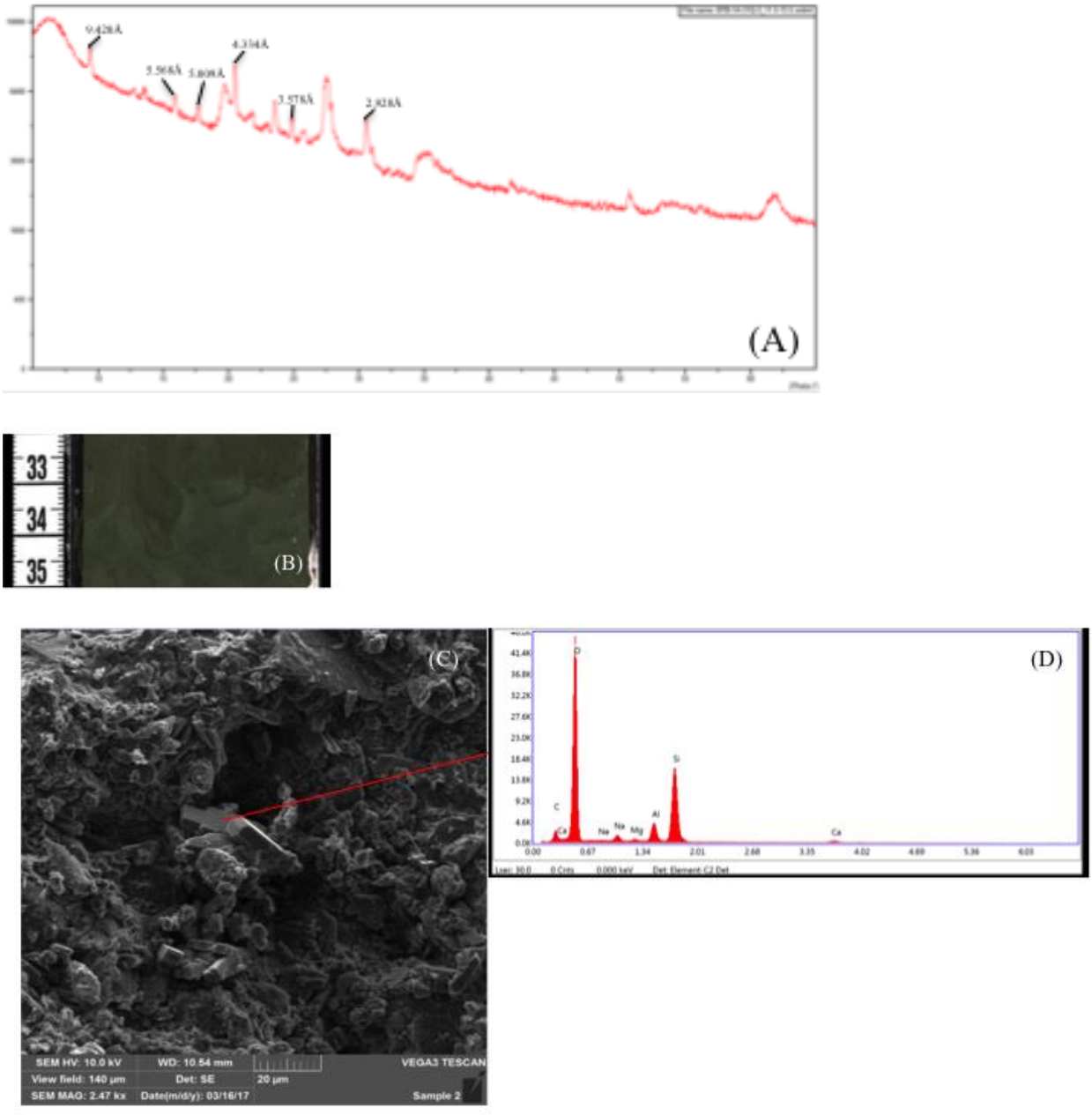

Figure 8 Analysis for chabazite-bearing sample BTB-1A-23Q-1_33.5-35.5 (64.83 mbs): (A) diffractogram showing peaks labeled with respective d-spacings, (B) core image described as "greenish-grey silts and fine sands, generally not well bedded, excellent evidence of soft

sediment deformation (possibly earthquake liquefaction events), few scattered laminae of coarse material, some calcite nodules, vivid green appears to mean weathered volcanic glass (C) SEM image showing cubic chabazite crystals among clay and possibly weathered wairakite, (D) EDS analysis describing the chemistry of chabazite containing Ca and Na with trace Mg.

3.2.4 Analcime facies

The Na-dominated analcime facies is the second most abundant in the BTB core. Although sharing a similar depth range with chabazite, spanning approximately 88m, the analcime facies is four times as common with 99 samples identified. Samples belonging in this facies contain mostly analcime with minor other related zeolites such as wairakite and natrolite. Wairakite shares a structure type with analcime although having Ca as the DEC, whereas natrolite shares Na as the respective DEC while belonging in a different structure type than analcime. X-ray diffraction evidence of high zeolite crystallinity is attributable to the abundance of euhedral analcime visible through SEM imagery (Figure 9). Although work is underway to examine the clay mineralogy in more detail, elevated levels of Mg relative to other observed intervals studied through EDS analyses suggests Mg-rich clay occurring with analcime at 81.81mbs in sample BTB-1A-28Q-1_141.5-143.5 (Figure 9). This facies onset occurs within the early clinoptilolite-heulandite facies and immediately above the termination of a phillipsite facies interval between 110.88-113.35mbs.

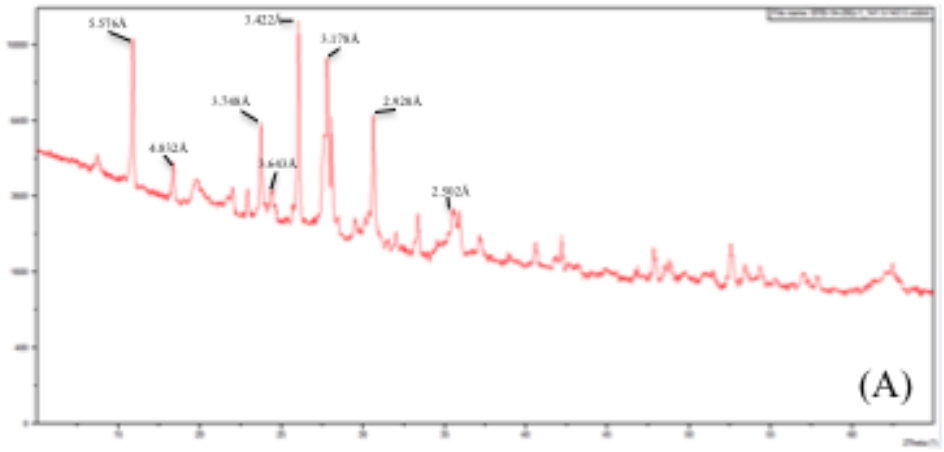

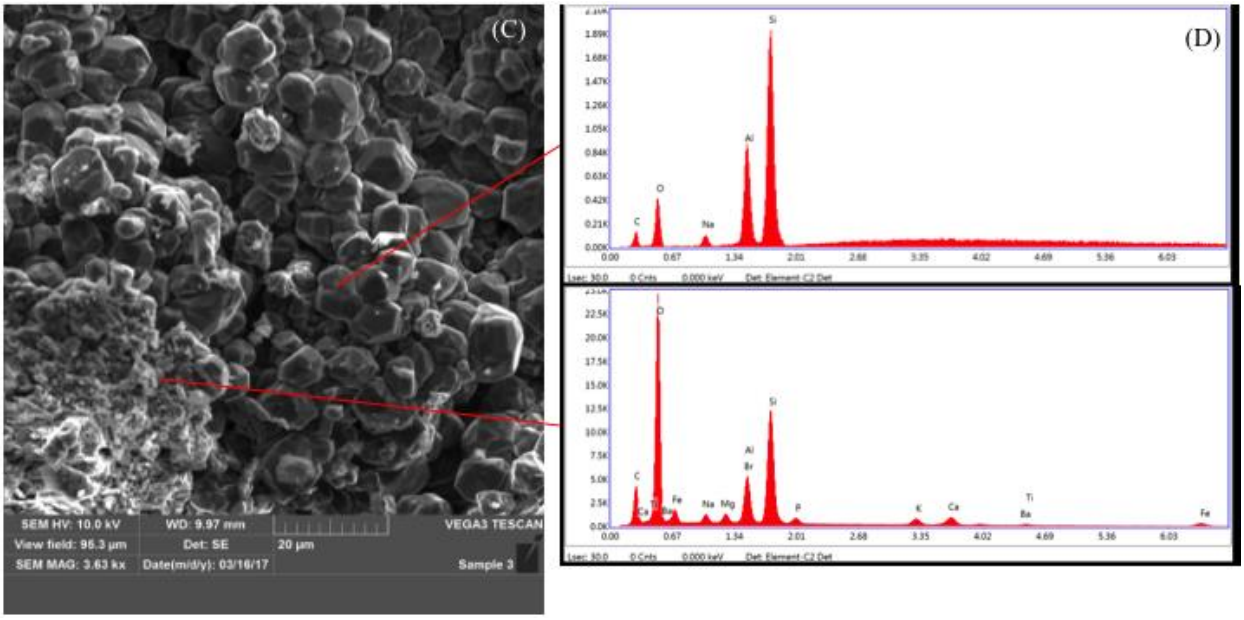

Figure 9 Analysis for analcime-bearing sample BTB-1A-28Q-1_141.5-143.5 (81.18 mbs): (A) diffractogram showing peaks labeled with respective d-spacings, (B) core image described as "dark black-grey course sand matrix, poorly sorted, small clasts, huge lithic fragments emplaced in matrix, some carbonate nodules indicative of poorly developed paleosols,

bedding with some bands of coarse grained material and some beds of grey and brown finer grained materials, bioturbation and mixed up bedding depositional environment, lithic zones most likely subaerial (C) SEM imagery depicting euhedral analcime crystals with clays, (D) EDS of analcime (top) occurring with clays consisting of Mg, Na, Ca, Fe, Ba, Ti, and P (bottom).

3.2.5 Diatomite facies

Diatomaceous material can be found throughout the majority of the top 50m of the core as well as a deeper interval around ~130mbs. The diatomites are typically zeolite-free intervals that only contain detrital clay mineral assemblages and opaline silica represented by diffuse diffraction peaks. In some cases diatomaceous sediments co-occur with all major zeolites at various depths. The deepest diatomite (~132-128mbs) marks the beginning of the first facies transition up-section with the occurrence of clinoptilolite at 129.05mbs at the top of the phillipsite facies. The remaining diatomites, termed diatomites 1-5 by Kingston et al. 2007, span approximately ~40.94m throughout the upper section of the core as mostly zeolite-free zones, with the exception of diatomites 1 and 2 existing in transitional facies associations. Diatomite 1 contains phillipsite, clinoptiolite-heulandite, chabazite, and analcime from samples observed throughout 53.27-50.07mbs. Phillipsite and chabazite are observed at 42.52mbs in diatomite 2.

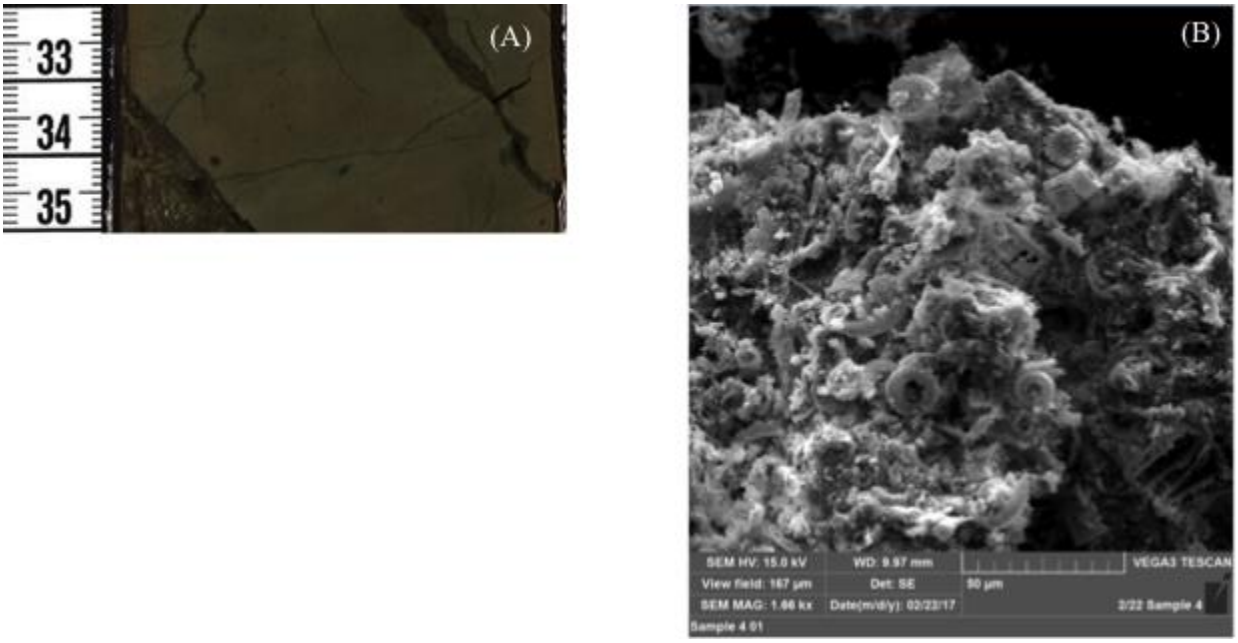

Figure 10 (A) Core and (B) SEM images from diatomite bearing sample BTB-45Q-1_33.5-35.5 (128.81 mbs).

4 DISCUSSION

4.1 Geochemical evolution of the Lake Baringo Basin & Paleohydrology

4.1.1 Zeolite geochemistry

Like most zeolites, volcaniclastic sediment accumulations of phillipsite, are generally alteration products replacing volcanic glass following reactions with alkaline waters. Phillipsite is found in a variety of geologic settings, but particularly in cavities of basaltic rocks replacing tuffs and abundant in deep ocean sediments (Lauf, 2014). Thermodynamic modeling of representative zeolite minerals found in saline-alkaline lakes (Figure 11A) shows phillipsite is stable at lower silica activities and is replaced by K-feldspar at elevated K+ concentrations. (Chipera and Apps, 2001). The phillipsite facies is representative for waters with relatively low Na/K ratios, such may occur in deep waters that are evaporatively enriched, but not hypersaline

(Kastner and Stonecipher, 1978; Stonecipher, 1978; Chipera and Apps, 2001; Deocampo and Jones, 2013).

Although clinoptilolite has a higher Si:Al ratio than heulandite (5.7 & 2.6, respectively), these minerals form a series and share many common identifiers, including XRD peak positions, DEC, and tetrahedral composition (Passaglia & Sheppard, 2001; Bish & Boak, 2001). These species cannot be easily distinguished based on X-ray powder diffraction alone due to difficulty in determining unit-cell parameter to changes in water content (Bish, 1984; Bish & Boak, 2001). For these reasons and for the purpose of this study, these minerals are combined into a single facies that occurs immediately after the phillipsite facies. Dominant extra-framework cations (DEC) for the series are primarily Ca-dominant, followed by Na and K, differing from the underlying phillipsite facies with DEC of K, Na, and Ca. The clinoptilolite-heulandite facies is the first transition facies between K-rich phillipsite and Na-rich Analcime, sharing properties with the basal phillipsite facies associated with deep-water conditions (Kastner & Stonecipher, 1978; Stonecipher, 1978; Chipera & Apps, 2001). The introduction of this facies suggests drastic environmental change with fluctuations to chabazite, analcime, and phillipsite facies throughout the rest of the core as represented by the sudden variations in mineralogy.

Chabazite is one of the most widespread natural zeolites with a variety of reported occurrences, such as vugs from plutonic rocks, volcanic, and metamorphic rocks, as well forming with association of many other zeolites, including, but not limited to analcime, heulandite-clinoptilolite, mordenite, and phillipsite (Passaglia & Sheppard, 2001). Sedimentary chabazite occurs in pyroclastic rocks diagentically altered in continental environments in both open and closed systems where it coexists with analcime, phillipsite, clinoptilolite-heulandite,

mordenite, and clay minerals (Passaglia & Sheppard, 2001). Chabazite shares DEC with the underlying clinoptilolite-heulandite facies Ca, Na, & K.

The analcime facies abundance and occurrence intervals throughout the core are suggestive for the highest concentration of brines and lack of availability of remaining non-Na cations. Regardless of silica saturation, analcime occurrence is dependent on Na availability relative to K & Ca.

Zeolite mineral assemblages are identified as varying facies occurring throughout the core. The behavior and pattern of these assemblages observed can be placed into distinct "zones" or certain depth intervals sharing similar variation in zeolite facies. Coupled with a geochemical stability diagram for zeolites occurring in saline-alkaline lacustrine systems, adapted from Chipera and Apps 2001, these zones are able to identify the geochemical history of the paleolake through K/Ca and Na/Ca ratios (Figure 11). Figure 11A shows zones depicted as color coded circles and numbers that illustrate the extent of the geochemistry of the paleolake. The range of stabilities for each mineral allows for identification of the geochemical history of paleolake waters through zones as a mineralogical approach at a terrestrial climate proxy.

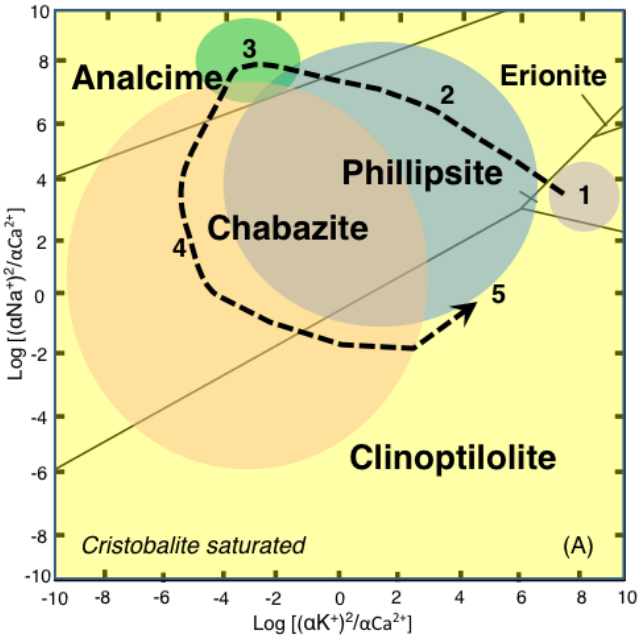

Zone 1 – Phillipsite primarily, w/ diatomite (116.12 – 227mbs)
Zone 2 – All zeolites, no diatomite (87.72 - 116.12mbs)
Zone 3 – Analcime only (70.18 - 87.72mbs)
Zone 4 – Zeolites w/o phillipsite (51.41 - 70.18mbs)
Zone 5* – All major facies, w/ diatomite (5.26 – 51.41mbs)

*Plots identically to Zone 2 (only difference is diatomite occurrence)

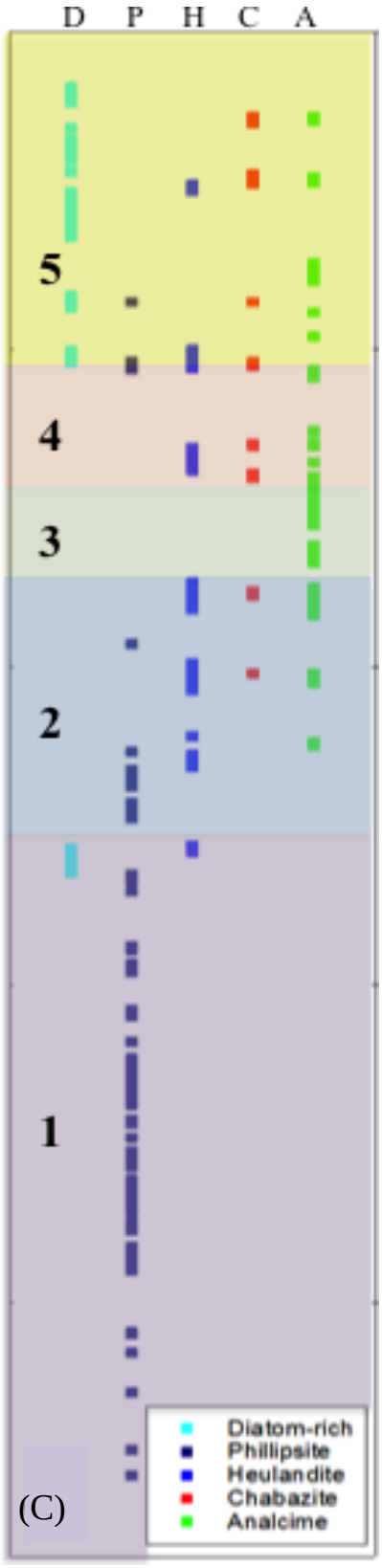

Figure 11 Thermodynamic stabilites for zeolites in saline-alkaline lake systems (modified from Chipera and Apps, 2001) with zones labeled as numbered color coded circles, (B) zone characteristics and depth, and (C) zones imposed over facies distribution plot

The largest zone, Zone 1, occupies nearly the entire lower half of the observed core spanning 111.18m (116.12-227.3mbs) with primarily the phillipsite facies. The onset of the clinoptilolite-heulandite facies occurring with the deepest diatomite around 129mbs is also present in zone 1. Zone 1 appears to be most geochemically stable interval until the diatomite occurrence at, reflecting indicators suggestive of environmental change. Zone 2 shows more variation in geochemical activity with all major zeolite facies occurring in the interval 87.72-116.12mbs, without diatom-rich material being observed. Zone 3 is similar to zone 1 for having a singular zeolite facies occupy a significant depth interval (70.18-87.72mbs) without the other major facies. Analcime is the only zeolite observed in zone 3; Na enrichment through depletion of Ca & K suggested by an absence of all other major facies indicative of geochemically stable conditions. The chabazite and clinoptilolite-heulandite facies are reintroduced in zone 4 (51.41-70.18mbs) without the phillipsite and diatomite facies. All major facies are observed in the top 49.15m of the core in Zone 5 (5.26-51.41mbs), including the Barsemoi diatomites (Deino et al., 2006; Kingston et al., 2007). A path can be constructed when coupling zones with the geochemical stabilities of the major zeolites, as seen in Figure 10. The lower part of the core can be interpreted as K-rich and Ca-poor with very high K/Ca and moderately high Na/Ca ratios, where the path begins on the K saturated boundary of the diagram. Traveling up-section through the core can be also observed as increasing Na/Ca and decreasing K/Ca with zones 2 and 3. Na/Ca decreases in zone 4 until the phillipsite facies reoccurrence in zone 5 with increasing K/Ca and Na/Ca.

The overall observed trend in mineralogy up-section, containing periods of increasing and decreasing Na/Ca and K/Ca ratios, depicts cyclical behavior in the paleolake basin geochemistry. The primary forcing of sediment flux may be attributed to either climatic or

tectonic sources, though climatic hypothesizes are being tested through these studies (Kingston et al., in review).

4.1.2 Paleohydrology

Geochemical evolution observed through mineralogical trends found in core material has the ability to be indicative of paleohydrological behavior in response to suggested climatic changes. The pattern created by zoning reflects increasing concentrations and compositional changes of surface and groundwater brines, along with increasing distance from sediment sources (Sheppard & Gude, 1968; Cohen, 2003). This allows analcime observed in core material to provide insights into the paleohydrological conditions of the lake using analcime occurrence as an indicator of increased salinity due to higher concentration of brines.

Paleolake Baringo is thought to have experienced salinity fluctuations based on zeolite facies intervals with representative DEC trending upsection from K-dominated to Na-dominated (Figure 11). The phillipsite facies can be observed during intervals of relatively deeper, fresher conditions with higher P/E ratios, with K+ mostly remaining in solution and not precipitating into authigenic minerals such as authigenic illite or K-feldspar (Hover and Ashley, 2002; Deocampo and Jones, 2013). The extent of the paleolake, inferred by cation availability recorded through zeolite occurrence, is able to determine the lake basin-type as well as salinity (Caroll & Bohacs, 1999).

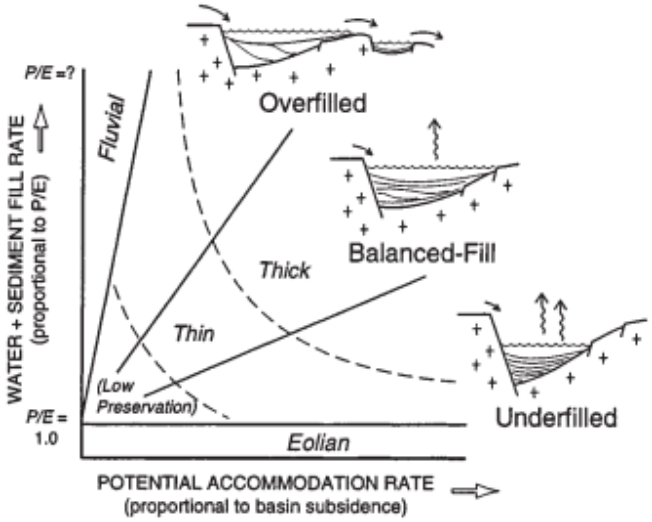

Figure 12 Ancient Lake Classification System (Carroll and Bohacs, 1999)

4.2 Implications for paleoclimate

Past climate reconstruction studies for Tugen Hills (Renaut et al., 2000; Ashley et al., 2006; Deino et al., 2006; Kingston et al., 2007; Trauth et al., 2010; Wilson et al., 2014) have been based on outcrops found along the lake margins and are not as continuous as the core material recovered through the HSPDP campaign. The Barsemoi diatomites in the upper portion of the core indicate that periods of deep-water conditions were associated with extreme wet/dry cycles, orbitally forced by precession at a time of peak eccentricity (Deino et al., 2006; Kingston et al., 2007). Regional paleoclimate studies for East Africa support claims of variability caused by orbital forcing through statistical methods and are removing inconsistencies between marine and other terrestrial records (deMenocal, 1995; Trauth et al., 2009).

The paleoclimate interpretation of Eastern Africa using mineralogical methods yields the important factor of variability. The occurrence in depth of authigenic zeolite mineral facies proxy as indicators recording sediment geochemistry changes through time. A perspective when observing the core in its entirety can lead to the conclusions of an up-section increase in aridity

from the increase in alkaline minerals and salinity. The Na/Ca increase is clearly noted through zone 3 as well as an overall abundance of the analcime facies. However, a single facies occurrence cannot determine climate conditions on its own. Facies are indicative of the sedimentary environment through the mineralogical scope at regional scales, but the zonation of facies' occurrence in depth and the variation of assemblages provide helpful information for determining the paleoenvironmental conditions.

While aridity intervals occur more frequently up-section, higher variability increases as well; especially in the intervals surrounding the diatomite facies. Ca is often below detection limits in saline-alkaline lake systems due to its removal through sulfates and carbonates, while Na and K can reach high concentrations (Chipera & Apps, 2001). Ca-dominant zeolites, such as chabazite, clinoptilolite, and heulandite, may be identified in the core as transitional periods indicating rapid environmental change from K-rich phillipsite to Na-rich analcime. The sequence of the Barsemoi diatomites, indicating humid climates with deep lake levels, contradicts the overall trend of aridity increase when only noting the Na/Ca ratio increase with the analcime facies. Singular trends in mineralogy are not strong enough to understand the overview of climatic behavior, although the spatial relationship and variability between facies may be suggestive of less stable conditions with more environmental change. Zones 2, 4, and 5 can be indicative of episodes experiencing changes in the environmental conditions reflected by the geochemical stabilities of the zeolite facies assemblages. Zones 1 and 3 are indicative of more stable environmental conditions; the abundance of primarily phillipsite may be interpreted as a humid period, whereas zone 3 provides insight into the increased saline conditions of the paleolake. The least stable conditions are observed from the fluctuations of zeolite facies with

the diatomite facies, suggesting rapid environmental change with varying DEC occurring simultaneously.

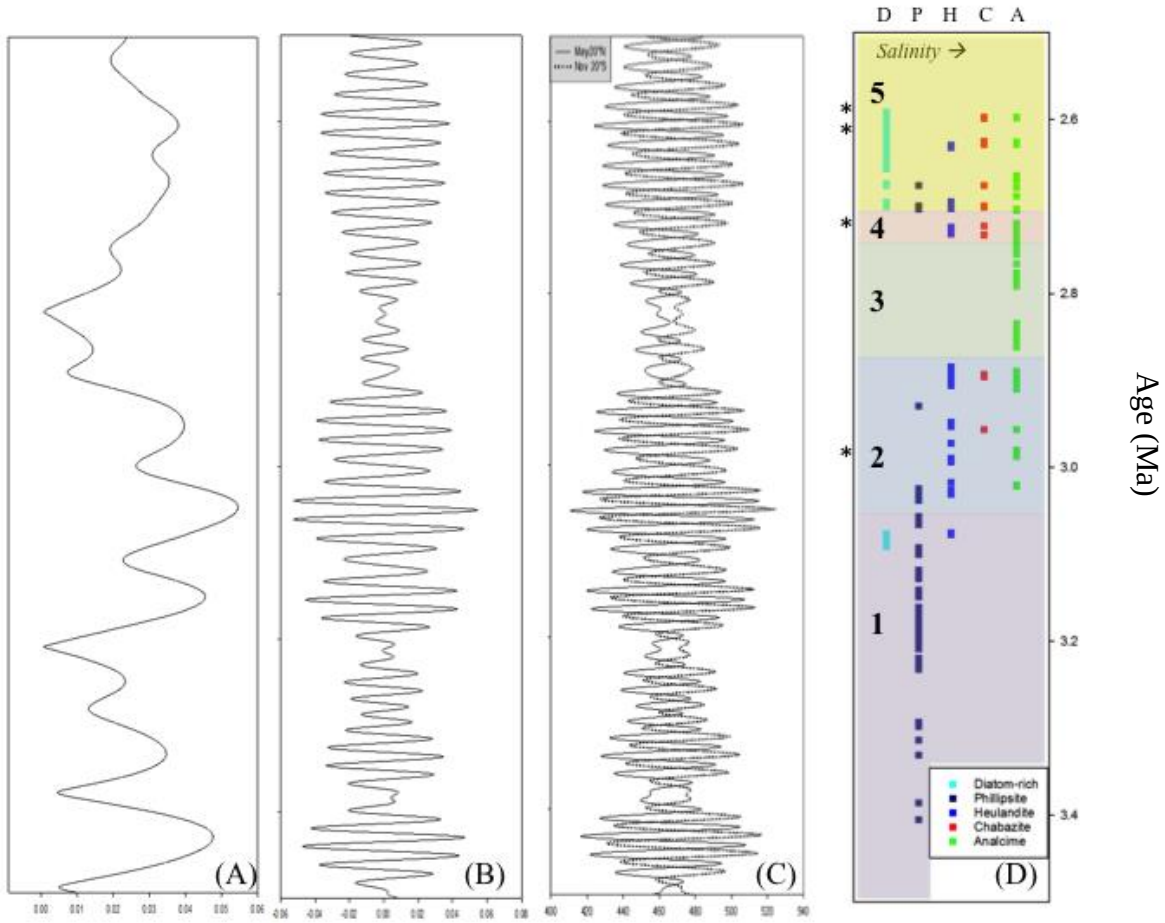

Figure 13 (A) Eccentricity, (B) precession, and (C) insolation curves (Laskar et al, 2004) compared to (D) zeolite facies occurrence plotted to age (Ma) with mineral zones shown. Dated tuff horizons (Table 3) marked as (*).

Table 3 $^{40}Ar/^{39}Ar$ tuff dates reported by Denio et al., 2006, with depth in the BTB core material using Table Interpolation age model, courtesy of Alan Deino.

Depth (mbs)	Dated Tuff Horizon Age (Ma)
5.74 – 6.23	2.587 (±0.005)
7.90 – 8.38	2.590 (±0.003)
61.62 – 62.10	2.718 (±0.005)
90.26 – 90.59	2.903 (±0.012)

Facies distribution plotted to age, rather than depth, tells nearly the same mineralogical story. The observed core holds a highly resolved stratigraphic record of the last events of the Pliocene leading to the onset of glaciation periods in the Pleistocene. The first facies transition event observed in the core, heulandite with the deepest diatomaceous material, approximately occurs during a global cooling trend around 3.07-3.09 Ma (Figure 12). The interval between the diatom-rich zones ~3.1-2.7 Ma depicts various zeolite mineral occurrences individually and simultaneously relative to other facies. Unstable conditions can be identified through periods of multiple facies such as zones 2, 4, and 5. These zones may be indicative of extensive environmental change reflected by varying lake paleochemistry. Zones 1 and 3 primarily exhibit stable environmental conditions. Zone 1 is K^+ rich being dominated by the phillipsite facies until heulandite is observed occurring with the deepest diatomite. Zone 3 is Na^+ rich with the analcime facies dominating, occurring prior to the Plio-Pleistocene boundary and the Barsemoi diatomites. Zone 3 is also a period of minimal eccentricity, precession, and insolation differences. The cyclical behavior of stable-unstable conditions might suggest rapid environmental changes recorded as events from zone transitions.

5 CONCLUSIONS

The mineralogical record observed from the HSPDP Tugen Hills drill core material holds a highly resolved stratigraphy data spanning events leading to the Plio-Pleistocene boundary (~2.58 Ma). X-ray diffraction and scanning electron microscope analyses have been used to identify the mineralogical behavior of the Baringo paleolake. The trends in zeolite mineralogy depict a pattern of stable and unstable paleoenvironmental conditions through distinct zones and facies assemblages. The lower portion of the core, zone 1, is indicative of stable environmental conditions until the transition to the clinoptilolite-heulandite facies occurring ~3.1 Ma (128mbs). The overlying zone 2 features the other major zeolite facies, clinoptilolite-heulandite, chabazite, and analcime, occurring simultaneously in the absence of diatomaceous material. Zone 3, populated primarily by the analcime facies, represents a relatively stable interval, likely with more saline lake waters. The observed interval is comparable to extensive periods of a single facies as observed in zone 1. The upper portion of the core, zones 4 and 5, represent the following period of instability and high amplitude of environmental change.

The overall trend observed in the core paleochemistry depicts a decrease in K/Ca and an increase in Na/Ca, with major fluctuations in between for facies transitions. Major environmental change recorded through mineralogy can be expressed as mineral zones, and used to infer the chemical changes in the basin.

Georgia State University is currently undergoing analysis for clay mineralogy through X-ray diffraction for selected intervals in each zone. Specific transitions observed may provide more paleoenvironmental insight through a higher resolution.

REFERENCES

Allen, D.J., Darling, W.G. 1992. Geothermics and hydrogeology of the Kenya Rift Valley between Lake Baringo and Lake Turkana. British Geology Survey Research Report SD/92/1, 39.

Ashley, G.M., Maitima Mworia, J., Muasya, A.M., Owen, R.B., Driese, S.G., Hover, V.C., Renaut, R.W., Goman, M.F., Mathai, S., Blatt, S.H. 2004. Sedimentation and recent history of a freshwater wetland in a semi-arid environment: Loboi Swamp, Kenya, East Africa. Sedimentology, 51, 1301-1321.

Ashley, G.M., Hover, Victoria, C., Driese, S.G., Roure, C.A., McBrearty, S., Owen, R.B., Renaut, R.W. 2006. A Changing Landscape in the semi-arid tropics: insights from paleosols, East Africa Rift, Kenya. Geological Society of America Abstracts with Programs, 38, 7, 531.

Amaoui, N., Hollnack, D. 2003. Neotectonics and extension direction of the Southern Kenya Rift, Lake Magadi area. Tectonophysics, 364, 71-83.

Bish, D.L. 1984. Effects of exchangeable cation composition on the thermal expansion/contraction of clinoptilolite. Clays & Clay Minerals, 32, 444-452.

Bish, D.L., Boak, J.M. 2001.Clinoptilolite-Heulandite Nomenclature, in: Bish, D.L., Ming, D.W. (Eds.), Natural Zeolites: Occurrence, Properties, Applications, The Mineralogical Society of America, Washington, DC, 45, 207-216.

Brindly, S.W., Brown, G. 1980. Crystal structure of clay minerals and their X-ray diffraction. Mineralogical Society, London.

Carroll, A.R., Bohacs, K.M. 1999. Stratigraphic classification of ancient lakes: Balancing tectonic and climatic controls. Geology, 27, 2, 99-102.

Chipera, S.J., Apps, J.A. 2001. Geochemical Stability of Natural Zeolites, in: Bish, D.L., Ming, D.W. (Eds.), Natural Zeolites: Occurrence, Properties, Applications, The Mineralogical Society of America, Washington, DC, 45, 118-161.

Campisano, C. et al. 2017. The Hominin Sites and Paleolakes Drilling Project: High-Resolution Paleoclimate Records from the East African Rift System and Their Implications for Understanding the Environmental Context of Hominin Evolution. PaleoAnthropology 2017:1-43

Chapman, G. R., Brook, M. 1978. Chronostratigraphy of the Baringo Basin, Kenya, in: Geological background to fossil man, edited by: Bishop, W. W., Scottish Academic Press, London, 207–223.

Clemens, S.C., Prell, W.L. 1991. One million year record of summer monsoon winds and continental aridity from the Owen Ridge (site 722), northwest Arabian Sea. Proceedings of the Ocean Drilling Program, Scientific Results, 117, 21, 365-388.

Cohen, A. 2003. Paleolimnology: The History and Evolution of Lake Systems. Oxford, New York. 230-231.

Cohen, A., Ashley, G.M., Potts, R., Behrensmeyer, A.K., Feibel, C., Quade, J. 2006. Paleoclimate and human evolution workshop. EOS Transactions AGU 87, 161, doi:10.1029/2006EO160008

Cohen, A., Umer, M. 2009. Connection scientific drilling and human evolution. EOS Transactions AGU 90, 122-122, doi: 10.1029/2009EO140010.

Cohen, A. et al. 2009. Understanding Paleoclimate and Human Evolution Through the Hominin Sites and Paleolakes Drilling Project, Scientific Drilling, 8, 60–65, doi:10.5194/sd-8-60-2009

Cohen, A. et al. 2016. The Hominin Sites and Paleolakes Drilling Project: inferring the environmental context of human evolution from eastern African rift lake deposits. Scientific Drilling, 21, 1-16. doi:10.5194/sd-21-1-2016.

Davies, T.D., Vincent, C.E., Beresford, A.K.C. 1985. July-August rainfall in West-Central Kenya. International Journal of Climatology, 5, 1, 17-33.

Deino, A.L., Hill, A. 2002. 40Ar/39Ar dating of the Chemeron Formation strata encompassing the site of hominin KNM-BC 1, Tugen Hills, Kenya. Journal of Human Evolution, 42, 141-151, doi: 10.1006/jhev.2001.0522.

Deino, A.L., Kingston, J.D., Glen, J.M., Edgar, R.K., Hill, A. 2006. Precessional forcing of lacustrine sedimentation in the late Cenozoic Chemeron Basin, Central Kenya Rift, and the calibration of the Gauss/Matuyama boundary. Earth and Planetary Science Letters, 247, 41-60.

Dunkley, P., Smith, M., Allen, D., Darling, W. 1993. The geothermal activity and geology of the northern sector of the Kenya Rift Valley. British Geological Survey Research Report SC/93/1, 185.

Harmand, S. et al 2015. 3.3 million year old stone tools from Lomekwi 3, West Turkana, Kenya, Nature, 521, 310–315, doi:10.1038/nature14464.

Hay, R.L. 1966. Zeolites and zeolitic reactions in sedimentary rocks. Geological Society of America Special Papers, 85, 130.

Hay, R.L. 1970. Silicate reactions in three lithofacies of a semi-arid basin, Olduvai Gorge, Tanzania. Mineralogical Society of America Special Paper, 3, 237-255.

Hay, R.L., Sheppard, R.A. 2001. Occurrence of Zeolites in Sedimentary Rocks: An Overview, in: Bish, D.L., Ming, D.W. (Eds.), Natural Zeolites: Occurrence, Properties, Applications, The Mineralogical Society of America, Washington, DC, 45, 69-104.

Hill, A. 1985. Early hominid from Baringo, Kenya. Nature, 315, 6016, 222-224.

Hill, A. 2002. Paleoanthropological research in the Tugen Hills, Kenya. Journal of Human Evolution, 42, 1-10.

Hover, V.C., Ashley, G.M. 2003. Geochemical signatures of paleodepositional and diagenetic environments: a STEM/AEM study of authigenic clay minerals from an arid rift basin, Olduvai Gorge, Tanzania. Clays and Clay Minerals, 51, 231-251.

Jansen, E., Sjoholm, J. 1991. Reconstruction of glaciation over the past 6 Myr from ice-borne deposits in the Norweigian Sea. Nature, 349, 600.

Johnson, C.R., McBrearty, S. 2010. 500,000 year old blades from the Kapthurin Formation, Kenya. Journal of Human Evolution, 58, 2, 193-200.

Kastner, M., Stonecipher, S.A. 1978. Zeolites in pelagic sediments of the Atlantic, Pacific, and Indian Oceans, in: Sand, L.B., Mumpton, F.A. (Eds.), Natural Zeolites: Occurrence, Properties, Use. Pergamon Press, New York, 199-220.

Kerrich, R., Renaut, R.W., Bonli, T. 2002. Trace-element compostion of cherts from alkaline lakes in the east African rift: a probe for ancient counterparts. SEPM Special Publication, 73, 275-294.

King, B.C. 1978. Structural and volcanic evolution of the Gregory Rift Valley. Geological Society, London Special Publications, 6, 29-54.

Kingston, J., Deino, A., Edgar, R., Hill, A. 2007. Astronomically forced climate change in the Kenyan Rift Valley 2.7-2.55 Ma: implications for the evolutions of early hominin ecosystems. Journal of Human Evolution, 53, 487-503.

Klein, C., Dutrow, B. 2007. Mineral Science, twenty-third ed. John Wiley & Sons, Inc., New Jersey.

Langella, A., Cappelletti, P., de' Gennaro, M. 2001. Zeolites in Closed Hydrologic Systems, in: Bish, D.L., Ming, D.W. (Eds.), Natural Zeolites: Occurrence, Properties, Applications, The Mineralogical Society of America, Washington, DC, 45, 235-260.

Laskar, J., Robutel, P., Joutel, F., Gastineau, M., Correia, A.C.M., Levrard, B. 2004. A long term numerical solution for the insolation quantities of the Earth. A&A, 428, 261-285. doi: 10.1051/0004-6361:20041335

Lauf, R.J. 2014. Collector's Guide to the Zeolite Group, Schiffer, Pennsylvania.

Le Turdu, C., Tiercelin, J.J., Coussement, C., Rolet, J., Renaut, R., Richert, J.P., Xavier, J.P., Coquelet, D. 1995. Basin structure and epositional patterns interpreted using a 3D remote sensing approach: the Baringo-Bogoria basins, central Kenya Rift, East Africa. Bulletin des Centre de Recherche Exploration-Production Elf-Aquitaine, 19, 1-37.

Le Turdu, C., Tiercelin, J.J., Richert, J.P., Rolet, J., Xavier, J.P., Renaut, R.W., Lezzar, K., Coussement, C. 1999. Influence of preexisting oblique discontinuities on the geometry and evolution of extension fault patterns: evidence from the Kenya Rift using SPOT imagery, in: Morley, C.K. (Ed.) Geoscience of Rift Systems – Evolution of East Africa, AAPG Studies in Geology, 44, 173-191.

McGregor, G.R., Nieuwolt, S. 1998. Tropical Climatology: An Introduction to the Climates of the Low Latitudes, 2nd Ed. John Wiley & Sons, Ltd. Chichester.

Mees, F., Stoops, G., Ranst, E.V., Paepe, R., Overloop, E.V. 2005. The Nature of Zeolite Occurences in Deposits of the Olduvai Basin, Northern Tanzania. Clay and Clay Minerals, 53, 6, 659-673.

deMenocal, P. 1995. Plio-Pleistocene African Climate. Science, 270, 5233, 53-59.

deMencocal, P., Ruddiman, W.F., Pokras, E.M. 1993. Influences of High- and Low-Latitude Processes on African Terrestrial Climate: Pleistocene Eolian Records from Equatorial Atlantic Ocean Drilling Program Site 663. Paleoceanography, 8, 2, 209-242.

Moore, D.M., Reynolds, R.C. 1989. X-ray Diffraction and the Identification and Analysis of Clay Minerals. Oxford university press, Oxford.

Nicholson, S.E. 1996. A review of dynamics and climate variability in Eastern Africa, in: Johnson, T.C., Odada, E.O. (Eds.), The Limnology, Climatology and Paleoclimatology of the East African Lakes. Gordon and Breach, Amsterdam, 25-76, 63-75.

Owen, R.B. 1981. Quaternary diatomaceous sediments and the geological evolution of lakes, Turkana, Baringo and Bogoria Kenya Rift Valley. Ph.D. dissertation, University of London, 465.

Panalytical. 2012. Introduction to PANalytical X'pert HighScore Plus v3.0. http://prism.mit.edu/xray/HighScore%20Plus%20Guide.pdf (accessed 04.05.17)

Pabalan, R.T., Bertetti, F.P. 2001. Cation-Exchange Properties of Natural Zeolites, in: Bish, D.L., Ming, D.W. (Eds.), Natural Zeolites: Occurrence, Properties, Applications, The Mineralogical Society of America, Washington, DC, 45, 69-104.

Passaglia, E., Sheppard, R.A., 2001. The Crystal Chemistry of Zeolites, in: Bish, D.L., Ming, D.W. (Eds.), Natural Zeolites: Occurrence, Properties, Applications, The Mineralogical Society of America, Washington, DC, 45, 69-104.

Rea, D.K. 1994. The paleoclimatic record provided by eolian deposition in the deep sea: The geologic history of wind. Reviews of Geophysics, 32, 2, 159-195.

Renaut, R.W., Tiercelin, J.J., Owen, R.B. 2000. Lake Baringo, Kenya Rift Valley, and its Pleistocene Precursors, in: Gierlowski-Kordesch, E.H., Kelts, K.R. (Eds.), Lake basins thorugh space and time. AAPG Studies in Geology, 46, 561-568.

Shackleton, N.J. et al. 1984. Oxygen isotope calibration of the onset of ice-rafting and history of glaciation in the North Atlantic region. Nature, 307, 620-623.

Shackleton, N.J., Berger, A., Peltier, W.R. 1990. An alternative astronomical calibration of the lower Pleistocene timescale based on ODP Site 677. Transactions of the Royal Soceity of Edinburgh: Earth Sciences, 81, 251-261.

Sheppard, R.A., Gude, A.J. 1968. Distribution and Genesis of Authigenic Silicate Minerals In Tuffs of Pleistocene Lake Tecopa, Inyo County California. Geological Survey Professional Paper 597, 24-30.

Sherwood, R. J., Ward, S. & Hill, A. 1996. Mandibular fossa anatomy of the Chemeron temporal bone (KNM-BC 1). Am. J. phys. Anthrop. Supplement 22, 214–215.

Stonecipher, S.A. 1978. Chemistry of deep-sea phillipsite, clinoptilolite, and host sediments, in: Sand, L.B., Mumpton, F.A. (Eds.), Natural Zeolites: Occurrence, Properties, Use. Pergamon Press, New York, 221-234.

Tiedemann, R., Sarnthen, M., Shackleton, N.J. 1994. Astronomic timescale for the Pliocene Atlantic $\delta^{18}O$ and dust flux record of Ocean Drilling Program site 659. Paleoceanography, 9, 4, 619-638.

Tiercelin, J.-J., Vincens, A. 1987. Le demi-graben de Baringo-Bogoria, Rift Gregory, Kenya. Bulletin des Centres de Recherces Exploration-Production Elf-Aquitaine, 11, 249-540.

Trauth, M.H., Maslin, M.A., Deino, A.L., Junginger, A., Lesoloyia, M., Odada, E.O., Olago, D.O., Olaka, L.A., Strecker, M.R., and Tiedemann, R., 2010. Human evolution in a

variable environment: The amplifier lakes of eastern Africa: Quaternary Science Reviews, 29, 2981– 2988, doi:10.1016/j.quascirev.2010.07.007.

Trauth, M.H., Larrasoana, J.C., Mudelsee, M. 2009. Trends, rhythms and events in Plio-Pleistocene African climate. Quaternary Science Reviews, 28, 5-6, 399-411.

Villmoare, B., Kimbel, W.H., Seyoum, C., Campisano, C.J., DiMaggio, E.N., Rowan, J., Braun, D.R., Arrowsmith, J.R., Reed, K.E. 2015. Early Homo at 2.8 Ma from Ledi-Geraru, Afar, Ethiopia. Science, 347, 1352–1355. doi:10.1126/science.aaa1343.

Walker, A., Leakey, R.E., Harris, J.M., Brown, F.H. 1986. 2.5-Myr Australopithecus boisei from west of Lake Turkana, Kenya. Nature, 322, 517-52, doi: 10.1038/322517a0.

Ward, S. and Hill, A. (1987), Pliocene hominid partial mandible from Tabarin, Baringo, Kenya. Am. J. Phys. Anthropol., 72: 21–37. Doi:10.1002/ajpa.1330720104.

Webster, P.J. 1987. The elementary monsoon, in: Fein, J.S., Stephens, P.L. (Eds), Monsoons. John Wiley, New York, 3-32.

Wilson, K. E., Maslin, M. A., Leng, M. J., Kingston, J. D., Deino, A. L., Edgar, R. K., Mackay, A. W. 2014. East African lake evidence for Pliocene millennial-scale climate variability, Geology, 42, 955–958.

Yuretich, R. 1982. Possible Influences upon Lake Development in the East African Rift Valleys. The Journal of Geology, 90, 3, 329-337.

APPENDIX: BULK MINERALOGY DATA

Section ID	Sampled Section Depth Top (cm)	Sampled Section Depth Bottom (cm)	Sampled MBS Top	XRD Bulk Mineralogy
HSPDP-BTB13-1A-1Q-1	1	3	5.26	Anorthoclase, anorthite, muscovite
HSPDP-BTB13-1A-1Q-1	17	19	5.42	Anorthoclase, albite, pyroxene, sanidine
HSPDP-BTB13-1A-1Q-1	33	35	5.58	Anorthoclase, sanidine, albite, diopside
HSPDP-BTB13-1A-1Q-1	49	51	5.74	Anorthoclase, albite, sanidine, pyroxene
HSPDP-BTB13-1A-1Q-1	65	67	5.9	Anorthoclase, albite, sanidine, pyroxene
HSPDP-BTB13-1A-1Q-1	81.5	83.5	6.07	Anorthoclase, abite, sanidine, muscovite
HSPDP-BTB13-1A-1Q-CC	12.5	14.5	6.23	Albite, Sanidine, Pyroxene, clays
HSPDP-BTB13-1A-2Q-1	0	2	6.6	Anorthoclase, cristobalite
HSPDP-BTB13-1A-2Q-1	16	18	6.76	Albite
HSPDP-BTB13-1A-2Q-1	32	34	6.92	Albite, Orthoclase, Anorthite
HSPDP-BTB13-1A-2Q-1	48	50	7.08	Anorthoclase, Albite
HSPDP-BTB13-1A-2Q-1	64.5	66.5	7.25	Albite, Anorthite
HSPDP-BTB13-1A-2Q-1	81	83	7.41	Na-feldspar, clays
HSPDP-BTB13-1A-2Q-1	97	99	7.57	Albite, Anorthite, Orthoclase
HSPDP-BTB13-1A-2Q-1	113	115	7.73	Albite
HSPDP-BTB13-1A-2Q-2	10	12	7.9	Anorthoclase, Tridymite(?)
HSPDP-BTB13-1A-2Q-2	26.5	28.5	8.06	Albite, Tridymite (?)
HSPDP-BTB13-1A-2Q-2	42.5	44.5	8.22	Albite, Orthoclase, organics
HSPDP-BTB13-1A-2Q-2	58.5	60.5	8.38	Albite, Orthoclase, Anorthite
HSPDP-BTB13-1A-2Q-2	75	77	8.55	Albite, muscovite, clay
HSPDP-BTB13-1A-2Q-2	90	92	8.69	Bytownite, tridymite, quartz, magnetite
HSPDP-BTB13-1A-2Q-2	100	102	8.73	Albite, tridymite, cristobalite
HSPDP-BTB13-1A-2Q-CC	8	10	8.97	Na-feldspar, tridymite
HSPDP-BTB13-1A-3Q-1	5	7	9.745	Dolomite
HSPDP-BTB13-1A-3Q-1	16.5	18.5	9.82	Mg-calcite
HSPDP-BTB13-1A-3Q-1	32.5	34.5	9.98	Palygorskite, dolomite
HSPDP-BTB13-1A-3Q-1	49	51	10.14	Bentonite?
HSPDP-BTB13-1A-3Q-1	58	60	10.16	Mg-calcite, Magnetite/Franklinite?
HSPDP-BTB13-1A-3Q-1	81	83	10.46	Muscovite, K-spar, Dolomite, Mg-calcite
HSPDP-BTB13-1A-3Q-1	97	99	10.62	Albite, Mg-Calcite
HSPDP-BTB13-1A-3Q-1	113	115	10.78	Muscovite, Albite, Pyroxene, Anorthite, K-spar
HSPDP-BTB13-1A-3Q-1	129	131	10.94	Muscovite, albite, orthoclase

HSPDP-BTB13-1A-3Q-1	145	147	11.1	Anorthoclase, Zeolite?
HSPDP-BTB13-1A-4Q-1	2	4	12.73	Albite, Anorthite
HSPDP-BTB13-1A-4Q-1	16	18	12.85	Anorthoclase, Albite, muscovite, sanidine, gypsum
HSPDP-BTB13-1A-4Q-1	32	34	13.01	Albite, Chabazite?
HSPDP-BTB13-1A-4Q-1	48	50	13.17	Albite, Orthoclase, zeolites?
HSPDP-BTB13-1A-4Q-1	64	66	13.33	Albite, muscovite, sanidine, diopside, natrolite, chabazite
HSPDP-BTB13-1A-4Q-1	80	82	13.49	Anorthoclase, Albite, Sanidine
HSPDP-BTB13-1A-4Q-1	95	97	13.63	Pyroxene, albite, anorthite, sanidine
HSPDP-BTB13-1A-4Q-2	15	17	13.82	Albite, sanidine, anorthite
HSPDP-BTB13-1A-4Q-2	31	33	13.98	Pyroxene, albite, analcime
HSPDP-BTB13-1A-4Q-2	47	49	14.14	Albite, anorthite, sanidine, gypsum
HSPDP-BTB13-1A-4Q-2	63	65	14.3	Anorthoclase, musocivte, albite
HSPDP-BTB13-1A-4Q-2	78	80	14.44	Albite, pyroxene, chabazite?
HSPDP-BTB13-1A-4Q-2	95	97	14.62	Albite, pyroxene, k-spar
HSPDP-BTB13-1A-4Q-2	111	113	14.78	Anorthoclase, albite, anorthite, sanidine
HSPDP-BTB13-1A-4Q-2	127	129	14.94	Albite, andesine, muscovite
HSPDP-BTB13-1A-4Q-2	143	145	15.1	Anorthoclase, Zeolite?
HSPDP-BTB13-1A-4Q-CC	5	7	15.175	Anorthoclase, Albite, K-spar, Muscovite
HSPDP-BTB13-1A-5Q-1	0.5	2.5	15.75	Anorthoclase, albite, sanidine, Mg-calcite
HSPDP-BTB13-1A-5Q-1	17	19	15.91	Anorthoclase, Albite, Pyroxene, K-spar, Muscovite
HSPDP-BTB13-1A-5Q-1	33.5	35.5	16.08	Anorthoclase, sanidine, clays
HSPDP-BTB13-1A-5Q-1	49.5	51.5	16.24	Albite, muscovite, andesine, mg-calcite
HSPDP-BTB13-1A-5Q-1	65.5	67.5	16.4	Albite, sanidine, sillimanite, pyroxene
HSPDP-BTB13-1A-5Q-1	81.5	83.5	16.56	Anorthoclase, sillimanite
HSPDP-BTB13-1A-5Q-1	97.5	99.5	16.72	Calcite, Anorthoclase
HSPDP-BTB13-1A-5Q-2	3	5	16.88	Qtz, Zeolite?
HSPDP-BTB13-1A-5Q-2	22	24	17.1	Anorthoclase, bytownite, orthoclase
HSPDP-BTB13-1A-5Q-2	35	37	17.2	Orthoclase, pyroxene, albite, calcite
HSPDP-BTB13-1A-5Q-2	51	53	17.36	Albite, orthoclase, mg-calcite
HSPDP-BTB13-1A-5Q-2	59	61	17.44	
HSPDP-BTB13-1A-5Q-2	67.5	69.5	17.53	Muscovite, quartz, clay
HSPDP-BTB13-1A-5Q-2	82	84	17.655	Anorthoclase
HSPDP-BTB13-1A-5Q-2	102	104	17.895	
HSPDP-BTB13-1A-5Q-CC	8	10	18	
HSPDP-BTB13-1A-6Q-1	2	4	18.83	Plag-Na, Qtz
HSPDP-BTB13-1A-6Q-1	16	18	18.95	Albite, Tridymite, Titanite
HSPDP-BTB13-1A-6Q-1	32	34	19.11	Muscovite, sanidine
HSPDP-BTB13-1A-6Q-1	48	50	19.27	Anorthoclase, muscovite

HSPDP-BTB13-1A-6Q-1	64	66	19.43	Muscovite, albite
HSPDP-BTB13-1A-6Q-1	78	80	19.55	Muscovite, Albite, K-spar
HSPDP-BTB13-1A-6Q-1	94	96	19.71	Albite, cristobalite
HSPDP-BTB13-1A-6Q-1	112	114	19.91	Albite
HSPDP-BTB13-1A-6Q-1	130	132	20.11	Mont, kspar
HSPDP-BTB13-1A-6Q-CC	7	9	20.23	Anorthoclase
HSPDP-BTB13-1A-7Q-1	4	6	21.92	Kspar, mont
HSPDP-BTB13-1A-7Q-1	16	18	22	Kspar, mont
HSPDP-BTB13-1A-7Q-1	32	34	22.16	Kpar, mont
HSPDP-BTB13-1A-7Q-1	51	53	22.38	Enstatite, albite, chabazite
HSPDP-BTB13-1A-7Q-1	64	66	22.48	Albite, chabazite, clay
HSPDP-BTB13-1A-7Q-1	80.5	82.5	22.65	Albite, chabazite, tridymite, magnesioferrite, mont
HSPDP-BTB13-1A-7Q-1	96.5	98.5	22.81	Albite, analcime, calcite, tridymite
HSPDP-BTB13-1A-7Q-1	112.5	114.5	22.97	Anorthite, kspar, analcime, mont
HSPDP-BTB13-1A-7Q-1	128.5	130.5	23.13	
HSPDP-BTB13-1A-7Q-2	2	4	23.29	Albite, anorthite, mont
HSPDP-BTB13-1A-7Q-2	19	21	23.47	Enstatite, albite, vermiculite
HSPDP-BTB13-1A-7Q-2	34	36	23.61	Albite, enstatite, analcime, vermiculite
HSPDP-BTB13-1A-7Q-2	50	52	23.77	Albite, enstatite, analcime, vermiculite, chabazite
HSPDP-BTB13-1A-7Q-2	66	68	23.93	Albite, chabazite, clay
HSPDP-BTB13-1A-7Q-2	82	84	24.09	Anorthoclase, clinoptilolite, mont
HSPDP-BTB13-1A-7Q-2	98	100	24.25	Anorthoclase, kspar, heulandite
HSPDP-BTB13-1A-7Q-2	114	116	24.41	Anorthoclase, clinoptilolite, mont
HSPDP-BTB13-1A-7Q-CC	8	10	24.65	Kspar, clinoptilolite, mont
HSPDP-BTB13-1A-8Y-1	10	12	25.075	Albite, heulandite, tridymite
HSPDP-BTB13-1A-8Y-1	20	22	25.065	Albite, clinoptilolite, vermiculite
HSPDP-BTB13-1A-8Y-1	38.5	40.5	25.22	Anorthoclase, vermiculite (?)
HSPDP-BTB13-1A-9Y-1	4.5	6.5	25.38	Anorthoclase, cristobalite
HSPDP-BTB13-1A-9Y-2	16	18	25.655	Albite, mont
HSPDP-BTB13-1A-9Y-2	28	30	25.71	Paragonite, vermiculite
HSPDP-BTB13-1A-9Y-2	45.5	47.5	25.87	Albite, mont
HSPDP-BTB13-1A-9Y-2	63	65	26.03	Albite, enstatite, muscovite
HSPDP-BTB13-1A-9Y-2	80.5	82.5	26.19	Albite, anorthite, tridymite
HSPDP-BTB13-1A-9Y-2	96	98	26.31	Albite, mont
HSPDP-BTB13-1A-9Y-2	115.5	117.5	26.51	Albite, mont
HSPDP-BTB13-1A-9Y-3	3	5	26.67	
HSPDP-BTB13-1A-9Y-3	20.5	22.5	26.83	Kspar, diopside, tridymite
HSPDP-BTB13-1A-9Y-3	38	40	26.99	Albite, mont
HSPDP-BTB13-1A-9Y-3	55.5	57.5	27.15	Albite

HSPDP-BTB13-1A-9Y-3	73	75	27.31	Albite, mont
HSPDP-BTB13-1A-9Y-3	88	90	27.415	Albite, mont
HSPDP-BTB13-1A-9Y-3	98	100	27.44	Kspar, mont
HSPDP-BTB13-1A-9Y-3	113	115	27.545	Mont
HSPDP-BTB13-1A-10Y-1	8	10	28.01	Kspar, mont
HSPDP-BTB13-1A-10Y-1	22	24	28.13	Kspar, mont
HSPDP-BTB13-1A-10Y-1	37.5	39.5	28.28	
HSPDP-BTB13-1A-10Y-1	50	52	28.365	Albite, mont
HSPDP-BTB13-1A-10Y-1	69.5	71.5	28.6	Albite, cristobalite
HSPDP-BTB13-1A-10Y-1	85.5	87.5	28.76	
HSPDP-BTB13-1A-10Y-1	101.5	103.5	28.92	
HSPDP-BTB13-1A-10Y-1	117.5	119.5	29.08	Paragonite, albite, clay
HSPDP-BTB13-1A-10Y-1	133.5	135.5	29.24	
HSPDP-BTB13-1A-10Y-2	3	5	29.445	Kspar, mica
HSPDP-BTB13-1A-10Y-2	23.5	25.5	29.69	Mica, clay
HSPDP-BTB13-1A-10Y-2	32.5	34.5	29.71	Mica, faujasite
HSPDP-BTB13-1A-10Y-2	48.5	50.5	29.87	Anorthoclase, mont
HSPDP-BTB13-1A-10Y-2	64.5	66.5	30.03	Anorthoclase, mont
HSPDP-BTB13-1A-10Y-2	80.5	82.5	30.19	
HSPDP-BTB13-1A-10Y-2	97	99	30.365	
HSPDP-BTB13-1A-10Y-2	112.5	114.5	30.51	Anorthoclase, magnesioferrite, mont
HSPDP-BTB13-1A-10Y-2	127	129	30.645	Paragonite, faujasite
HSPDP-BTB13-1A-10Y-2	144	146	30.825	Anorthoclase
HSPDP-BTB13-1A-11Y-1	6	8	31.02	Kspar, mica
HSPDP-BTB13-1A-11Y-1	21.5	23.5	31.16	Kspar, mont
HSPDP-BTB13-1A-11Y-1	38	40	31.33	
HSPDP-BTB13-1A-11Y-1	54.5	56.5	31.49	
HSPDP-BTB13-1A-11Y-1	71	73	31.65	Kspar, tridymite, mont
HSPDP-BTB13-1A-11Y-1	84	86	31.745	Kspar, faujasite
HSPDP-BTB13-1A-11Y-1	110	112	32.1	Blodite?
HSPDP-BTB13-1A-11Y-1	120.5	122.5	32.14	
HSPDP-BTB13-1A-11Y-1	137	139	32.31	Kspar
HSPDP-BTB13-1A-11Y-2	5	7	32.47	
HSPDP-BTB13-1A-11Y-2	21.5	23.5	32.63	
HSPDP-BTB13-1A-11Y-2	38	40	32.8	Anorthoclase, cristobalite
HSPDP-BTB13-1A-11Y-2	54.5	56.5	32.96	
HSPDP-BTB13-1A-11Y-2	71	73	33.12	
HSPDP-BTB13-1A-11Y-2	87.5	89.5	33.29	
HSPDP-BTB13-1A-11Y-2	104	106	33.45	Albite, andesine, muscovite, sanidine
HSPDP-BTB13-1A-11Y-2	120.5	122.5	33.61	
HSPDP-BTB13-1A-11Y-2	135	137	33.74	

HSPDP-BTB13-1A-11Y-CC	4.5	6.5	33.93	
HSPDP-BTB13-1A-12Y-1	10	12	34.1	
HSPDP-BTB13-1A-12Y-1	26	28	34.26	Anorthoclase, enstatite, sanidine, cristobalite
HSPDP-BTB13-1A-12Y-1	42.5	44.5	34.43	
HSPDP-BTB13-1A-12Y-1	58.5	60.5	34.59	
HSPDP-BTB13-1A-12Y-1	75	77	34.75	
HSPDP-BTB13-1A-12Y-1	91.5	93.5	34.92	
HSPDP-BTB13-1A-12Y-1	108	110	35.08	Albite, anorthite
HSPDP-BTB13-1A-12Y-1	124.5	126.5	35.25	Albite, kspar, tridymite, clay
HSPDP-BTB13-1A-12Y-1	140.5	142.5	35.41	Anorthoclase, albite, mont
HSPDP-BTB13-1A-12Y-2	6.5	8.5	35.57	Enstatite, albite, cristobalite
HSPDP-BTB13-1A-12Y-2	21	23	35.69	
HSPDP-BTB13-1A-12Y-2	39.5	41.5	35.9	
HSPDP-BTB13-1A-12Y-2	56	58	36.06	
HSPDP-BTB13-1A-12Y-2	72.5	74.5	36.23	
HSPDP-BTB13-1A-12Y-2	88.5	90.5	36.39	Kspar, analcime, Cristobalite, natron
HSPDP-BTB13-1A-12Y-2	105	107	36.55	
HSPDP-BTB13-1A-12Y-2	121.5	123.5	36.72	
HSPDP-BTB13-1A-12Y-2	138	140	36.88	
HSPDP-BTB13-1A-13Y-1	0	2	37.05	
HSPDP-BTB13-1A-13Y-1	16	18	37.21	Albite, anorthite, muscovite, sanidine, analcime
HSPDP-BTB13-1A-13Y-1	33.5	35.5	37.4	Albite, enstatite, analcime
HSPDP-BTB13-1A-13Y-1	49	51	37.54	
HSPDP-BTB13-1A-13Y-1	65	67	37.7	Albite, sanidine, enstatite, analcime
HSPDP-BTB13-1A-13Y-1	81.5	83.5	37.87	Albite, anorthite, sanidine, analcime
HSPDP-BTB13-1A-13Y-1	103	105	38.13	
HSPDP-BTB13-1A-13Y-1	114.5	116.5	38.2	Albite, enstatite, sanidine, analcime
HSPDP-BTB13-1A-13Y-1	131	133	38.36	
HSPDP-BTB13-1A-13Y-2	6.5	8.5	38.53	Anorthoclase, enstatite, sanidine, analcime
HSPDP-BTB13-1A-13Y-2	23	25	38.69	
HSPDP-BTB13-1A-13Y-2	39.5	41.5	38.86	Albite, enstatite, analcime
HSPDP-BTB13-1A-13Y-2	56	58	39.02	
HSPDP-BTB13-1A-13Y-2	72	74	39.18	Albite, sanidine, anorthite, analcime
HSPDP-BTB13-1A-13Y-2	88.5	90.5	39.35	
HSPDP-BTB13-1A-13Y-2	105	107	39.51	
HSPDP-BTB13-1A-13Y-2	121.5	123.5	39.68	
HSPDP-BTB13-1A-13Y-2	138	140	39.84	
HSPDP-BTB13-1A-14Y-1	0.5	2.5	40.11	
HSPDP-BTB13-1A-14Y-1	15	17	40.23	Albite, palygorskite, kao

HSPDP-BTB13-1A-14Y-1	42	44	40.605	Albite, kao
HSPDP-BTB13-1A-14Y-1	52.5	54.5	40.66	Muscovite, Albite, dolomite, kao
HSPDP-BTB13-1A-14Y-1	67	69	40.78	Albite, kao
HSPDP-BTB13-1A-14Y-1	86.5	88.5	41.01	Palygorskite, qtz, kao
HSPDP-BTB13-1A-14Y-1	99	101	41.09	
HSPDP-BTB13-1A-14Y-1	115.5	117.5	41.26	Quartz, palygorskite, ti-oxide, kao
HSPDP-BTB13-1A-14Y-1	131	133	41.4	Albite, kao
HSPDP-BTB13-1A-14Y-2	12	14	41.52	Albite, Palygorskiite, dolomite
HSPDP-BTB13-1A-14Y-2	31.5	33.5	41.74	Albite, palygorskite
HSPDP-BTB13-1A-14Y-2	44	46	41.835	Albite, palygorskite
HSPDP-BTB13-1A-14Y-2	62	64	42.03	Anorthite, magnesioferrite, qtz
HSPDP-BTB13-1A-14Y-2	80.5	82.5	42.23	Albite, cristobalite
HSPDP-BTB13-1A-14Y-2	97	99	42.4	
HSPDP-BTB13-1A-14Y-CC	6	8	42.52	Chabazite, Plag-Na, Phillipsite
HSPDP-BTB13-1A-15Y-1	34	36	43.47	Albite, kspar, cristobalite
HSPDP-BTB13-1A-15Y-1	52	54	43.65	Albite, enstatite
HSPDP-BTB13-1A-15Y-1	68	70	43.8	Albite
HSPDP-BTB13-1A-15Y-1	86	88	43.98	
HSPDP-BTB13-1A-15Y-1	102	104	44.13	Plag-Na, K-spar, Analcime, Zeolite?
HSPDP-BTB13-1A-15Y-1	119	121	44.29	Albite, analcime
HSPDP-BTB13-1A-15Y-1	138.5	140.5	44.505	Plag-Na, K-spar, Zeolite?
HSPDP-BTB13-1A-15Y-2	2	4	44.62	Albite, kspar
HSPDP-BTB13-1A-15Y-2	19	21	44.79	Albite, anorthite, kspar
HSPDP-BTB13-1A-15Y-2	36	38	44.95	albite, kspar, anorthite
HSPDP-BTB13-1A-15Y-2	53	55	45.12	Albite, kspar
HSPDP-BTB13-1A-15Y-2	70	72	45.28	Kspar
HSPDP-BTB13-1A-15Y-2	87	89	45.45	
HSPDP-BTB13-1A-15Y-2	104	106	45.61	Anorthite, cristobalite
HSPDP-BTB13-1A-15Y-2	121	123	45.78	
HSPDP-BTB13-1A-15Y-2	138	140	45.94	Albite, kspar, cristobalite
HSPDP-BTB13-1A-15Y-CC	2.5	4.5	46.08	Anorthoclase
HSPDP-BTB13-1A-16Q-1	7.5	9.5	46.27	Anorthoclase, K-spar, Cristobalite, Zeolite?
HSPDP-BTB13-1A-16Q-CC	3	5	46.43	Anorthoclase
HSPDP-BTB13-1A-17Q-1	0.5	2.5	46.59	Albite, palygorskite
HSPDP-BTB13-1A-17Q-1	17	19	46.76	Plag-Na, Cristobalite, K-spar, Zeolite?
HSPDP-BTB13-1A-17Q-1	33.5	35.5	46.92	Albite, mica
HSPDP-BTB13-1A-17Q-1	50	52	47.08	
HSPDP-BTB13-1A-17Q-1	66.5	68.5	47.25	Plag-Na, K-spar, Zeolite?
HSPDP-BTB13-1A-17Q-1	85	87	47.45	Anorthoclase, kspar, albite

HSPDP-BTB13-1A-17Q-1	99.5	101.5	47.57	Albite, kspar, analcime, cristobalite
HSPDP-BTB13-1A-17Q-1	117	119	47.75	
HSPDP-BTB13-1A-17Q-2	1.5	3.5	47.9	Kspar, anorthite, analcime, pyroxene
HSPDP-BTB13-1A-17Q-2	18	20	48.06	Albite, tridymite
HSPDP-BTB13-1A-17Q-2	34.5	36.5	48.22	Plag-Na, K-spar, Zeolite?
HSPDP-BTB13-1A-17Q-2	50	52	48.36	Anorthoclase, kspar
HSPDP-BTB13-1A-17Q-2	66	68	48.515	Albite, analcime, cristobalite
HSPDP-BTB13-1A-17Q-2	84	86	48.71	
HSPDP-BTB13-1A-17Q-2	100.5	102.5	48.87	
HSPDP-BTB13-1A-17Q-2	116	118	49.02	
HSPDP-BTB13-1A-17Q-2	132	134	49.165	Anorthoclase, albite, analcime, mont
HSPDP-BTB13-1A-18Q-1	10.5	12.5	49.36	Albite, kspar, analcime
HSPDP-BTB13-1A-18Q-1	27	29	49.53	Albite, gypsum, analcime
HSPDP-BTB13-1A-18Q-1	43.5	45.5	49.69	Albite, kspar, tridymite
HSPDP-BTB13-1A-18Q-1	60	62	49.85	Albite, palygorskite
HSPDP-BTB13-1A-18Q-1	79	81	50.065	Albite, clinoptilolite, tridymite
HSPDP-BTB13-1A-18Q-1	93	95	50.18	Plag-Na, K-spar, Zeolite?
HSPDP-BTB13-1A-18Q-1	109.5	111.5	50.34	Anorthoclase, clinoptilolite
HSPDP-BTB13-1A-18Q-1	126	128	50.5	Anorthoclase, Clinoptilolite, Zeolite?
HSPDP-BTB13-1A-18Q-1	142.5	144.5	50.66	Anorthoclase, Clinoptilolite
HSPDP-BTB13-1A-18Q-2	13.5	15.5	50.82	Clinoptilolite, Plag-Ca
HSPDP-BTB13-1A-18Q-2	29	31	50.97	Anorthite, clinoptilolite
HSPDP-BTB13-1A-18Q-2	50.5	52.5	51.23	Clinoptilolite, Plag-Ca
HSPDP-BTB13-1A-18Q-2	65	67	51.35	
HSPDP-BTB13-1A-18Q-2	79.5	81.5	51.47	Clinoptilolite, fe-oxide
HSPDP-BTB13-1A-18Q-2	96	98	51.64	Clinoptilolite, ti-oxide
HSPDP-BTB13-1A-18Q-2	111.5	113.5	51.78	Heulandite, rutile
HSPDP-BTB13-1A-18Q-2	129	131	51.96	Chabazite, Phillipsite, Feldspar/Zeolite?
HSPDP-BTB13-1A-18Q-2	141.5	143.5	52.04	Chabazite, analcime
HSPDP-BTB13-1A-18Q-CC	15	17	52.27	Chabazite, kspar, palygorskite
HSPDP-BTB13-1A-19Q-1	14	16	52.45	Pyroxene, anorthite, chabazite
HSPDP-BTB13-1A-19Q-1	30	32	52.61	Gypsum, chabazite, kspar
HSPDP-BTB13-1A-19Q-1	46.5	48.5	52.78	Albite, clinoptilolite, kaolinite(?)
HSPDP-BTB13-1A-19Q-1	63	65	52.94	Anorthite, clinoptilolite, cristobalite, mont
HSPDP-BTB13-1A-19Q-1	79.5	81.5	53.11	Plag-Ca, Phillipsite
HSPDP-BTB13-1A-19Q-1	95.5	97.5	53.27	Plag-Ca, Anorthoclase, Natrolite
HSPDP-BTB13-1A-19Q-1	112	114	53.43	Kspar, mg-calcite, tridymite, cristobalite
HSPDP-BTB13-1A-19Q-1	128.5	130.5	53.6	Plag-Na, K-spar, Zeolite?
HSPDP-BTB13-1A-19Q-1	143	145	53.72	Albite, diopside, vaterite
HSPDP-BTB13-1A-19Q-2	16	18	53.92	Enstatite, albite, magnetite

HSPDP-BTB13-1A-19Q-2	32	34	54.08	
HSPDP-BTB13-1A-19Q-2	50	52	54.275	Kspar, albite, analcime, gypsum
HSPDP-BTB13-1A-19Q-2	65	67	54.41	Enstatite, albite, wairakite
HSPDP-BTB13-1A-19Q-2	82	84	54.59	Plag-Na, Mg-calcite, Qtz, K-spar
HSPDP-BTB13-1A-19Q-2	97.5	99.5	54.74	Albite, anorthite, kspar
HSPDP-BTB13-1A-19Q-2	114	116	54.9	Plag-Na, K-spar
HSPDP-BTB13-1A-19Q-2	130.5	132.5	55.07	Anorthoclase, kspar, mont, cristobalite
HSPDP-BTB13-1A-19Q-CC	3	5	55.23	Plag-Na, Cristobalite, K-spar, Zeolite?
HSPDP-BTB13-1A-20Q-1	3.5	5.5	55.4	Albite, kspar, pyroxene, cristobalite
HSPDP-BTB13-1A-20Q-1	19.5	21.5	55.56	
HSPDP-BTB13-1A-20Q-1	36	38	55.72	
HSPDP-BTB13-1A-20Q-1	52.5	54.5	55.89	Pyroxene, albite, muscovite, cristobalite
HSPDP-BTB13-1A-20Q-1	70	72	56.07	Plag-Na, Cristobalite, K-spar, Zeolite?
HSPDP-BTB13-1A-20Q-1	85	87	56.21	Plag-Na, Cristobalite, K-spar, Zeolite?
HSPDP-BTB13-1A-20Q-1	101.5	103.5	56.38	Anorthoclase, anorthite
HSPDP-BTB13-1A-20Q-1	116	118	56.5	Albite, palygorskite, kspar, tridymite
HSPDP-BTB13-1A-20Q-2	15	17	56.7	Albite, kspar, palygorskite, cristobalite
HSPDP-BTB13-1A-20Q-2	31.5	33.5	56.86	Anorthoclase, albite
HSPDP-BTB13-1A-20Q-2	48	50	57.03	Albite, palygorskite, kspar
HSPDP-BTB13-1A-20Q-2	72	74	57.345	Anorthoclase, Albite, K-spar, Muscovite
HSPDP-BTB13-1A-20Q-2	81	83	57.36	Anorthoclase, albite
HSPDP-BTB13-1A-20Q-2	97	99	57.52	
HSPDP-BTB13-1A-20Q-2	113.5	115.5	57.68	Anorthoclase, cristobalite, mont
HSPDP-BTB13-1A-20Q-2	130	132	57.85	Anorthoclase, cristobalite, mont
HSPDP-BTB13-1A-20Q-3	6	8	58.01	Anorthoclase, anorthite
HSPDP-BTB13-1A-20Q-3	18	20	58.085	Albite, anorthite
HSPDP-BTB13-1A-21Q-1	0	2	58.4	Anorthoclase, kspar, mont
HSPDP-BTB13-1A-21Q-1	17.5	19.5	58.58	Anorthoclase, albite, cristobalite
HSPDP-BTB13-1A-21Q-1	33	35	58.72	Albite, palygorskite, anorthite
HSPDP-BTB13-1A-21Q-1	49.5	51.5	58.88	Albite, palygorskite, anorthite
HSPDP-BTB13-1A-21Q-1	66	68	59.04	Anorthoclase, mg-calcite, gobbinsite, cristobalite
HSPDP-BTB13-1A-21Q-1	82.5	84.5	59.2	Albite, anorthite, palygorskite, calcite, cristobalite
HSPDP-BTB13-1A-21Q-1	99	101	59.36	Albite, diopside, dolomite
HSPDP-BTB13-1A-21Q-1	115.5	117.5	59.52	Albite, diopside, cristobalite
HSPDP-BTB13-1A-21Q-1	132	134	59.68	Albite, diopside, cristobalite
HSPDP-BTB13-1A-21Q-1	148.5	150.5	59.84	Albite, anorthite, diopside
HSPDP-BTB13-1A-21Q-2	14.5	16.5	60.01	Anorthoclase, enstatite, diopside
HSPDP-BTB13-1A-21Q-2	31	33	60.17	Sanidine, orthoclase, diopside
HSPDP-BTB13-1A-21Q-2	47.5	49.5	60.33	Anorthite, Mg-Calcite, palygorskite

HSPDP-BTB13-1A-21Q-2	62	64	60.45	Anorthoclase, diopside, cristobalite
HSPDP-BTB13-1A-21Q-2	80.5	82.5	60.65	
HSPDP-BTB13-1A-21Q-2	96	98	60.79	
HSPDP-BTB13-1A-21Q-2	113.5	115.5	60.97	Anorthite, albite, enstatite
HSPDP-BTB13-1A-21Q-2	130	132	61.13	Albite, anorthite, orthoclase
HSPDP-BTB13-1A-21Q-2	144	146	61.245	Albite, anorthite, pyroxene
HSPDP-BTB13-1A-22Q-1	0.5	2.5	61.45	Anorthoclase, kspar, analcime, cristobalite
HSPDP-BTB13-1A-22Q-1	17.5	19.5	61.62	Anorthoclase, analcime, cristobalite
HSPDP-BTB13-1A-22Q-1	34.5	36.5	61.78	Albite, enstatite
HSPDP-BTB13-1A-22Q-1	51.5	53.5	61.94	Albite, anorthite, analcime
HSPDP-BTB13-1A-22Q-1	68.5	70.5	62.1	Albite, sepiolite, mg-calcite, cristobalite
HSPDP-BTB13-1A-22Q-1	85.5	87.5	62.26	Albite, muscovite, analcime, cristobalite
HSPDP-BTB13-1A-22Q-1	102.5	104.5	62.43	Albite, analcime, mg-calcite, cristobalite
HSPDP-BTB13-1A-22Q-1	119.5	121.5	62.59	
HSPDP-BTB13-1A-22Q-2	0.5	2.5	62.75	Anorthoclase, albite, analcime
HSPDP-BTB13-1A-22Q-2	17.5	19.5	62.91	Albite, enstatite, sanidine, jadeite, analcime
HSPDP-BTB13-1A-22Q-2	34.5	36.5	63.07	Enstatite, albite, analcime
HSPDP-BTB13-1A-22Q-2	51.5	53.5	63.23	
HSPDP-BTB13-1A-22Q-2	68.5	70.5	63.39	Albite, kspar, tridymite
HSPDP-BTB13-1A-22Q-2	85.5	87.5	63.56	Albitem anorthite, palygorskite
HSPDP-BTB13-1A-22Q-2	102.5	104.5	63.72	Albite, paragonite, cristobalite
HSPDP-BTB13-1A-22Q-2	119.5	121.5	63.88	Albite, paragonite, cristobalite
HSPDP-BTB13-1A-23Q-1	0.5	2.5	64.5	Albite, anorthite
HSPDP-BTB13-1A-23Q-1	17	19	64.67	Albite, palygorskite, diopside
HSPDP-BTB13-1A-23Q-1	33.5	35.5	64.83	Albite, wairakite (z), chabazite, natrolite
HSPDP-BTB13-1A-23Q-1	50	52	64.99	
HSPDP-BTB13-1A-23Q-1	66.5	68.5	65.15	Anorthoclase, chabazite, wairakite, palygorskite
HSPDP-BTB13-1A-23Q-1	83	85	65.31	
HSPDP-BTB13-1A-23Q-1	101	103	65.495	Albite, clinoptilolite
HSPDP-BTB13-1A-23Q-1	116	118	65.63	Anorthoclase, albite, kspar, palygorskite, cristobalite
HSPDP-BTB13-1A-23Q-1	132.5	134.5	65.79	anorthoclase, albite, muscovite
HSPDP-BTB13-1A-23Q-1	149	151	65.95	
HSPDP-BTB13-1A-23Q-2	12	14	66.11	Albite, clinoptilolite, quartz
HSPDP-BTB13-1A-23Q-2	28.5	30.5	66.27	Albite, clinoptilolite, quartz
HSPDP-BTB13-1A-23Q-2	45	47	66.43	
HSPDP-BTB13-1A-23Q-2	61.5	63.5	66.59	Albite, clinoptilolite, qtz
HSPDP-BTB13-1A-23Q-2	78	80	66.75	Albite, clinoptilolite
HSPDP-BTB13-1A-23Q-2	94.5	96.5	66.91	Albite, clinoptilolite, heulandite (Z)
HSPDP-BTB13-1A-23Q-2	111	113	67.07	Anorthoclase, clinoptilolite
HSPDP-BTB13-1A-23Q-2	127.5	129.5	67.23	Albite, clinoptilolite

HSPDP-BTB13-1A-23Q-2	144	146	67.39	Anorthoclase, kspar, clinoptilolite
HSPDP-BTB13-1A-24Q-1	0.5	2.5	67.56	Albite, clinoptilolite
HSPDP-BTB13-1A-24Q-1	17	19	67.72	Albite, kspar, palygorskite, analcime
HSPDP-BTB13-1A-24Q-1	33.5	35.5	67.89	Anorthoclase
HSPDP-BTB13-1A-24Q-1	49.5	51.5	68.05	Kspar, palygorskite
HSPDP-BTB13-1A-24Q-1	66	68	68.21	Paragonite, albite, qtz
HSPDP-BTB13-1A-24Q-1	82.5	84.5	68.38	Anorthoclase, cristobalite, qtz
HSPDP-BTB13-1A-24Q-1	99	101	68.54	Magnesioferrite, rutile
HSPDP-BTB13-1A-24Q-1	115.5	117.5	68.71	Paragonite, titanite
HSPDP-BTB13-1A-24Q-1	132	134	68.87	Enstatite, magnetite
HSPDP-BTB13-1A-24Q-2	4.5	6.5	69.03	Clinoptilolite, pyrite
HSPDP-BTB13-1A-24Q-2	21	23	69.2	
HSPDP-BTB13-1A-24Q-2	37.5	39.5	69.36	Kspar, bassanite, magnetite, pyrite, clays
HSPDP-BTB13-1A-24Q-2	54	56	69.53	Anorthite, chabazite, pyrite
HSPDP-BTB13-1A-24Q-2	70	72	69.69	Chabazite, pyrite
HSPDP-BTB13-1A-24Q-2	86.5	88.5	69.85	Anorthite, chabazite
HSPDP-BTB13-1A-24Q-2	103	105	70.02	Enstatite, analcime, magnetite, mg-calcite
HSPDP-BTB13-1A-24Q-2	119.5	121.5	70.18	Enstatite, analcime, chabazite
HSPDP-BTB13-1A-24Q-2	136	138	70.35	
HSPDP-BTB13-1A-24Q-2	150	152	70.465	
HSPDP-BTB13-1A-25Q-1	7	9	70.67	Albite, anorthite, sanidine, analcime
HSPDP-BTB13-1A-25Q-1	23.5	25.5	70.84	Albite, analcime, anorthite, muscovite
HSPDP-BTB13-1A-25Q-1	39.5	41.5	71	Enstatite, albite, analcime
HSPDP-BTB13-1A-25Q-1	56	58	71.16	Albite, anorthite, analcime
HSPDP-BTB13-1A-25Q-1	72.5	74.5	71.33	
HSPDP-BTB13-1A-25Q-1	89	91	71.49	Albite, enstatite, analcime
HSPDP-BTB13-1A-25Q-1	105	107	71.65	Albite, anorthite, analcime
HSPDP-BTB13-1A-25Q-1	121.5	123.5	71.82	
HSPDP-BTB13-1A-25Q-2	4.5	6.5	72.015	Albite, anorthite, analcime
HSPDP-BTB13-1A-25Q-2	21	23	72.175	Albite, anorthite, analcime, clinopyroxene
HSPDP-BTB13-1A-25Q-2	37.5	39.5	72.345	Albite, anorthite, sanidine, analcime
HSPDP-BTB13-1A-25Q-2	54	56	72.505	Albite, anorthite, clay, analcime, fe-oxide
HSPDP-BTB13-1A-25Q-2	70	72	72.66	Albite, pyroxene, analcime, clay
HSPDP-BTB13-1A-25Q-2	86.5	88.5	72.83	
HSPDP-BTB13-1A-25Q-2	103	105	72.99	Albite, anorthite, analcime, kspar, fe-oxide
HSPDP-BTB13-1A-25Q-2	119.5	121.5	73.165	Albite, analcime, kspar, fe-oxide
HSPDP-BTB13-1A-25Q-2	134.5	136.5	73.3	Albite, anorthite, kspar, analcime
HSPDP-BTB13-1A-25Q-3	14	16	73.46	Albite, anorthite, analcime, fe-oxide
HSPDP-BTB13-1A-26Q-1	0.5	2.5	73.65	Albite, anorthite, analcime, clays
HSPDP-BTB13-1A-26Q-1	17	19	73.81	
HSPDP-BTB13-1A-26Q-1	33.5	35.5	73.98	Albite, K-spar, Analcime

HSPDP-BTB13-1A-26Q-1	50	52	74.14	Albite, anorthite, muscovite, analcime
HSPDP-BTB13-1A-26Q-1	66.5	68.5	74.31	Albite, kspar, anorthite, clay, analcime, fe-oxide
HSPDP-BTB13-1A-26Q-1	81	83	74.43	
HSPDP-BTB13-1A-26Q-1	100	102	74.645	Anorthoclase, na-plag, analcime, kspar, fe-oxide
HSPDP-BTB13-1A-26Q-1	115.5	117.5	74.8	
HSPDP-BTB13-1A-26Q-1	132	134	74.96	Albite, analcime, clay
HSPDP-BTB13-1A-26Q-2	4	6	75.12	
HSPDP-BTB13-1A-26Q-2	20.5	22.5	75.28	Anorthoclase, albite, analcime
HSPDP-BTB13-1A-26Q-2	37	39	75.45	Albite, analcime, clay
HSPDP-BTB13-1A-26Q-2	53.5	55.5	75.61	Anorthoclase, analcime, anorthite, kspar, fe-oxide, clay, cristobalite
HSPDP-BTB13-1A-26Q-2	70	72	75.78	Analcime, anorthoclase, albite, clinopyroxene
HSPDP-BTB13-1A-26Q-2	86	88	75.94	Albite, mica, kspar, analcime
HSPDP-BTB13-1A-26Q-2	102.5	104.5	76.1	
HSPDP-BTB13-1A-26Q-2	119	121	76.27	Albite, pyroxene, analcime, clay
HSPDP-BTB13-1A-26Q-2	135.5	137.5	76.43	
HSPDP-BTB13-1A-26Q-3	8	10	76.545	Anorthoclase, analcime, anorthite, fe-oxide
HSPDP-BTB13-1A-27Q-1	7	9	76.76	
HSPDP-BTB13-1A-27Q-1	23.5	25.5	76.92	Albite, analcime, clay
HSPDP-BTB13-1A-27Q-1	40	42	77.08	Na-plag, analcime, fe-oxide
HSPDP-BTB13-1A-27Q-1	56.5	58.5	77.24	Albite, pyroxene, analcime, cristobalite
HSPDP-BTB13-1A-27Q-1	73	75	77.41	
HSPDP-BTB13-1A-27Q-1	89.5	91.5	77.57	Albite, muscovite, analcime, magnetite
HSPDP-BTB13-1A-27Q-1	106	108	77.73	Albite, fe-oxide, clinopyroxene
HSPDP-BTB13-1A-27Q-1	122.5	124.5	77.89	
HSPDP-BTB13-1A-27Q-1	139	141	78.05	Kspar, na-plag, clay
HSPDP-BTB13-1A-27Q-2	10.5	12.5	78.22	
HSPDP-BTB13-1A-27Q-2	27	29	78.38	Albite, kspar, cristobalite
HSPDP-BTB13-1A-27Q-2	43.5	45.5	78.54	Kspar, albite, mica, tridymite
HSPDP-BTB13-1A-27Q-2	60	62	78.7	Albite, kspar, cristobalite, clay
HSPDP-BTB13-1A-27Q-2	76.5	78.5	78.86	Albite, enstatite, kspar
HSPDP-BTB13-1A-27Q-2	93	95	79.03	
HSPDP-BTB13-1A-27Q-2	109.5	111.5	79.19	Albite, anorthite, kspar, clay
HSPDP-BTB13-1A-27Q-2	126	128	79.35	Albite, anorthite, clay
HSPDP-BTB13-1A-27Q-2	142.5	144.5	79.51	Albite, kspar, sepiolite
HSPDP-BTB13-1A-27Q-3	13	15	79.68	Anorthoclase, pyroxene, cristobalite
HSPDP-BTB13-1A-28Q-1	10	12	79.84	Albite, anorthite
HSPDP-BTB13-1A-28Q-1	26.5	28.5	80.01	Albite, anorthite, clay
HSPDP-BTB13-1A-28Q-1	43	45	80.17	Albite, clinopyroxene
HSPDP-BTB13-1A-28Q-1	59.5	61.5	80.34	Anorthoclase, albite, palygorskite

HSPDP-BTB13-1A-28Q-1	76	78	80.5	Anorthoclase, albite
HSPDP-BTB13-1A-28Q-1	92	94	80.66	Kspar
HSPDP-BTB13-1A-28Q-1	110	112	80.855	Albite, analcime, magnetite
HSPDP-BTB13-1A-28Q-1	125	127	80.99	Analcime, Anorthoclase, Albite, Anorthite, Pyroxene, Magnetite
HSPDP-BTB13-1A-28Q-1	141.5	143.5	81.16	Albite, analcime, magnetite
HSPDP-BTB13-1A-28Q-2	12.5	14.5	81.32	Albite, analcime, magnetite, galena
HSPDP-BTB13-1A-28Q-2	29	31	81.48	Albite, kspar, analcime
HSPDP-BTB13-1A-28Q-2	45.5	47.5	81.65	Analcime, albite, pyroxene, fe-oxide
HSPDP-BTB13-1A-28Q-2	61.5	63.5	81.81	
HSPDP-BTB13-1A-28Q-2	78	80	81.97	Albite, Anorthoclase, K-spar, Muscovite, Analcime, Pyroxene
HSPDP-BTB13-1A-28Q-2	94.5	96.5	82.14	Anorthoclase, Albite, K-spar, Analcime, Magnetite
HSPDP-BTB13-1A-28Q-2	111	113	82.3	
HSPDP-BTB13-1A-28Q-2	127.5	129.5	82.47	Albite, Ca-plag, analcime, pyroxene, fe-oxide
HSPDP-BTB13-1A-29Q-1	0	2	82.79	
HSPDP-BTB13-1A-29Q-1	13	15	82.81	Anorthoclase, Albite, Anorthite, Analcime, K-spar, Pyroxene
HSPDP-BTB13-1A-29Q-1	42	44	83.12	
HSPDP-BTB13-1A-29Q-2	9	11	83.44	Anorthite, kspar, analcime, pyroxene, fe-oxide
HSPDP-BTB13-1A-29Q-2	30	32	83.61	K-spar, Analcime, Plag-Na, Zeolite?
HSPDP-BTB13-1A-29Q-2	51	53	83.77	
HSPDP-BTB13-1A-29Q-2	93	95	84.1	Pyroxene, albite, fe-oxide, cristobalite
HSPDP-BTB13-1A-29Q-3	8.5	10.5	84.26	
HSPDP-BTB13-1A-30Q-1	8	10	84.42	Albite, clay, calcite, cristobalite
HSPDP-BTB13-1A-30Q-1	24.5	26.5	84.59	
HSPDP-BTB13-1A-30Q-2	13.5	15.5	84.75	Anorthoclase, pyroxene, cristobalite
HSPDP-BTB13-1A-30Q-2	29.5	31.5	84.91	Anorthoclase, mica, cristobalite
HSPDP-BTB13-1A-30Q-2	46	48	85.07	
HSPDP-BTB13-1A-30Q-2	60	62	85.185	Albite, calcite, olivine, cristobalite
HSPDP-BTB13-1A-31Q-1	0.5	2.5	85.85	Plag-Na, muscovite, kspar, cristobalite
HSPDP-BTB13-1A-31Q-1	16.5	18.5	86.01	Anorthoclase, albite, palygorskite
HSPDP-BTB13-1A-31Q-1	33	35	86.17	Albite, palygorskite, cristobalite
HSPDP-BTB13-1A-31Q-1	49.5	51.5	86.34	Anorthoclase, palygorskite, diopside
HSPDP-BTB13-1A-31Q-1	66	68	86.5	Anorthoclase, Cristobalite
HSPDP-BTB13-1A-31Q-1	84.5	86.5	86.715	Anorthite, muscovite, clinoptilolite
HSPDP-BTB13-1A-31Q-1	98.5	100.5	86.83	Muscovite, heulandite, anorthite
HSPDP-BTB13-1A-31Q-1	115	117	86.99	Clinoptilolite, Plag-Ca, Magnetite?
HSPDP-BTB13-1A-31Q-1	131.5	133.5	87.16	Heulandite/Clinoptilolite, Plag-Na, K-spar
HSPDP-BTB13-1A-31Q-2	7	9	87.31	Heulandite/Clinoptilolite

HSPDP-BTB13-1A-31Q-2	23.5	25.5	87.48	Clinoptilolite, natrolite, gypsum, anorthite
HSPDP-BTB13-1A-31Q-2	39.5	41.5	87.64	Heulandite, anorthite, clay
HSPDP-BTB13-1A-31Q-2	56	58	87.8	Albite, gypsum, cristobalite
HSPDP-BTB13-1A-31Q-2	72.5	74.5	87.97	
HSPDP-BTB13-1A-31Q-2	89	91	88.13	Albite, tridymite, chabazite, mont
HSPDP-BTB13-1A-31Q-2	108	110	88.35	Clinoptilolite, anorthite, mont
HSPDP-BTB13-1A-31Q-2	121.5	123.5	88.46	Palygorskite, heulandite, wairakite, cristobalite
HSPDP-BTB13-1A-31Q-2	138	140	88.62	Chabazite, clinoptilolite, cristobalite, anorthite
HSPDP-BTB13-1A-31Q-3	11.5	13.5	88.79	Chabazite, anorthite
HSPDP-BTB13-1A-32Q-1	24	26	89.125	
HSPDP-BTB13-1A-32Q-1	56	58	89.44	Anorthite, heulandite
HSPDP-BTB13-1A-32Q-1	72.5	74.5	89.61	
HSPDP-BTB13-1A-32Q-1	89	91	89.77	Enstatite, analcime, cristobalite
HSPDP-BTB13-1A-32Q-1	105	107	89.93	Anorthite, albite, analcime, cristobalite
HSPDP-BTB13-1A-32Q-1	121.5	123.5	90.1	Anorthite, clinoptilolite, fe-oxide, analcime, cristobalite
HSPDP-BTB13-1A-32Q-1	138	140	90.26	Albite, clay, analcime
HSPDP-BTB13-1A-32Q-2	7.5	9.5	90.43	
HSPDP-BTB13-1A-32Q-2	24	26	90.59	Anorthite, muscovite, clinoptilolite
HSPDP-BTB13-1A-32Q-2	40	42	90.75	Anorthoclase, albite, palygorskite
HSPDP-BTB13-1A-32Q-2	56.5	58.5	90.92	Albite, muscovite, cristobalite, clinoptiloite
HSPDP-BTB13-1A-32Q-2	73	75	91.08	Albite, kspar
HSPDP-BTB13-1A-32Q-2	89.5	91.5	91.25	Anorthite, palygorskite, analcime, dolomite
HSPDP-BTB13-1A-32Q-2	105.5	107.5	91.41	Anorthite, muscovite, analcime
HSPDP-BTB13-1A-32Q-2	122	124	91.57	Anorthite, analcime, dolomite
HSPDP-BTB13-1A-32Q-2	138.5	140.5	91.74	Albite, Anorthite, K-spar, Analcime, Magentite
HSPDP-BTB13-1A-33Q-1	0.5	2.5	91.93	Albite, analcime, palygorskite
HSPDP-BTB13-1A-33Q-1	17	19	92.1	Kspar, vaterite, calcite
HSPDP-BTB13-1A-33Q-1	33.5	35.5	92.26	Albite, anorthite
HSPDP-BTB13-1A-33Q-1	50	52	92.42	Anorthoclase, cristobalite
HSPDP-BTB13-1A-33Q-1	66.5	68.5	92.58	Enstatite, albite, palygorskite
HSPDP-BTB13-1A-33Q-1	83	85	92.74	Albite, enstatite, clay
HSPDP-BTB13-1A-33Q-1	99.5	101.5	92.9	Albite, mg-calcite, clay
HSPDP-BTB13-1A-33Q-1	116	118	93.07	Albite, kspar, cristobalite
HSPDP-BTB13-1A-33Q-1	132.5	134.5	93.23	Albite, anorthite, cristobalite, clay
HSPDP-BTB13-1A-33Q-1	147	149	93.35	Albite, anorthite, kspar, clay
HSPDP-BTB13-1A-33Q-2	16	18	93.55	Albite, anorthite, mica
HSPDP-BTB13-1A-33Q-2	32.5	34.5	93.71	
HSPDP-BTB13-1A-33Q-2	49	51	93.87	Kspar, albite, tridymite, vermiculite

HSPDP-BTB13-1A-33Q-2	65.5	67.5	94.03	Albite, diopside, tridymite, vermiculite
HSPDP-BTB13-1A-33Q-2	82	84	94.19	Albite, anorthite, tridymite
HSPDP-BTB13-1A-33Q-2	98.5	100.5	94.36	
HSPDP-BTB13-1A-33Q-2	115	117	94.52	Albite, mont
HSPDP-BTB13-1A-33Q-2	131.5	133.5	94.68	Albite, tridymite, mont
HSPDP-BTB13-1A-33Q-3	2.5	4.5	94.84	Albite, tridymite, mica
HSPDP-BTB13-1A-34Q-1	3	5	95.01	Albite, anorthite
HSPDP-BTB13-1A-34Q-1	19.5	21.5	95.17	Anorthite, kspar, magnetite, tridymite
HSPDP-BTB13-1A-34Q-1	36	38	95.33	Albite, kspar, clay
HSPDP-BTB13-1A-34Q-1	52.5	54.5	95.5	Albite, anrothite, palygorskite
HSPDP-BTB13-1A-34Q-1	69	71	95.66	
HSPDP-BTB13-1A-34Q-1	85.5	87.5	95.82	Enstatite, albite, cristobalite
HSPDP-BTB13-1A-34Q-1	102	104	95.99	Albite, mont
HSPDP-BTB13-1A-34Q-1	118.5	120.5	96.15	Albite, bloedite, cristobalite
HSPDP-BTB13-1A-34Q-1	135	137	96.31	Albite, anorthite, phillipsite, tridymite, magnetite
HSPDP-BTB13-1A-34Q-2	6	8	96.47	Albite
HSPDP-BTB13-1A-34Q-2	22.5	24.5	96.63	Albite, enstatite
HSPDP-BTB13-1A-34Q-2	39	41	96.8	Anorthoclase, albite
HSPDP-BTB13-1A-34Q-2	55.5	57.5	96.96	
HSPDP-BTB13-1A-34Q-2	72	74	97.12	Anorthite, mont, cristobalite
HSPDP-BTB13-1A-34Q-2	86	88	97.235	Anorthite, mont, rutile
HSPDP-BTB13-1A-34Q-2	105	107	97.45	Albite, anorthite
HSPDP-BTB13-1A-34Q-2	121.5	123.5	97.61	Albite, cristobalite
HSPDP-BTB13-1A-34Q-2	138	140	97.77	Albite, anorthite, mica
HSPDP-BTB13-1A-34Q-3	8.5	10.5	97.94	Anorthoclase, albite
HSPDP-BTB13-1A-35Q-1	6.5	8.5	98.1	Anorthoclase, calcite, tridymite
HSPDP-BTB13-1A-35Q-1	23	25	98.26	Albite, cristobalite
HSPDP-BTB13-1A-35Q-1	39	41	98.42	Anorthoclase, diopside
HSPDP-BTB13-1A-35Q-1	55.5	57.5	98.59	Albite, tridymite, mont
HSPDP-BTB13-1A-35Q-1	72	74	98.75	Anorthoclase, albite, dolomite
HSPDP-BTB13-1A-35Q-1	88.5	90.5	98.92	Albite, cristobalite, mont
HSPDP-BTB13-1A-35Q-1	105	107	99.08	Albite, kspar, sepiolite
HSPDP-BTB13-1A-35Q-1	119	121	99.195	Anorthite, albite, mg-calcite, cristobalite
HSPDP-BTB13-1A-35Q-1	138	140	99.415	Anorthoclase, heulandite
HSPDP-BTB13-1A-35Q-2	12.5	14.5	99.57	Albite, mg-calcite, clinoptilolite, cristobalite
HSPDP-BTB13-1A-35Q-2	29	31	99.74	Kspar, clinoptilolite, clay
HSPDP-BTB13-1A-35Q-2	45.5	47.5	99.9	Anorthite, clinoptilolite, mordenite (heulandite), tridymite
HSPDP-BTB13-1A-35Q-2	62	64	100.07	Albite, clinoptilolite, clays
HSPDP-BTB13-1A-35Q-2	78.5	80.5	100.23	Anorthite, tridymite
HSPDP-BTB13-1A-35Q-2	94.5	96.5	100.39	Kspar, diopside, tridymite, cristobalite

HSPDP-BTB13-1A-35Q-2	111	113	100.56	Anorthite, clinoptilolite, fe-oxide
HSPDP-BTB13-1A-35Q-2	127.5	129.5	100.72	
HSPDP-BTB13-1A-35Q-3	2	4	100.9	
HSPDP-BTB13-1A-35Q-3	14	16	100.975	Albite, quartz, analcime, cristobalite
HSPDP-BTB13-1A-36Q-1	13	15	101.21	Albite, gypsum, clay
HSPDP-BTB13-1A-36Q-1	32	34	101.425	Albite, cristobalite, anorthite
HSPDP-BTB13-1A-36Q-1	46	48	101.54	Anorthoclase, qtz
HSPDP-BTB13-1A-36Q-1	59.5	61.5	101.64	Anorthoclase, heulandite
HSPDP-BTB13-1A-36Q-1	77.5	79.5	101.835	
HSPDP-BTB13-1A-36Q-1	95.5	97.5	102.03	Paragonite, analcime, faujasite
HSPDP-BTB13-1A-36Q-1	112	114	102.19	Anorthoclase, muscovite, wairakite, mont
HSPDP-BTB13-1A-36Q-1	128.5	130.5	102.35	Albite, anorthite, analcime, mont
HSPDP-BTB13-1A-36Q-1	143	145	102.48	Kspar, analcime, mont
HSPDP-BTB13-1A-36Q-2	14.5	16.5	102.68	Albite, mg-calcite, analcime
HSPDP-BTB13-1A-36Q-2	31	33	102.84	Albite, clinoptilolite, dolomite
HSPDP-BTB13-1A-36Q-2	47.5	49.5	103.01	Albite, heulandite
HSPDP-BTB13-1A-36Q-2	64	66	103.17	Albite, heulandite, mica
HSPDP-BTB13-1A-36Q-2	80.5	82.5	103.33	Albite, heulandite, mica
HSPDP-BTB13-1A-36Q-2	97	99	103.5	Anorthoclase, heulandite
HSPDP-BTB13-1A-36Q-2	113.5	115.5	103.66	Anorthoclase, anorthite, heulandite
HSPDP-BTB13-1A-36Q-2	134	136	103.9	Albite, mont, cristobalite
HSPDP-BTB13-1A-36Q-2	145	147	103.955	Albite, clay
HSPDP-BTB13-1A-37Q-1	3	5	104.15	Albite, kaolinite
HSPDP-BTB13-1A-37Q-1	19.5	21.5	104.32	Albite
HSPDP-BTB13-1A-37Q-1	35.5	37.5	104.48	Albite
HSPDP-BTB13-1A-37Q-1	52	54	104.64	Anorthoclase, albite
HSPDP-BTB13-1A-37Q-1	68	70	104.8	Anorthoclase, albite, clay
HSPDP-BTB13-1A-37Q-1	86	88	104.995	Anorthoclase, albite, mont
HSPDP-BTB13-1A-37Q-1	101	103	105.13	Anorthoclase, cristobalite
HSPDP-BTB13-1A-37Q-1	117.5	119.5	105.3	Albite, gordaite
HSPDP-BTB13-1A-37Q-1	136	138	105.5	Albite, anorthite
HSPDP-BTB13-1A-37Q-2	9	11	105.62	Albite, enstatite, fe-oxide
HSPDP-BTB13-1A-37Q-2	25	27	105.78	Anorthoclase, albite, mont
HSPDP-BTB13-1A-37Q-2	41.5	43.5	105.94	Anorthoclase, anorthite, mont
HSPDP-BTB13-1A-37Q-2	62	64	106.19	Anorthoclase, albite, mont
HSPDP-BTB13-1A-37Q-2	76	78	106.305	Albite, anorthite
HSPDP-BTB13-1A-37Q-2	90.5	92.5	106.43	Pyroxene, anorthoclase, anorthite, fe-oxide, ti-oxide
HSPDP-BTB13-1A-37Q-2	117.5	119.5	106.805	Albite, anorthite
HSPDP-BTB13-1A-37Q-2	123.5	125.5	106.76	Albite
HSPDP-BTB13-1A-37Q-2	140	142	106.93	Albite, anorthite, clay
HSPDP-BTB13-1A-37Q-3	8	10	107.04	

HSPDP-BTB13-1A-38Q-1	9	11	107.26	Anorthoclase, Cristobalite, Zeolite?
HSPDP-BTB13-1A-38Q-1	25.5	27.5	107.42	Albite, tridymite, anorthite
HSPDP-BTB13-1A-38Q-1	42	44	107.59	Anorthoclase, vermiculite
HSPDP-BTB13-1A-38Q-1	58.5	60.5	107.75	Anorthoclase, Cristobalite, Zeolite?
HSPDP-BTB13-1A-38Q-1	75	77	107.92	Albite, tridymite
HSPDP-BTB13-1A-38Q-1	91.5	93.5	108.08	Anorthoclase, mont
HSPDP-BTB13-1A-38Q-1	108	110	108.25	Anorthoclase, mont, magadiite
HSPDP-BTB13-1A-38Q-1	126.5	128.5	108.45	Anorthoclase, albite, kspar, tridymite
HSPDP-BTB13-1A-38Q-1	138	140	108.52	Albite, anorthite, mont
HSPDP-BTB13-1A-38Q-2	16.5	18.5	108.74	Albite, tridymite
HSPDP-BTB13-1A-38Q-2	33	35	108.91	Albite, tridymite, mica
HSPDP-BTB13-1A-38Q-2	49.5	51.5	109.07	Anorthoclase
HSPDP-BTB13-1A-38Q-2	66	68	109.24	Albite, pyroxene
HSPDP-BTB13-1A-38Q-2	82.5	84.5	109.4	Kspar, tridymite
HSPDP-BTB13-1A-38Q-2	99	101	109.57	Albite, kspar, tridymite, magnetite
HSPDP-BTB13-1A-38Q-2	115.5	117.5	109.73	Albite, cristobalite
HSPDP-BTB13-1A-38Q-2	132	134	109.9	Albite, kspar, tridymite, cristobalite
HSPDP-BTB13-1A-38Q-3	7.5	9.5	110.06	Albite, cristobalite, anorthite
HSPDP-BTB13-1A-39Q-1	3.5	5.5	110.28	Albite, anorthite, clinopyroxene, clay
HSPDP-BTB13-1A-39Q-1	17	19	110.39	Albite, gypsum, jarosite, pyrite
HSPDP-BTB13-1A-39Q-1	33.5	35.5	110.55	Kspar, muscovite, diopside
HSPDP-BTB13-1A-39Q-1	50	52	110.72	Anorthoclase, paragonite
HSPDP-BTB13-1A-39Q-1	66.5	68.5	110.88	Albite, heulandite, cristobalite
HSPDP-BTB13-1A-39Q-1	83	85	111.05	Albite, paragonite, kspar
HSPDP-BTB13-1A-39Q-1	99.5	101.5	111.21	Albite, anorthite, clays
HSPDP-BTB13-1A-39Q-1	116	118	111.38	Albite, pyrite, clay
HSPDP-BTB13-1A-39Q-1	132.5	134.5	111.54	Anorthite, kspar, sepiolite, cristobalite
HSPDP-BTB13-1A-39Q-2	5	7	111.71	
HSPDP-BTB13-1A-39Q-2	21.5	23.5	111.87	Anorthite, palygorskite, natrolite
HSPDP-BTB13-1A-39Q-2	38	40	112.04	
HSPDP-BTB13-1A-39Q-2	54.5	56.5	112.2	Albite, anorthite, muscovite
HSPDP-BTB13-1A-39Q-2	71	73	112.37	Plag-Na, Pyrite, K-spar, Natrolite, Zeolite?
HSPDP-BTB13-1A-39Q-2	87.5	89.5	112.53	Albite, enstatite, kspar, pyrite, clay
HSPDP-BTB13-1A-39Q-2	104	106	112.7	
HSPDP-BTB13-1A-39Q-2	120.5	122.5	112.86	Kspar, pyrite, cristobalite
HSPDP-BTB13-1A-39Q-2	137	139	113.03	Anorthoclase, albite, kspar, palygorskite
HSPDP-BTB13-1A-39Q-3	11.5	13.5	113.19	Anorthoclase, kspar
HSPDP-BTB13-1A-40Q-1	8	10	113.35	Albite, phillipsite, quartz
HSPDP-BTB13-1A-40Q-1	24.5	26.5	113.51	Kspar, mont
HSPDP-BTB13-1A-40Q-1	41	43	113.68	Albite, enstatite, fe-oxide
HSPDP-BTB13-1A-40Q-1	57.5	59.5	113.84	Kspar, heulandite

HSPDP-BTB13-1A-40Q-1	74	76	114	Albite, tridymite, heulandite
HSPDP-BTB13-1A-40Q-1	90.5	92.5	114.17	Anorthite, clinoptilolite, tridymite, mont
HSPDP-BTB13-1A-40Q-1	107	109	114.33	Albite, heulandite
HSPDP-BTB13-1A-40Q-1	123.5	125.5	114.49	Anorthoclase, heulandite
HSPDP-BTB13-1A-40Q-1	139	141	114.64	Albite, heulandite, kaolinite(?)
HSPDP-BTB13-1A-40Q-2	10.5	12.5	114.82	Anorthoclase, mica, clinoptilolite
HSPDP-BTB13-1A-40Q-2	27	29	114.98	Albite, clinoptilolite
HSPDP-BTB13-1A-40Q-2	43.5	45.5	115.14	Albite, clinoptilolite, mont
HSPDP-BTB13-1A-40Q-2	60	62	115.31	Kspar, mordenite
HSPDP-BTB13-1A-40Q-2	76.5	78.5	115.47	Albite, anorthite, clinoptilolite?
HSPDP-BTB13-1A-40Q-2	93	95	115.63	
HSPDP-BTB13-1A-40Q-2	109.5	111.5	115.8	Albite, clinoptilolite
HSPDP-BTB13-1A-40Q-2	126	128	115.96	Kspar, sepiolite, faujasite
HSPDP-BTB13-1A-40Q-2	142.5	144.5	116.12	Anorthoclase, Phillipsite
HSPDP-BTB13-1A-40Q-3	13.5	15.5	116.28	Albite, clay
HSPDP-BTB13-1A-41Q-1	13	15	116.45	Anorthoclase, mica
HSPDP-BTB13-1A-41Q-1	29.5	31.5	116.62	Kspar, sepiolite
HSPDP-BTB13-1A-41Q-1	46	48	116.78	Anorthite, mica
HSPDP-BTB13-1A-41Q-1	62.5	64.5	116.95	Albite, sepiolite
HSPDP-BTB13-1A-41Q-1	79	81	117.11	Anorthoclase, tridymite, sepiolite
HSPDP-BTB13-1A-41Q-1	95	97	117.27	Albite, phillipsite, fe-oxide, clay
HSPDP-BTB13-1A-41Q-1	111.5	113.5	117.44	Anorthoclase, Cristobalite, Phillipsite
HSPDP-BTB13-1A-41Q-1	128	130	117.6	Orthoclase, muscovite
HSPDP-BTB13-1A-41Q-2	5.5	7.5	117.76	Albite, mica, phillipsite
HSPDP-BTB13-1A-41Q-2	21.5	23.5	117.92	Albite, fe-oxide, clay
HSPDP-BTB13-1A-41Q-2	38	40	118.09	Anorthoclase, phillipsite, anorthite
HSPDP-BTB13-1A-41Q-2	54.5	56.5	118.25	Phillipsite, qtz, sodalite, sepiolite
HSPDP-BTB13-1A-41Q-2	71	73	118.42	Albite, pyroxenes
HSPDP-BTB13-1A-41Q-2	87.5	89.5	118.58	Paragonite, albite, phillipsite, sepiolite, anorthite
HSPDP-BTB13-1A-41Q-2	104	106	118.75	Phillipsite, nacrite, anorthite
HSPDP-BTB13-1A-41Q-2	120	122	118.91	
HSPDP-BTB13-1A-41Q-2	136.5	138.5	119.07	Albite, dickite, sepiolite
HSPDP-BTB13-1A-41Q-3	12.5	14.5	119.23	Kspar, magadiite, cristobalite
HSPDP-BTB13-1A-42Q-1	4	6	119.4	Albite, mont
HSPDP-BTB13-1A-42Q-1	22	24	119.58	Albite, clay
HSPDP-BTB13-1A-42Q-1	55	57	119.89	Albite, kaolinite, vermiculite
HSPDP-BTB13-1A-42Q-1	71	73	120.04	Kaolinite, sepiolite, anorthite
HSPDP-BTB13-1A-42Q-1	89	91	120.22	
HSPDP-BTB13-1A-42Q-1	93	41	120.81	
HSPDP-BTB13-1A-42Q-1	106	108	120.39	Sepiolite
HSPDP-BTB13-1A-42Q-1	122	124	120.53	

HSPDP-BTB13-1A-42Q-1	139	141	120.7	Anorthoclase, anorthite
HSPDP-BTB13-1A-42Q-2	13.5	15.5	120.87	Albite, apatite (CaF), goethite, cristobalite
HSPDP-BTB13-1A-42Q-2	30.5	32.5	121.04	Anorthoclase, enstatite, kspar
HSPDP-BTB13-1A-42Q-2	47.5	49.5	121.2	Albite, anorthite
HSPDP-BTB13-1A-42Q-2	64.5	66.5	121.37	Anorthoclase, phillipsite, mont
HSPDP-BTB13-1A-42Q-2	81.5	83.5	121.53	Anorthoclase, paragonite, phillipsite
HSPDP-BTB13-1A-42Q-2	98.5	100.5	121.69	Anorthoclase, anorthite, phillipsite, cristobalite
HSPDP-BTB13-1A-42Q-3	6.5	8.5	121.86	Anorthoclase, gobbinsite, cristobalite
HSPDP-BTB13-1A-42Q-3	24	26	122.035	Phillipsite, dolomite, nacrite
HSPDP-BTB13-1A-42Q-3	35	37	122.085	Albite, anorthite, phillipsite, dickite
HSPDP-BTB13-1A-42Q-3	57.5	59.5	122.35	Anorthoclase, phillipsite, paragonite, hematite, cristobalite
HSPDP-BTB13-1A-43Q-1	10.5	12.5	122.52	Kspar, titanite, magnetite
HSPDP-BTB13-1A-43Q-1	27	29	122.68	Enstatite, fe-oxide, anorthite
HSPDP-BTB13-1A-43Q-1	43.5	45.5	122.85	Anorthoclase, phillipsite, hematite, cristobalite
HSPDP-BTB13-1A-43Q-1	60	62	123.01	Anorthoclase, hematite, cristobalite
HSPDP-BTB13-1A-43Q-1	76	78	123.17	
HSPDP-BTB13-1A-43Q-1	92.5	94.5	123.34	Albite, gobbinsite, hematite
HSPDP-BTB13-1A-43Q-1	109	111	123.5	Anorthoclase, Cristobalite, Phillipsite
HSPDP-BTB13-1A-43Q-1	125.5	127.5	123.67	
HSPDP-BTB13-1A-43Q-2	0.5	2.5	123.82	Anorthite, phillipsite, fe-oxide
HSPDP-BTB13-1A-43Q-2	17	19	123.99	Anorthoclase, gobbinsite, hematite, mont
HSPDP-BTB13-1A-43Q-2	33.5	35.5	124.15	Anorthoclase, hematite, cristobalite, vermiculite, anorthite
HSPDP-BTB13-1A-43Q-2	49.5	51.5	124.31	Anorthoclase, gobbinsite, hematite, cristobalite
HSPDP-BTB13-1A-43Q-2	66	68	124.48	Albite, gobbinsite, hematite, mont
HSPDP-BTB13-1A-43Q-2	80.5	82.5	124.6	
HSPDP-BTB13-1A-43Q-2	101	103	124.85	Albite, gobbinsite, hematite, cristobalite
HSPDP-BTB13-1A-43Q-2	115.5	117.5	124.97	Anorthoclase, hematite
HSPDP-BTB13-1A-43Q-3	3	5	125.13	Anorthoclase, vermiculite
HSPDP-BTB13-1A-43Q-3	19	21	125.29	Albite, pyroxene, quartz
HSPDP-BTB13-1A-44Q-1	4	6	125.535	Albite, mont, cristobalite
HSPDP-BTB13-1A-44Q-1	17	19	125.63	Anorthoclase, hematite, vermiculite
HSPDP-BTB13-1A-44Q-1	33.5	35.5	125.79	Anorthoclase, cristobalite, mont
HSPDP-BTB13-1A-44Q-1	49	51	125.93	Anorthoclase, hematite, vermiculite
HSPDP-BTB13-1A-44Q-1	66.5	68.5	126.11	Anorthoclase, vermiculite
HSPDP-BTB13-1A-44Q-1	83	85	126.28	Anorthoclase, hematite, mont
HSPDP-BTB13-1A-44Q-1	99.5	101.5	126.44	Albite, hematite, cristobalite, mont
HSPDP-BTB13-1A-44Q-1	116	118	126.6	Anorthoclase, mont
HSPDP-BTB13-1A-44Q-1	132.5	134.5	126.76	Albite, hematite

HSPDP-BTB13-1A-44Q-2	2	4	126.93	Anorthoclase, albite
HSPDP-BTB13-1A-44Q-2	19	21	127.095	Plag-Na, K-spar, Zeolite?
HSPDP-BTB13-1A-44Q-2	35	37	127.25	Anorthoclase, hematite, cristobalite, mont
HSPDP-BTB13-1A-44Q-2	51.5	53.5	127.41	Kspar, hematite, cristobalite
HSPDP-BTB13-1A-44Q-2	68	70	127.58	Anorthoclase, hematite
HSPDP-BTB13-1A-44Q-2	84.5	86.5	127.74	Gobbinsite, anorthite
HSPDP-BTB13-1A-44Q-2	101	103	127.9	Anorthoclase, mont
HSPDP-BTB13-1A-44Q-2	117.5	119.5	128.06	Magnetite, clinoptilolite
HSPDP-BTB13-1A-44Q-2	134	136	128.23	
HSPDP-BTB13-1A-44Q-3	3.5	5.5	128.39	Albite, muscovite
HSPDP-BTB13-1A-45Q-1	4.5	6.5	128.56	orthopyroxene, heulandite, quartz
HSPDP-BTB13-1A-45Q-1	21	23	128.72	Clinoptilolite, anorthite
HSPDP-BTB13-1A-45Q-1	33.5	35.5	128.81	Clinoptilolite
HSPDP-BTB13-1A-45Q-1	53.5	55.5	129.05	Kspar, clinoptilolite, clay
HSPDP-BTB13-1A-45Q-1	70	72	129.21	Albite, faujasite
HSPDP-BTB13-1A-45Q-1	85.5	87.5	129.36	Albite, anorthite
HSPDP-BTB13-1A-45Q-2	14	16	129.54	Kpar, sepiolite, mica
HSPDP-BTB13-1A-45Q-2	30.5	32.5	129.7	Albite, sepiolite, cristobalite
HSPDP-BTB13-1A-45Q-2	47	49	129.87	
HSPDP-BTB13-1A-45Q-2	63.5	65.5	130.03	
HSPDP-BTB13-1A-45Q-2	80	82	130.2	Albite, muscovite, magadiite
HSPDP-BTB13-1A-45Q-2	96.5	98.5	130.36	Albite, dickite, anorthite
HSPDP-BTB13-1A-46Q-1	1	3	131.575	Kaolinite, rutile
HSPDP-BTB13-1A-46Q-1	16	18	131.69	Kaolinite, mont
HSPDP-BTB13-1A-46Q-2	15.5	17.5	131.89	Albite, mont
HSPDP-BTB13-1A-46Q-2	43	45	132.24	Albite, anorthite, clay
HSPDP-BTB13-1A-46Q-2	50.5	52.5	132.21	Anorthoclase, paragonite
HSPDP-BTB13-1A-46Q-2	68	70	132.37	Anorthoclase, cristobalite
HSPDP-BTB13-1A-46Q-2	85.5	87.5	132.54	Albite, enstatite, fe-oxide, clay
HSPDP-BTB13-1A-46Q-2	103	105	132.7	Albite, phillipsite, hematite, cristobalite, mont
HSPDP-BTB13-1A-46Q-2	120.5	122.5	132.86	
HSPDP-BTB13-1A-46Q-3	2	4	133.02	Enstatite, albite, fe-oxide, dolomite
HSPDP-BTB13-1A-46Q-3	19.5	21.5	133.18	
HSPDP-BTB13-1A-46Q-3	37	39	133.35	Anorthoclase, hematite, dolomite, mont
HSPDP-BTB13-1A-46Q-3	54.5	56.5	133.51	Albite, hematite, cristobalite
HSPDP-BTB13-1A-46Q-3	72	74	133.67	Anorthoclase, phillipsite, cristobalite
HSPDP-BTB13-1A-46Q-3	89.5	91.5	133.83	Anorthoclase, albite, hematite, dickite, cristobalite, mont
HSPDP-BTB13-1A-46Q-3	107	109	133.99	Albite, hematite, cristobalite, anorthite
HSPDP-BTB13-1A-46Q-3	124.5	126.5	134.16	Anorthoclase, hematite, cristobalite
HSPDP-BTB13-1A-46Q-3	142	144	134.32	Anorthoclase, cristobalite

HSPDP-BTB13-1A-47Q-1	6	8	134.56	Albite, hematite, anorthite
HSPDP-BTB13-1A-47Q-1	18.5	20.5	134.65	Albite, enstatite
HSPDP-BTB13-1A-47Q-1	35	37	134.81	Anorthoclase, diopside, cristobalite, clay
HSPDP-BTB13-1A-47Q-1	51.5	53.5	134.98	Anorthoclase, cristobalite
HSPDP-BTB13-1A-47Q-1	64.5	66.5	135.075	Kspar, tridymite, magnesioferrite
HSPDP-BTB13-1A-47Q-1	84	86	135.3	Enstatite, albite, phillipsite, clay
HSPDP-BTB13-1A-47Q-1	107	109	135.595	Albite, fe-oxide, clay
HSPDP-BTB13-1A-47Q-1	118	120	135.65	Anorthoclase, hematite, cristobalite
HSPDP-BTB13-1A-47Q-1	134	136	135.805	Albite, mica
HSPDP-BTB13-1A-47Q-2	6.5	8.5	135.96	Kspar, mont
HSPDP-BTB13-1A-47Q-2	23	25	136.12	Anorthoclase, magnesioferrite, cristobalite, mont
HSPDP-BTB13-1A-47Q-2	39.5	41.5	136.29	Albite, magnesioferrite, mont
HSPDP-BTB13-1A-47Q-2	56	58	136.45	Anorthoclase, cristobalite, mont
HSPDP-BTB13-1A-47Q-2	72.5	74.5	136.62	Anorthoclase, cristobalite
HSPDP-BTB13-1A-47Q-2	89	91	136.78	Albite, cristobalite, clay
HSPDP-BTB13-1A-47Q-2	105.5	107.5	136.95	Plag-Na, K-spar, Zeolite?
HSPDP-BTB13-1A-47Q-2	122	124	137.11	Anorthoclase, cristobalite, mont
HSPDP-BTB13-1A-47Q-2	138.5	140.5	137.28	
HSPDP-BTB13-1A-47Q-3	12	14	137.46	Albite, mont
HSPDP-BTB13-1A-47Q-3	26.5	28.5	137.59	Anorthoclase, cristobalite, mont
HSPDP-BTB13-1A-48Q-1	14	16	137.81	Anorthoclase, cristobalite, mont
HSPDP-BTB13-1A-48Q-1	28.5	30.5	137.93	Albite, mica, clay
HSPDP-BTB13-1A-48Q-1	52	54	138.24	Anorthoclase, mont
HSPDP-BTB13-1A-48Q-1	61.5	63.5	138.26	Anorthoclase
HSPDP-BTB13-1A-48Q-1	78	80	138.42	Anorthoclase
HSPDP-BTB13-1A-48Q-1	88	90	138.455	Anorthoclase, cristobalite, mont
HSPDP-BTB13-1A-48Q-2	15.5	17.5	138.75	Anorthoclase, Cristobalite, Zeolite?
HSPDP-BTB13-1A-48Q-2	32	34	138.92	Anorthoclase, diopside, calcite
HSPDP-BTB13-1A-48Q-2	48.5	50.5	139.08	Anorthoclase, cristobalite
HSPDP-BTB13-1A-48Q-2	65	67	139.24	Kspar, cristobalite, mont
HSPDP-BTB13-1A-48Q-2	77	79	139.315	
HSPDP-BTB13-1A-48Q-2	98	100	139.57	Anorthoclase, cristobalite, mont
HSPDP-BTB13-1A-48Q-2	114.5	116.5	139.74	
HSPDP-BTB13-1A-48Q-2	128	130	139.84	Albite, mont
HSPDP-BTB13-1A-48Q-3	8	10	140.06	Anorthoclase, mont
HSPDP-BTB13-1A-48Q-3	24.5	26.5	140.23	Albite, sodalite, dolomite, anorthite
HSPDP-BTB13-1A-48Q-3	41	43	140.39	
HSPDP-BTB13-1A-48Q-3	57.5	59.5	140.55	Anorthoclase, qtz, cristobalite
HSPDP-BTB13-1A-49Q-1	2	4	140.72	Albite, enstatite, mica
HSPDP-BTB13-1A-49Q-1	18.5	20.5	140.89	
HSPDP-BTB13-1A-49Q-1	25	27	140.85	

HSPDP-BTB13-1A-49Q-1	73	75	141.65	Albite, enstatite
HSPDP-BTB13-1A-49Q-1	78	80	141.585	Albite, anorthite, quartz
HSPDP-BTB13-1A-49Q-1	84	86	141.54	Albite, quartz, sodalite
HSPDP-BTB13-1A-49Q-1	95	97	141.595	Albite, anorthite, sepiolite
HSPDP-BTB13-1A-49Q-2	8	10	141.815	Anorthoclase
HSPDP-BTB13-1A-49Q-2	27	29	142.03	Albite, cristobalite, mont
HSPDP-BTB13-1A-49Q-2	38	40	142.085	Anorthoclase, cristobalite, mont
HSPDP-BTB13-1A-49Q-2	60	62	142.36	Albite, cristobalite
HSPDP-BTB13-1A-49Q-2	72	74	142.435	Albite, mont
HSPDP-BTB13-1A-49Q-2	92.5	94.5	142.68	Anorthoclase
HSPDP-BTB13-1A-49Q-3	2.5	4.5	142.85	Anorthoclase
HSPDP-BTB13-1A-49Q-3	20	22	143.03	
HSPDP-BTB13-1A-49Q-3	34	36	143.145	Albite, qtz
HSPDP-BTB13-1A-50Q-1	2	4	143.79	Anorthoclase, hematite, mont, vermiculite
HSPDP-BTB13-1A-50Q-1	16.5	18.5	143.92	Albite, phillipsite, clay
HSPDP-BTB13-1A-50Q-1	33	35	144.08	Anorthoclase, tridymite, clay
HSPDP-BTB13-1A-50Q-1	49	51	144.24	Anorthoclase, blodite (ev), pyroxene, tridymite, clay
HSPDP-BTB13-1A-50Q-1	65.5	67.5	144.41	
HSPDP-BTB13-1A-50Q-1	82	84	144.57	Albite, phillipsite, clay
HSPDP-BTB13-1A-50Q-1	98.5	100.5	144.74	Albite, anorthite
HSPDP-BTB13-1A-50Q-1	115	117	144.9	
HSPDP-BTB13-1A-50Q-1	131.5	133.5	145.07	
HSPDP-BTB13-1A-50Q-2	5	7	145.23	Albite, anorthite, clay
HSPDP-BTB13-1A-50Q-2	20	22	145.365	Anorthoclase, anorthite
HSPDP-BTB13-1A-50Q-2	38	40	145.56	
HSPDP-BTB13-1A-50Q-2	54.5	56.5	145.73	Albite, magnetite, sepiolite
HSPDP-BTB13-1A-50Q-2	71	73	145.89	Kspar, enstatite
HSPDP-BTB13-1A-50Q-2	87	89	146.05	Albite, anorthite, clay
HSPDP-BTB13-1A-50Q-2	103.5	105.5	146.22	Anorthoclase, muscovite, serpentine
HSPDP-BTB13-1A-50Q-2	120	122	146.38	
HSPDP-BTB13-1A-50Q-2	136.5	138.5	146.55	
HSPDP-BTB13-1A-50Q-3	10	12	146.71	Anorthoclase, phillipsite, quartz, clay
HSPDP-BTB13-1A-51Q-1	7	9	146.87	Phillipsite, anorthite, clay
HSPDP-BTB13-1A-51Q-1	23.5	25.5	147.04	Albite, anorthite, clay
HSPDP-BTB13-1A-51Q-2	7	9	147.19	Albite, phillipsite, clay
HSPDP-BTB13-1A-51Q-2	23.5	25.5	147.36	Albite, mica
HSPDP-BTB13-1A-51Q-2	40	42	147.52	Albite, phillipsite, qtz, clay
HSPDP-BTB13-1A-51Q-2	56.5	58.5	147.69	Anorthoclase, qtz
HSPDP-BTB13-1A-51Q-2	72.5	74.5	147.85	Anorthoclase, mont
HSPDP-BTB13-1A-51Q-2	89	91	148.01	Albite, phillipsite, quartz, clay
HSPDP-BTB13-1A-51Q-2	105.5	107.5	148.18	Anorthoclase, mont

HSPDP-BTB13-1A-51Q-2	122	124	148.34	Anorthoclase, mont
HSPDP-BTB13-1A-51Q-3	6	8	148.51	
HSPDP-BTB13-1A-51Q-3	20.5	22.5	148.63	Albite, tridymite, clay
HSPDP-BTB13-1A-52Q-1	13.5	15.5	148.84	Abite, sepiolite, calcite, magnesioferrite, cristobalite
HSPDP-BTB13-1A-52Q-1	32	34	149.04	Anorthoclase, hematite
HSPDP-BTB13-1A-52Q-1	44	46	149.115	Anorthoclase, hematite, mont
HSPDP-BTB13-1A-52Q-1	63	65	149.33	Anorthoclase, hematite, sepiolite
HSPDP-BTB13-1A-52Q-1	79.5	81.5	149.5	Anorthoclase, hematite
HSPDP-BTB13-1A-52Q-1	95.5	97.5	149.66	Anorthoclase, mont
HSPDP-BTB13-1A-52Q-1	112	114	149.82	Albite, mont
HSPDP-BTB13-1A-52Q-1	127	129	149.955	Albite, vermiculite
HSPDP-BTB13-1A-52Q-2	14	16	150.15	Anorthoclase, calcite
HSPDP-BTB13-1A-52Q-2	30.5	32.5	150.32	Albite, calcite, cristobalite, clays
HSPDP-BTB13-1A-52Q-2	47	49	150.48	Albite, clinopyroxene, fe-oxide, cristobalite clay
HSPDP-BTB13-1A-52Q-2	63.5	65.5	150.65	Anorthite, albite, clay
HSPDP-BTB13-1A-52Q-3	1.5	3.5	150.8	
HSPDP-BTB13-1A-52Q-3	18	20	150.97	Albite, clinopyroxene, clay
HSPDP-BTB13-1A-53Q-1	3	5	151.13	Kspar, anorthite, hematite
HSPDP-BTB13-1A-53Q-1	19.5	21.5	151.3	
HSPDP-BTB13-1A-53Q-1	35.5	37.5	151.46	Anorthoclase, calcite, cristobalite, mont
HSPDP-BTB13-1A-53Q-1	52	54	151.62	Albite, fe-oxides, mica
HSPDP-BTB13-1A-53Q-1	68.5	70.5	151.79	Enstatite, albite, hematite, cristobalite, mont
HSPDP-BTB13-1A-53Q-1	85	87	151.95	
HSPDP-BTB13-1A-53Q-1	101	103	152.11	Anorthoclase, mg-calcite, cristobalite, mont
HSPDP-BTB13-1A-53Q-1	117.5	119.5	152.28	Anorthite, mg-calcite, cristobalite, mont
HSPDP-BTB13-1A-53Q-1	134	136	152.44	Anorthite, mont
HSPDP-BTB13-1A-53Q-2	1.5	3.5	152.61	Anorthite, mont
HSPDP-BTB13-1A-53Q-2	18	20	152.77	Albite, mg-calcite, fe-oxide, mont
HSPDP-BTB13-1A-54Q-1	4	6	152.93	Mg-calcite, Plag-Na, Qtz, Fe-oxides
HSPDP-BTB13-1A-54Q-1	20.5	22.5	153.09	
HSPDP-BTB13-1A-54Q-1	41	43	153.29	Albite, hematite, anorthite, cristobalite
HSPDP-BTB13-1A-54Q-1	53.5	55.5	153.42	Anorthoclase, mont, cristobalite
HSPDP-BTB13-1A-54Q-1	70	72	153.58	Anorthoclase, anorthite, hematite, cristobalite, mont
HSPDP-BTB13-1A-54Q-1	86.5	88.5	153.74	Albite, mordenite, vermiculite
HSPDP-BTB13-1A-54Q-1	103	105	153.91	Anorthite, phillipsite, hematite, cristobalite
HSPDP-BTB13-1A-54Q-1	119.5	121.5	154.07	Anorthoclase, anorthite, mont
HSPDP-BTB13-1A-54Q-1	136	138	154.23	Albite, enstatite, quartz, fe-oxides, clays
HSPDP-BTB13-1A-54Q-2	9	11	154.39	

HSPDP-BTB13-1A-54Q-2	25.5	27.5	154.56	Kspar, fe-oxide, clay
HSPDP-BTB13-1A-54Q-2	42	44	154.72	Albite, enstatite, fe-oxide, clay
HSPDP-BTB13-1A-54Q-2	58.5	60.5	154.88	
HSPDP-BTB13-1A-54Q-2	74	76	155.03	Albite, phillipsite, clinopyroxene, fe-oxide, clay
HSPDP-BTB13-1A-54Q-2	91.5	93.5	155.21	
HSPDP-BTB13-1A-54Q-2	108	110	155.37	Kspar, fe-oxides, cristobalite
HSPDP-BTB13-1A-54Q-2	124.5	126.5	155.53	Anorthoclase, clinopyroxene, fe-oxide, clay
HSPDP-BTB13-1A-54Q-2	140	142	155.68	Anorthoclase, magenesioferrite, mont
HSPDP-BTB13-1A-54Q-3	14	16	155.86	Anorthoclase, gobbinsite, magnesioferrite, mont
HSPDP-BTB13-1A-55Q-1	8	10	156.02	Anorthoclase, gobbinsite, hematite, vermiculite
HSPDP-BTB13-1A-55Q-1	24.5	26.5	156.18	Anorthoclase, calcite, mont
HSPDP-BTB13-1A-55Q-1	41	43	156.35	
HSPDP-BTB13-1A-55Q-1	57.5	59.5	156.51	Albite, hematite, mont
HSPDP-BTB13-1A-55Q-1	74	76	156.67	Anorthoclase, hematite, vermiculite
HSPDP-BTB13-1A-55Q-1	90.5	92.5	156.84	Anorthoclase
HSPDP-BTB13-1A-55Q-1	107	109	157	Kspar, albite, dickite, hematite
HSPDP-BTB13-1A-55Q-1	123.5	125.5	157.17	
HSPDP-BTB13-1A-55Q-1	140	142	157.33	Anorthoclase, hematite, mont
HSPDP-BTB13-1A-55Q-2	14.5	16.5	157.49	Albite, paragonite, gobbinsite, hematite, mont
HSPDP-BTB13-1A-55Q-2	31	33	157.66	Anorthoclase, Cristobalite, Zeolite?
HSPDP-BTB13-1A-55Q-2	47.5	49.5	157.82	Anorthoclase, hematite, gobbinsite, mont
HSPDP-BTB13-1A-55Q-2	64	66	157.98	Anorthoclase, Cristobalite, Zeolite?
HSPDP-BTB13-1A-55Q-2	80.5	82.5	158.15	Anorthite, hematite, gobbinsite
HSPDP-BTB13-1A-55Q-2	97	99	158.31	Albite, gobbinsite, hematite, cristobalite, mont
HSPDP-BTB13-1A-55Q-2	113.5	115.5	158.47	Anorthoclase
HSPDP-BTB13-1A-55Q-2	130	132	158.64	Anorthoclase, gobbinsite, hematite
HSPDP-BTB13-1A-55Q-3	5	7	158.8	Anorthoclase
HSPDP-BTB13-1A-55Q-3	20	22	158.935	Anorthoclase, phillipsite, hematite, sepiolite
HSPDP-BTB13-1A-56Q-1	13	15	159.11	Albite, gobbinsite, mont
HSPDP-BTB13-1A-56Q-1	30	32	159.29	Anorthoclase, qtz
HSPDP-BTB13-1A-56Q-1	46.5	48.5	159.46	Anorthoclase, gobbinsite, mont
HSPDP-BTB13-1A-56Q-1	63	65	159.62	Albite, clays, kspar
HSPDP-BTB13-1A-56Q-1	79.5	81.5	159.79	
HSPDP-BTB13-1A-56Q-1	95.5	97.5	159.95	Mica, faujasite
HSPDP-BTB13-1A-56Q-1	112	114	160.11	Anorthoclase, mica, anorthite
HSPDP-BTB13-1A-56Q-1	128.5	130.5	160.28	
HSPDP-BTB13-1A-56Q-2	6.5	8.5	160.44	Anorthoclase, enstatite

HSPDP-BTB13-1A-56Q-2	22.5	24.5	160.6	Albite, enstatite, zeolite(?)
HSPDP-BTB13-1A-56Q-2	39	41	160.76	Albite, palygorskite
HSPDP-BTB13-1A-56Q-2	55.5	57.5	160.93	Albite, kspar, palygorskite
HSPDP-BTB13-1A-56Q-2	72	74	161.09	Albite, kspar
HSPDP-BTB13-1A-56Q-2	88.5	90.5	161.26	Albite, enstatite
HSPDP-BTB13-1A-56Q-2	105	107	161.42	Albite, sepiolite, magnetite
HSPDP-BTB13-1A-56Q-2	121.5	123.5	161.59	Albite, phillipsite, muscovite, cristobalite
HSPDP-BTB13-1A-56Q-3	8	10	161.75	Albite, enstatite, zeolite
HSPDP-BTB13-1A-57Q-1	0.5	2.5	161.94	Albite, paragonite, gobbinsite
HSPDP-BTB13-1A-57Q-1	17	19	162.11	Anorthoclase, phillipsite, muscovite, cristobalite
HSPDP-BTB13-1A-57Q-2	1	3	162.27	Albite, kspar
HSPDP-BTB13-1A-57Q-2	17.5	19.5	162.44	Albite, phillipsite, sepiolite
HSPDP-BTB13-1A-57Q-2	34	36	162.6	Enstatite, albite, phillipsite
HSPDP-BTB13-1A-57Q-2	50.5	52.5	162.77	Albite, phillipsite, sepiolite, cristobalite
HSPDP-BTB13-1A-57Q-2	67	69	162.93	Paragonite, albite, dickite
HSPDP-BTB13-1A-57Q-2	83.5	85.5	163.1	Albite, sepiolite, gobbinsite
HSPDP-BTB13-1A-57Q-2	100	102	163.26	Albite, paragonite, gobbinsite
HSPDP-BTB13-1A-57Q-2	116.5	118.5	163.43	Albite, phillipsite, sepiolite
HSPDP-BTB13-1A-57Q-3	8	10	163.59	Albite, anorthite
HSPDP-BTB13-1A-57Q-3	24.5	26.5	163.75	Anorthite, Kspar, sepiolite, magnetite
HSPDP-BTB13-1A-57Q-3	41	43	163.91	Anorthoclase, albite, kspar, palygorskite, magadiite
HSPDP-BTB13-1A-57Q-3	57.5	59.5	164.08	Albite, phillipsite, sepiolite, nacrite, cristobalite
HSPDP-BTB13-1A-57Q-3	74	76	164.24	Albite, anorthite, palygorskite, cristobalite
HSPDP-BTB13-1A-57Q-3	90.5	92.5	164.41	Albite, phillipsite, palygorskite, cristobalite
HSPDP-BTB13-1A-57Q-3	107	109	164.57	Anorthoclase, palygorskite, cristobalite
HSPDP-BTB13-1A-57Q-3	123.5	125.5	164.74	Albite, phillipsite, paragonite, hematite, cristobalite
HSPDP-BTB13-1A-57Q-3	140	142	164.9	Albite, hematite, dolomite, cristobalite
HSPDP-BTB13-1A-57Q-CC	4	6	165	Albite, anorthite, cristobalite
HSPDP-BTB13-1A-58Q-1	14.5	16.5	165.23	Anorthoclase, phillipsite, anorthite
HSPDP-BTB13-1A-58Q-1	31	33	165.39	Albite, palygorskite, hematite, dolomite, cristobalite
HSPDP-BTB13-1A-58Q-1	47.5	49.5	165.56	Albite, palygorskite, phillipsite, hematite, cristobalite
HSPDP-BTB13-1A-58Q-1	63.5	65.5	165.72	Albite, phillipsite, palygorskite, hematite, dolomite, cristobalite
HSPDP-BTB13-1A-58Q-1	80	82	165.88	
HSPDP-BTB13-1A-58Q-2	1	3	166.05	Phillipsite, palygorskite, hematite, cristobalite
HSPDP-BTB13-1A-58Q-2	17	19	166.21	Albite, phillipsite, palygorskite, hematite, cristobalite

HSPDP-BTB13-1A-58Q-2	33.5	35.5	166.37	Phillipsite, palygorskite, hematite
HSPDP-BTB13-1A-58Q-2	50	52	166.54	Albite, palygorskite, cristobalite
HSPDP-BTB13-1A-58Q-2	66.5	68.5	166.7	Albite, pyroxene, zeolite(?), clays
HSPDP-BTB13-1A-58Q-2	82.5	84.5	166.86	Anorthoclase, cristobalite
HSPDP-BTB13-1A-58Q-2	99	101	167.03	Anorthoclase, phillipsite, magnesioferrite
HSPDP-BTB13-1A-58Q-3	15	17	167.19	Anorthoclase, phillipsite
HSPDP-BTB13-1A-58Q-3	31.5	33.5	167.36	Anorthoclase, gobbinsite
HSPDP-BTB13-1A-59Q-1	0	2	168.13	Anorthoclase, cristobalite
HSPDP-BTB13-1A-59Q-1	16.5	18.5	168.29	Albite, tridymite, calcite, hematite
HSPDP-BTB13-1A-59Q-1	33	35	168.45	Anorthoclase, gobbinsite
HSPDP-BTB13-1A-59Q-1	49.5	51.5	168.61	Anorthoclase, gobbinsite, hematite
HSPDP-BTB13-1A-59Q-1	66	68	168.77	Anorthoclase, Cristobalite, Zeolite?
HSPDP-BTB13-1A-59Q-1	82.5	84.5	168.93	Anorthoclase, phillipsite, magnesioferrite, hematite
HSPDP-BTB13-1A-59Q-1	99	101	169.09	Anorthoclase, gobbinsite, magnesioferrite, hematite
HSPDP-BTB13-1A-59Q-1	115.5	117.5	169.25	Anorthoclase, gobbinsite
HSPDP-BTB13-1A-59Q-1	132	134	169.41	Anorthoclase, cristobalite
HSPDP-BTB13-1A-59Q-2	5	7	169.57	Anorthoclase
HSPDP-BTB13-1A-59Q-2	21.5	23.5	169.73	Anorthoclase, gobbinsite, cristobalite
HSPDP-BTB13-1A-59Q-2	38	40	169.89	Anorthoclase, gobbinsite
HSPDP-BTB13-1A-59Q-2	54.5	56.5	170.05	Anorthoclase, clay, fe-oxides
HSPDP-BTB13-1A-59Q-2	71	73	170.21	Anorthoclase, Albite, K-spar, Pyroxene
HSPDP-BTB13-1A-59Q-2	87.5	89.5	170.37	Anorthoclase, clay, fe-oxides
HSPDP-BTB13-1A-59Q-2	104	106	170.53	Anorthoclase, mica, clay, cristobalite
HSPDP-BTB13-1A-59Q-2	120.5	122.5	170.69	Albite, muscovite, serpentine, fe-oxide
HSPDP-BTB13-1A-59Q-2	137	139	170.85	Albite, paragonite, clay
HSPDP-BTB13-1A-59Q-3	11	13	171.02	Albite, serpentine, clay, fe-oxide
HSPDP-BTB13-1A-60Q-1	1	3	171.19	Albite, phillipsite, clay, fe-oxide
HSPDP-BTB13-1A-60Q-1	16	18	171.34	Anorthoclase, gobbinsite, hematite
HSPDP-BTB13-1A-60Q-1	32.5	34.5	171.5	Kspar, hematite, gobbinsite
HSPDP-BTB13-1A-60Q-1	49	51	171.66	Albite, gobbinsite
HSPDP-BTB13-1A-60Q-1	65.5	67.5	171.83	Albite, hematite, gobbinsite
HSPDP-BTB13-1A-60Q-1	82	84	171.99	Albite, phillipsite, hematite, magnesioferrite
HSPDP-BTB13-1A-60Q-1	98.5	100.5	172.15	Albite, gobbinsite, hematite, dolomite
HSPDP-BTB13-1A-60Q-1	115	117	172.31	Anorthoclase, clays
HSPDP-BTB13-1A-60Q-1	131.5	133.5	172.48	Anorthoclase, Hematite?, Zeolite?
HSPDP-BTB13-1A-60Q-2	10.5	12.5	172.64	Albite, palygorskite, dolomite, hematite, cristobalite
HSPDP-BTB13-1A-60Q-2	27	29	172.8	Albite, palygorskite, hematite, dolomite
HSPDP-BTB13-1A-60Q-2	43.5	45.5	172.96	Albite, sepiolite, hematite, dolomite, cristobalite

HSPDP-BTB13-1A-60Q-2	60	62	173.13	Albite, palygorskite, dolomite, hematite
HSPDP-BTB13-1A-60Q-2	76.5	78.5	173.29	Albite, palygorskite, hematite
HSPDP-BTB13-1A-60Q-2	93	95	173.45	Albite, sepiolite, hematite, dolomite
HSPDP-BTB13-1A-60Q-2	109.5	111.5	173.61	Albite, palygorskite, dolomite, hematite, cristobalite
HSPDP-BTB13-1A-60Q-2	126	128	173.78	Albite, palygorskite, kspar, hematite, cristobalite
HSPDP-BTB13-1A-60Q-3	5.5	7.5	173.94	Albite, tridymite, hematite, dolomite
HSPDP-BTB13-1A-60Q-3	22	24	174.1	Albite, palygorskite, phillipsite, dolomite, maghemite
HSPDP-BTB13-1A-61Q-1	3.5	5.5	174.27	Anorthite, Albite, Muscovite, K-spar, Pyroxene
HSPDP-BTB13-1A-61Q-1	20	22	174.43	Albite, Anorthite, K-spar
HSPDP-BTB13-1A-61Q-1	36.5	38.5	174.6	
HSPDP-BTB13-1A-61Q-1	53	55	174.76	Albite, Anorthite, K-spar, Muscovite, Pyroxene, Mg.calcite
HSPDP-BTB13-1A-61Q-1	69.5	71.5	174.93	Albite, Anorthite, K-spar, Nepheline, Pyroxene, Mg-calcite
HSPDP-BTB13-1A-61Q-1	86	88	175.09	Anorthoclase, calcite, cristobalite
HSPDP-BTB13-1A-61Q-1	102.5	104.5	175.26	Anorthoclase, qtz
HSPDP-BTB13-1A-61Q-1	118.5	120.5	175.42	Anorthoclase, anorthite, gobbinsite
HSPDP-BTB13-1A-61Q-1	135	137	175.58	Anorthoclase, Qtz, Zeolite?
HSPDP-BTB13-1A-61Q-2	7	9	175.74	Albite, Andesine, Vermiculite
HSPDP-BTB13-1A-61Q-2	23.5	25.5	175.9	Anorthoclase, qtz
HSPDP-BTB13-1A-61Q-2	40	42	176.07	Anorthoclase, qtz
HSPDP-BTB13-1A-61Q-2	56.5	58.5	176.23	Phillipsite, anorthite
HSPDP-BTB13-1A-61Q-2	73	75	176.4	Albite, Anorthite, K-spar
HSPDP-BTB13-1A-61Q-2	89.5	91.5	176.56	Anorthoclase, qtz
HSPDP-BTB13-1A-61Q-2	106	108	176.73	Albite, phillipsite
HSPDP-BTB13-1A-61Q-2	122.5	124.5	176.89	Anorthoclase, cristobalite
HSPDP-BTB13-1A-61Q-2	137	139	177.02	Anorthoclase, phillipsite, anorthite
HSPDP-BTB13-1A-62Q-1	0.5	2.5	177.29	Albite
HSPDP-BTB13-1A-62Q-1	17	19	177.45	Albite, Anorthite, K-spar
HSPDP-BTB13-1A-62Q-1	33	35	177.61	Anorthoclase, palygorskite, cristobalite
HSPDP-BTB13-1A-62Q-1	49.5	51.5	177.78	Anorthoclase, anorthite, calcite, cristobalite
HSPDP-BTB13-1A-62Q-1	66	68	177.94	Anorthoclase, Plag-Ca, Phillipsite
HSPDP-BTB13-1A-62Q-1	82.5	84.5	178.11	Anorthoclase, calcite, cristobalite
HSPDP-BTB13-1A-62Q-1	99	101	178.27	Anorthoclase, phillipsite, cristobalite, qtz
HSPDP-BTB13-1A-62Q-1	115.5	117.5	178.44	Anorthoclase, cristobalite, qtz
HSPDP-BTB13-1A-62Q-1	132	134	178.6	Anorthoclase, cristobalite, qtz
HSPDP-BTB13-1A-62Q-2	8	10	178.77	Anorthoclase, Albite, Phillipsite, Muscovite, K-spar, Anorthite
HSPDP-BTB13-1A-62Q-2	24	26	178.93	Anorthoclase, anorthite

HSPDP-BTB13-1A-62Q-2	40.5	42.5	179.09	Anorthoclase, muscovite, kspar
HSPDP-BTB13-1A-62Q-2	57	59	179.26	Anorthoclase, gobbinsite
HSPDP-BTB13-1A-62Q-2	73.5	75.5	179.42	Anorthoclase, muscovite, albite, dickite
HSPDP-BTB13-1A-62Q-2	89.5	91.5	179.58	Kspar, muscovite, anorthite
HSPDP-BTB13-1A-62Q-2	106	108	179.75	Albite, muscovite, tridymite
HSPDP-BTB13-1A-62Q-2	122.5	124.5	179.91	Albite, K-spar, Magadiite
HSPDP-BTB13-1A-62Q-3	4	6	180.08	
HSPDP-BTB13-1A-63Q-1	0.5	2.5	180.33	Anorthoclase, Magadiite
HSPDP-BTB13-1A-63Q-1	8	10	180.485	Anorthoclase, cristobalite, qtz
HSPDP-BTB13-1A-63Q-1	24	26	180.64	Anorthoclase, phillipsite, qtz, cristobalite
HSPDP-BTB13-1A-63Q-1	40.5	42.5	180.8	
HSPDP-BTB13-1A-63Q-1	57	59	180.96	Anorthoclase, qtz
HSPDP-BTB13-1A-63Q-1	73.5	75.5	181.13	Anorthoclase, qtz
HSPDP-BTB13-1A-63Q-1	89.5	91.5	181.285	Albite, Pyroxene, Magadiite, Qtz
HSPDP-BTB13-1A-63Q-1	106	108	181.445	Albite, Anorthite, Muscovite, K-spar
HSPDP-BTB13-1A-63Q-1	122.5	124.5	181.605	
HSPDP-BTB13-1A-63Q-2	3	5	181.63	Albite, Anorthite, K-spar, Qtz
HSPDP-BTB13-1A-63Q-2	19.5	21.5	181.8	Albite, pyroxene, clay
HSPDP-BTB13-1A-63Q-2	36	38	181.96	Albite, kspar, clays
HSPDP-BTB13-1A-63Q-2	52.5	54.5	182.12	Albite, Phillipsite, Muscovite, K-spar
HSPDP-BTB13-1A-63Q-2	69	71	182.29	Anorthoclase, albite, clay
HSPDP-BTB13-1A-63Q-2	85.5	87.5	182.45	Albite, anorthite, phillipsite
HSPDP-BTB13-1A-63Q-2	102	104	182.61	Anorthoclase, kspar, clay, cristobalite
HSPDP-BTB13-1A-63Q-2	118.5	120.5	182.78	Albite, paragonite, phillipsite, anorthite
HSPDP-BTB13-1A-63Q-3	7.5	9.5	182.94	Albite, clay, kspar, dolomite
HSPDP-BTB13-1A-63Q-3	24	26	183.1	Albite, clay, kspar, cristobalite
HSPDP-BTB13-1A-63Q-3	40.5	42.5	183.27	Albite, serpentine, anorthite
HSPDP-BTB13-1A-64Q-1	5.5	7.5	183.43	Anorthoclase, albite, clay
HSPDP-BTB13-1A-64Q-1	22	24	183.59	Albite, kspar, gobbinsite
HSPDP-BTB13-1A-64Q-1	38.5	40.5	183.76	
HSPDP-BTB13-1A-64Q-1	55	57	183.92	Albite, muscovite, kspar, phillipsite
HSPDP-BTB13-1A-64Q-1	87.5	89.5	184.25	Albite, phillipsite, palygorskite, hematite, cristobalite
HSPDP-BTB13-1A-64Q-1	104	106	184.41	Albite, muscovite, hematite
HSPDP-BTB13-1A-64Q-1	120.5	122.5	184.58	Albite, phillipsite, palygorskite, hematite
HSPDP-BTB13-1A-64Q-2	4.5	6.5	184.74	Kspar, phillipsite, muscovite, hematite, cristobalite
HSPDP-BTB13-1A-64Q-2	21	23	184.9	Anorthoclase, hematite, magnesioferrite, cristobalite, sepiolite
HSPDP-BTB13-1A-64Q-2	37.5	39.5	185.07	Anorthite, phillipsite, hematite
HSPDP-BTB13-1A-64Q-2	53.5	55.5	185.23	Anorthoclase, palygoskite, hematite, dolomite, cristobalite

HSPDP-BTB13-1A-64Q-2	70	72	185.39	Palygorskite, phillipsite, kspar, magnesioferrite, cristobalite
HSPDP-BTB13-1A-64Q-2	86.5	88.5	185.56	Anorthoclase, anorthite, magnesioferrite, hematite, cristobalite
HSPDP-BTB13-1A-64Q-2	103	105	185.72	Anorthite, phillipsite, hematite
HSPDP-BTB13-1A-64Q-2	119.5	121.5	185.89	Albite, anorthite, tridymite
HSPDP-BTB13-1A-64Q-3	4	6	186.05	Anorthoclase, anorthite, diopside
HSPDP-BTB13-1A-64Q-3	20.5	22.5	186.22	Anorthoclase, phillipsite, mont
HSPDP-BTB13-1A-65Q-1	0.5	2.5	186.42	Anorthoclase, phillipsite, cristobalite
HSPDP-BTB13-1A-65Q-1	17	19	186.59	Anorthoclase, Cristobalite, Fe-oxides
HSPDP-BTB13-1A-65Q-1	33.5	35.5	186.75	Kspar, hematite
HSPDP-BTB13-1A-65Q-1	50	52	186.91	Anorthoclase, albite, diopside, hematite
HSPDP-BTB13-1A-65Q-1	66.5	68.5	187.08	Anorthoclase, hematite, cristobalite
HSPDP-BTB13-1A-65Q-1	83	85	187.24	Anorthoclase, Albite, Pyroxene, K-spar
HSPDP-BTB13-1A-65Q-1	99.5	101.5	187.4	Albite, Anorthite, Phillipsite, Pyroxene, Magnetite, Hematite
HSPDP-BTB13-1A-65Q-1	116	118	187.57	
HSPDP-BTB13-1A-65Q-2	1	3	187.73	Anorthoclase, muscovite, phillipsite, fe-oxide, cristobalite
HSPDP-BTB13-1A-65Q-2	17.5	19.5	187.89	Albite, phillipsite, clay, fe-oxide, cristobalite
HSPDP-BTB13-1A-65Q-2	34	36	188.06	Albite, phillipsite, clay, fe-oxide, cristobalite
HSPDP-BTB13-1A-65Q-2	50.5	52.5	188.22	Albite, pyroxene, fe-oxides, cristobalite
HSPDP-BTB13-1A-65Q-2	67	69	188.38	Albite, Phillipsite, K-spar, Pyroxene
HSPDP-BTB13-1A-65Q-2	83.5	85.5	188.55	Albite, phillipsite, fe-oxide, cristobalite
HSPDP-BTB13-1A-65Q-2	100	102	188.71	Albite, phillipsite, muscovite, cristobalite
HSPDP-BTB13-1A-65Q-2	116.5	118.5	188.87	Albite, mica
HSPDP-BTB13-1A-65Q-2	133	135	189.04	Anorthoclase, clay, fe-oxide, quartz
HSPDP-BTB13-1A-65Q-2	149.5	151.5	189.2	Anorthoclase, mica, clay, fe-oxide
HSPDP-BTB13-1A-65Q-3	15	17	189.36	
HSPDP-BTB13-1A-66Q-1	5.5	7.5	189.53	Albite, paragonite, pyroxene
HSPDP-BTB13-1A-66Q-1	22	24	189.69	Albite, anorthite, mica
HSPDP-BTB13-1A-66Q-1	38	40	189.85	Albite, muscovite
HSPDP-BTB13-1A-66Q-1	54.5	56.5	190.02	Anorthoclase, fe-oxide, cristobalite, mica
HSPDP-BTB13-1A-66Q-1	71	73	190.18	
HSPDP-BTB13-1A-66Q-1	87.5	89.5	190.35	Anorthoclase, Pyroxene, K-spar, Albite, Hematite, Zeolite?
HSPDP-BTB13-1A-66Q-1	104	106	190.51	
HSPDP-BTB13-1A-66Q-1	120.5	122.5	190.68	Anorthoclase, Pyroxene, Anorthite, Magnetite, Cristobalite
HSPDP-BTB13-1A-66Q-1	137	139	190.84	Anorthoclase, Cristobalite, Fe-oxieds, Zeolite?
HSPDP-BTB13-1A-66Q-2	13	15	191	

HSPDP-BTB13-1A-66Q-3	10	12	191.17	Enstatite, anorthoclase, phillipsite, muscovite, fe-oxide
HSPDP-BTB13-1A-66Q-3	26.5	28.5	191.33	Albite, hematite, anorthite
HSPDP-BTB13-1A-66Q-3	42.5	44.5	191.49	
HSPDP-BTB13-1A-66Q-3	59	61	191.66	Albite, hematite, mont
HSPDP-BTB13-1A-66Q-3	75.5	77.5	191.82	Anorthoclase, hematite, cristobalite
HSPDP-BTB13-1A-66Q-3	92	94	191.99	Anorthoclase, hematite, cristobalite
HSPDP-BTB13-1A-66Q-3	108.5	110.5	192.15	Anorthoclase, hematite, mont
HSPDP-BTB13-1A-66Q-3	125	127	192.32	Albite, phillipsite, fe-oxide, mica
HSPDP-BTB13-1A-67Q-1	0	2	192.52	Albite, muscovite, phillipsite, fe-oxide, cristobalite
HSPDP-BTB13-1A-67Q-1	16.5	18.5	192.69	Anorthoclase, phillipsite, hematite, cristobalite
HSPDP-BTB13-1A-67Q-1	33	35	192.85	Anorthoclase, hematite, cristobalite, mont
HSPDP-BTB13-1A-67Q-1	49.5	51.5	193.02	Anorthoclase, hematite, mont, cristobalite
HSPDP-BTB13-1A-67Q-1	66	68	193.18	Albite, phillipsite, hematite, qtz
HSPDP-BTB13-1A-67Q-1	82	84	193.34	Albite, kspar, fe-oxide, cristobalite, clay
HSPDP-BTB13-1A-67Q-1	98.5	100.5	193.51	Anorthoclase, hematite, mont
HSPDP-BTB13-1A-67Q-1	115	117	193.67	
HSPDP-BTB13-1A-67Q-1	131.5	133.5	193.84	Albite, phillipsite, fe-oxide, cristobalite, clay
HSPDP-BTB13-1A-67Q-2	7.5	9.5	194	Anorthoclase, Zeolite?
HSPDP-BTB13-1A-67Q-2	24	26	194.17	
HSPDP-BTB13-1A-67Q-2	40.5	42.5	194.33	Albite, mica, phillipsite, fe-oxide
HSPDP-BTB13-1A-67Q-2	56.5	58.5	194.49	
HSPDP-BTB13-1A-67Q-2	73	75	194.66	Albite, phillipsite, clay
HSPDP-BTB13-1A-67Q-2	89.5	91.5	194.82	Albite, phillipsite, fe-oxide, clay
HSPDP-BTB13-1A-67Q-2	106	108	194.99	Albite, muscovite, phillipsite, fe-oxide, clay
HSPDP-BTB13-1A-67Q-2	122.5	124.5	195.15	Anorthite, fe-oxide
HSPDP-BTB13-1A-68Q-1	0.5	2.5	195.57	
HSPDP-BTB13-1A-68Q-1	16.5	18.5	195.73	
HSPDP-BTB13-1A-68Q-1	33	35	195.89	
HSPDP-BTB13-1A-68Q-2	7	9	196.125	Anorthoclase, albite, mont
HSPDP-BTB13-1A-68Q-2	20	22	196.22	
HSPDP-BTB13-1A-68Q-2	36.5	38.5	196.38	Albite, diopside, fe-oxide, cristobalite, clay
HSPDP-BTB13-1A-68Q-2	53	55	196.55	Albite, anorthite, fe-oxide, clay
HSPDP-BTB13-1A-68Q-2	66.5	68.5	196.65	
HSPDP-BTB13-1A-68Q-2	85.5	87.5	196.87	
HSPDP-BTB13-1A-68Q-2	102	104	197.04	
HSPDP-BTB13-1A-69Q-1	0	2	198.61	
HSPDP-BTB13-1A-69Q-1	16.5	18.5	198.77	Albite, hematite, mont
HSPDP-BTB13-1A-69Q-1	33	35	198.94	Anorthoclase, musocvite, fe-oxide, clay

HSPDP-BTB13-1A-69Q-1	49.5	51.5	199.1	Anorthoclase, fe-oxide, clay
HSPDP-BTB13-1A-69Q-1	66	68	199.26	Enstatite, albite, hematite
HSPDP-BTB13-1A-69Q-1	82.5	84.5	199.43	Anorthoclase, enstatite, fe-oxide, cristobalite
HSPDP-BTB13-1A-69Q-1	99	101	199.59	Albite, dolomite, hematite, mont
HSPDP-BTB13-1A-69Q-1	115.5	117.5	199.75	
HSPDP-BTB13-1A-69Q-1	132	134	199.92	Albite, fe-oxide, serpentine
HSPDP-BTB13-1A-69Q-1	148.5	150.5	200.08	Anorthoclase, hematite, mont, anorthite
HSPDP-BTB13-1A-69Q-2	14	16	200.25	Albite, mica
HSPDP-BTB13-1A-69Q-2	30.5	32.5	200.41	Albite, hematite, mont
HSPDP-BTB13-1A-69Q-2	47	49	200.57	
HSPDP-BTB13-1A-69Q-2	63.5	65.5	200.74	Albite, diopside, mont
HSPDP-BTB13-1A-69Q-2	80	82	200.9	Albite, mica, clay
HSPDP-BTB13-1A-69Q-2	96.5	98.5	201.06	Albite, kspar, mont
HSPDP-BTB13-1A-69Q-2	113	115	201.23	Albite, tridymite, mont
HSPDP-BTB13-1A-69Q-2	129.5	131.5	201.39	Anorthoclase, Zeolite?
HSPDP-BTB13-1A-69Q-2	146	148	201.55	Albite, mont, cristobalite
HSPDP-BTB13-1A-70Q-1	6	8	201.72	Anorthoclase, hematite, mont
HSPDP-BTB13-1A-70Q-1	22.5	24.5	201.89	Enstatite, albite, mg-calcite, mont
HSPDP-BTB13-1A-70Q-1	38.5	40.5	202.05	Albite, anorthite, vermiculite
HSPDP-BTB13-1A-70Q-1	64	66	202.39	Albite, Fe-oxides, zeolite
HSPDP-BTB13-1A-70Q-1	71.5	73.5	202.38	Anorthite, albite, mg-calcite
HSPDP-BTB13-1A-70Q-1	88	90	202.54	
HSPDP-BTB13-1A-70Q-2	1	3	202.7	Albite, sepiolite
HSPDP-BTB13-1A-70Q-2	17.5	19.5	202.87	
HSPDP-BTB13-1A-70Q-2	34	36	203.03	
HSPDP-BTB13-1A-70Q-2	50	52	203.19	Albite, calcite, chlorite(?)
HSPDP-BTB13-1A-70Q-2	66.5	68.5	203.36	
HSPDP-BTB13-1A-70Q-2	99.5	101.5	203.69	
HSPDP-BTB13-1A-70Q-3	16	18	204.01	
HSPDP-BTB13-1A-71Q-1	0.5	2.5	204.71	Plag-Na, Plag-Ca, Phillipsite
HSPDP-BTB13-1A-71Q-1	35	37	204.87	Albite, qtz, hematite, cristobalite
HSPDP-BTB13-1A-71Q-1	69.5	71.5	205.04	Anorthoclase, muscovite, phillipsite
HSPDP-BTB13-1A-72Q-1	9	11	205.2	
HSPDP-BTB13-1A-72Q-1	25.5	27.5	205.37	Anorthoclase, mg-calcite, fe-oxide, clay
HSPDP-BTB13-1A-72Q-1	42	44	205.53	
HSPDP-BTB13-1A-72Q-1	58.5	60.5	205.7	Albite, pyroxene, mg-calcite, fe-oxide, clay
HSPDP-BTB13-1A-72Q-1	75	77	205.86	Albite, mg-calcite, fe-oxide, clay
HSPDP-BTB13-1A-72Q-2	4	6	206.02	Anorthite, albite, mg-calcite, magnesioferrite, sepiolite, cristobalite
HSPDP-BTB13-1A-72Q-2	20.5	22.5	206.18	Albite, clinopyroxene, cristobalite
HSPDP-BTB13-1A-72Q-2	37	39	206.35	

HSPDP-BTB13-1A-72Q-2	53.5	55.5	206.51	
HSPDP-BTB13-1A-72Q-2	70	72	206.68	Albite, pyroxene, fe-oxide, clay
HSPDP-BTB13-1A-72Q-3	10.5	12.5	206.84	
HSPDP-BTB13-1A-72Q-3	27	29	207.01	Anorthoclase, clinopyroxene, hematite, chlorite(?)
HSPDP-BTB13-1A-73Q-1	0.5	2.5	207.76	Albite, quartz, fe-oxide, clay
HSPDP-BTB13-1A-73Q-1	17.5	19.5	207.93	Albite, phillipsite, barite, fe-oxide
HSPDP-BTB13-1A-73Q-1	34.5	36.5	208.09	
HSPDP-BTB13-1A-73Q-1	51.5	53.5	208.26	Albite, fe-oxide, clay
HSPDP-BTB13-1A-73Q-1	68.5	70.5	208.42	Albite, mg-calcite, fe-oxide, clay
HSPDP-BTB13-1A-73Q-1	85.5	87.5	208.58	Albite, mg-calcite, fe-oxide, clay
HSPDP-BTB13-1A-73Q-1	102.5	104.5	208.75	
HSPDP-BTB13-1A-73Q-1	119.5	121.5	208.91	Albite, fe-oxide, clay
HSPDP-BTB13-1A-73Q-1	136.5	138.5	209.08	Albite, pyroxene, fe-oxide, clay
HSPDP-BTB13-1A-73Q-2	0.5	2.5	209.23	Mg-calcite, Anorthoclase, Fe-oxides, Zeolite?
HSPDP-BTB13-1A-73Q-2	17.5	19.5	209.4	Albite, pyroxene, clays, fe-oxide
HSPDP-BTB13-1A-73Q-2	34.5	36.5	209.56	Albite, mg-calcite, fe-oxide, clay
HSPDP-BTB13-1A-73Q-2	51.5	53.5	209.73	Anorthoclase, hematite, mont
HSPDP-BTB13-1A-73Q-2	68.5	70.5	209.89	Anorthoclase, hematite, mont
HSPDP-BTB13-1A-73Q-2	85.5	87.5	210.05	Anorthoclase, hematite, mont
HSPDP-BTB13-1A-73Q-2	102.5	104.5	210.22	Anorthoclase, fe-oxide, clay
HSPDP-BTB13-1A-73Q-2	119.5	121.5	210.38	Albite, fe-oxide, clay
HSPDP-BTB13-1A-73Q-2	136.5	138.5	210.55	
HSPDP-BTB13-1A-74Q-1	0.5	2.5	210.79	Anorthoclase, Fe-oxides, Zeolite?
HSPDP-BTB13-1A-74Q-1	8	10	210.87	Albite, hematite, anorthite, faujasite(?)
HSPDP-BTB13-1A-74Q-1	24.5	26.5	211.03	Anorthoclase, hematite, mont
HSPDP-BTB13-1A-74Q-1	41	43	211.19	Albite, hematite, quartz, mica
HSPDP-BTB13-1A-75Q-1	1	3	211.35	Anorthoclase, sillimanite, hematite
HSPDP-BTB13-1A-75Q-1	17.5	19.5	211.52	Anorthoclase, mont
HSPDP-BTB13-1A-75Q-1	37	39	211.74	Anorthoclase, mont
HSPDP-BTB13-1A-75Q-1	50.5	52.5	211.85	Albite, anorthite
HSPDP-BTB13-1A-75Q-1	67	69	212.01	Anorthoclase, mont
HSPDP-BTB13-1A-75Q-1	83.5	85.5	212.18	Anorthoclase, vermiculite
HSPDP-BTB13-1A-75Q-2	7.5	9.5	212.34	Anorthoclase, Zeolite?
HSPDP-BTB13-1A-75Q-2	24	26	212.5	Anorthoclase, Zeolite?, Fe & Ti-oxieds
HSPDP-BTB13-1A-75Q-2	40.5	42.5	212.67	Anatase
HSPDP-BTB13-1A-75Q-2	57	59	212.83	Phillipsite, hematite, anatase, vermiculite
HSPDP-BTB13-1A-75Q-2	73	75	212.99	Fe & Ti oxides, mont
HSPDP-BTB13-1A-75Q-2	88	90	213.125	Phillipsite, mont, anatase
HSPDP-BTB13-1A-76Q-1	23.5	25.5	214	Anorthoclase, Zeolite?

HSPDP-BTB13-1A-76Q-1	33.5	35.5	213.87	Albite, phillipsite, hematite
HSPDP-BTB13-1A-76Q-1	50	52	214.03	Anorthoclase, hematite, mont
HSPDP-BTB13-1A-76Q-1	66.5	68.5	214.19	Anorthoclase, phillipsite, hematite
HSPDP-BTB13-1A-76Q-1	83	85	214.35	Anorthoclase, phillipsite, mont
HSPDP-BTB13-1A-76Q-1	99.5	101.5	214.52	
HSPDP-BTB13-1A-76Q-2	15	17	214.68	Anorthoclase, Zeolite?
HSPDP-BTB13-1A-76Q-2	31.5	33.5	214.84	Anorthoclase, qtz, hematite
HSPDP-BTB13-1A-76Q-2	48	50	215	Anorthoclase, phillipsite, hematite
HSPDP-BTB13-1A-76Q-2	64.5	66.5	215.16	Albite, anorthite
HSPDP-BTB13-1A-76Q-2	81	83	215.32	Albite, hematite, qtz
HSPDP-BTB13-1A-76Q-2	97.5	99.5	215.49	Anorthoclase, qtz
HSPDP-BTB13-1A-76Q-3	14	16	215.65	Anorthoclase, Zeolite?
HSPDP-BTB13-1A-76Q-3	30.5	32.5	215.81	Anorthoclase, qtz, mont
HSPDP-BTB13-1A-76Q-3	47	49	215.97	Anorthoclase, qtz, mont
HSPDP-BTB13-1A-76Q-3	63.5	65.5	216.14	
HSPDP-BTB13-1A-76Q-3	80	82	216.3	Anorthoclase, hematite, vermiculite
HSPDP-BTB13-1A-76Q-3	96.5	98.5	216.46	Albite, kaolinite, hematite, mont
HSPDP-BTB13-1A-76Q-4	6.5	8.5	216.62	Anorthoclase, nacrite, hematite, mont
HSPDP-BTB13-1A-77Q-1	10	12	216.79	Anorthoclase, Zeolite?, Fe-oxieds
HSPDP-BTB13-1A-77Q-1	26.5	28.5	216.96	Dickite, hematite, rutile, mont
HSPDP-BTB13-1A-77Q-1	43	45	217.12	
HSPDP-BTB13-1A-77Q-1	59.5	61.5	217.29	Hematite, rutile, mont
HSPDP-BTB13-1A-77Q-1	76	78	217.45	
HSPDP-BTB13-1A-77Q-1	92	94	217.61	Sillimanite, hematite, magnesioferrite
HSPDP-BTB13-1A-77Q-1	108.5	110.5	217.78	Anorthoclase, kaolinite, hematite, anatase, mont
HSPDP-BTB13-1A-77Q-1	125	127	217.94	Kaolinite, hematite, rutile, anatase, montmorillonite
HSPDP-BTB13-1A-77Q-2	13	15	218.11	Albite, kaolinite, hematite, rutile, cristobalite
HSPDP-BTB13-1A-77Q-2	29.5	31.5	218.27	Anorthoclase, hematite, vermiculite
HSPDP-BTB13-1A-77Q-2	46	48	218.44	Anorthoclase, kaolinite, hematite, rutile, anatase
HSPDP-BTB13-1A-77Q-2	62.5	64.5	218.6	Anorthoclase, hematite, gobbinsite, mont
HSPDP-BTB13-1A-78Q-1	2	4	219.29	Anorthoclase, hematite, mont
HSPDP-BTB13-1A-78Q-1	16.5	18.5	219.42	Anorthoclase, Mg-calcite, Fe-oxides, Zeolite?
HSPDP-BTB13-1A-78Q-1	33	35	219.58	Anorthoclase, diopside, hematite
HSPDP-BTB13-1A-78Q-1	49	51	219.74	Anorthoclase, mg-calcite, hematite, mont
HSPDP-BTB13-1A-78Q-2	6	8	219.9	Anorthoclase, mg-calcite, hematite, qtz
HSPDP-BTB13-1A-79Q-1	6.5	8.5	220.07	Anorthoclase, Mg-calcite, Fe-oxides, Zeolite?
HSPDP-BTB13-1A-79Q-1	23	25	220.23	Anorthoclase,mica, fe-oxide, mg-calcite
HSPDP-BTB13-1A-79Q-1	39.5	41.5	220.4	Anorthoclase, mg-calcite, hematite, mont

HSPDP-BTB13-1A-79Q-1	56	58	220.56	Rutile, cristobalite, mont
HSPDP-BTB13-1A-79Q-1	72.5	74.5	220.73	Anorthoclase, mont
HSPDP-BTB13-1A-79Q-1	89	91	220.89	Anorthoclase, hematite, mont
HSPDP-BTB13-1A-79Q-1	105	107	221.05	Anorthoclase, Zeolite?
HSPDP-BTB13-1A-79Q-1	121.5	123.5	221.22	Kspar, magnesioferrite, mont, cristobalite
HSPDP-BTB13-1A-79Q-2	28.5	30.5	221.55	Anorthoclase
HSPDP-BTB13-1A-79Q-2	61.5	63.5	221.88	Anorthoclase, pyroxene
HSPDP-BTB13-1A-79Q-2	78	80	222.04	Anorthoclase, dickite, hematite, mont
HSPDP-BTB13-1A-79Q-2	94	96	222.2	Albite, hematite, vermiculite
HSPDP-BTB13-1A-79Q-2	110.5	112.5	222.37	Anorthoclase, phillipsite, hematite, mont
HSPDP-BTB13-1A-79Q-3	2	4	222.52	Albite, anorthoclase, vermiculite
HSPDP-BTB13-1A-80Q-1	0.5	2.5	223.06	Mg-calcite, Anorthoclase, Fe-oxide, Zeolite?
HSPDP-BTB13-1A-80Q-1	17	19	223.22	Phillipsite, clays, fe-oxides
HSPDP-BTB13-1A-80Q-1	33.5	35.5	223.39	
HSPDP-BTB13-1A-80Q-1	50	52	223.55	Anorthite, sepiolite
HSPDP-BTB13-1A-80Q-1	83	85	223.88	Anorthoclase, Zeolite?
HSPDP-BTB13-1A-80Q-1	99	101	224.04	Anorthoclase, anorthite, magnesioferrite, mont
HSPDP-BTB13-1A-80Q-2	7	9	224.2	
HSPDP-BTB13-1A-80Q-2	23.5	25.5	224.37	Albite, kaolinite, hematite, cristobalite, mont
HSPDP-BTB13-1A-80Q-2	40	42	224.53	Anorthoclase, Zeolite?, Fe-oxides
HSPDP-BTB13-1A-80Q-2	56	58	224.69	Anorthoclase, gobbinsite, fe-oxides, mont
HSPDP-BTB13-1A-80Q-2	72.5	74.5	224.86	Anorthoclase, dickite, hematite, mont
HSPDP-BTB13-1A-80Q-2	89	91	225.02	Anorthoclase, fe-oxides, mont
HSPDP-BTB13-1A-80Q-2	105.5	107.5	225.19	Orthoclase, phillipsite, magnesioferrite, cristobalite, mont
HSPDP-BTB13-1A-81Q-1	0.5	2.5	226.09	Anorthite, clay
HSPDP-BTB13-1A-81Q-1	20	22	226.26	Anorthoclase, fe-oxide, clay
HSPDP-BTB13-1A-81Q-1	39.5	41.5	226.42	
HSPDP-BTB13-1A-81Q-1	59	61	226.59	Clays, fe-oxide, ti-oxide
HSPDP-BTB13-1A-81Q-1	78.5	80.5	226.75	
HSPDP-BTB13-1A-81Q-1	98	100	226.91	
HSPDP-BTB13-1A-81Q-2	17	19	227.07	Anorthoclase, Zeolite?, Ti-oxides
HSPDP-BTB13-1A-81Q-2	36.5	38.5	227.24	Albite, phillipsite, clay, fe-oxide, cristobalite, ti-oxide
HSPDP-BTB13-1A-81Q-2	56	58	227.4	Anorthoclase, palygorskite, nacrite, hematite, anatase
HSPDP-BTB13-1A-81Q-2	75.5	77.5	227.56	
HSPDP-BTB13-1A-81Q-2	95	97	227.73	Kaolinite, hematite, rutile, cristobalite